ISSN: 2687 - 4539

CHAOS

THEORY AND APPLICATIONS

IN APPLIED SCIENCES AND ENGINEERING

VOLUME 4, ISSUE 1, MARCH 2022

AN INTERDISCIPLINARY JOURNAL OF NONLINEAR SCIENCE

ISSN: 2687 - 4539

CHAOS

THEORY AND APPLICATIONS

IN APPLIED SCIENCES AND ENGINEERING

Chaos Theory and Applications (CHTA)
Volume: 4 – Issue No: 1 (March 2022)
https://dergipark.org.tr/en/pub/chaos/issue/63571

Editorial Advisory Board Members

Language Editors

Technical Coordinator

ISSN: 2687 - 4539

CHAOS

THEORY AND APPLICATIONS

IN APPLIED SCIENCES AND ENGINEERING

Chaos Theory and Applications (CHTA)
Volume: 4 – Issue No: 1 (March 2022)
https://dergipark.org.tr/en/pub/chaos/issue/63571

Contents

CHAOS
Theory and Applications
in Applied Sciences and Engineering

e-ISSN: 2687-4539
EDITORIAL
Vol.4 / No.1 / 2022 / pp.1-3

Chaos Theory and Applications: The Physical Evidence, Mechanism are Important in Chaotic Systems

Jun Ma *,[1]
*Department of Physics, Lanzhou University of Technology, Lanzhou 730050, China.

ABSTRACT This editorial is presented for readers and researchers in the field of nonlinear dynamics, including dynamical control, synchronization stability and control, fractional order approach, boundary condition, memristive system, functional neural circuit, Hamilton energy and Lyapunov function. These short comments and clarifications are helpful to explain the motive of scientific research, physical principle and potential application of nonlinear circuits, statistical analysis and schemes, and thus the report and papers may become readable and instructive.

KEYWORDS
Time delay
Memristors
Hamilton energy
Fractional order

Most of the deterministic dynamical systems with nonlinear terms can be tamed in the intrinsic parameters or excited by using external stimulus for inducing chaotic states, and numerical solutions can be detected under reliable algorithm, as a result, Poincare section and Lyapunov exponent spectrum are calculated to predict the parameter regions for generating chaos. For experimental series of some variables, power spectrum analysis becomes available and dense orbits are confirmed in the phase space when chaos keeps survival. In experimental way, many nonlinear circuits are useful to reproduce the dynamical properties of the chaotic systems, some of the intrinsic parameters of electric components can be adjusted to change the energy exchange, output voltage from capacitor and channel current across each branch circuit. For most of the isolated nonlinear circuits, the standard electric components are ideal and linear relation for the input and output variables, while nonlinear components can be rebuilt by using equivalent branch circuits.

It is claimed that many chaotic and hyperchaotic systems can be used for secure communication and image encryption. On the other hand, some nonlinear circuits can be modified and improved as neural circuits, which similar firing patterns such as quiescent, spiking, bursting and chaotic modes can be reproduced as those series from biological neurons. An isolated nonlinear circuit has finite power release and it just describes the local kinetics of multi-agent and networks, therefore, the energy pumping along the coupling channel becomes a challenge by regulating the physical properties via external physical field. That is, it is important to clarify some of the physical principles and mechanism (Ma *et al.* 2019) before imposing any theoretical schemes for synchronization and control of chaos.

Existence of Solutions means controllability in the dynamical systems. In fact, before starting any control scheme, it is critical to confirm that reliable solutions can be obtained in theoretical or numerical way. For example, the numerical solution becomes divergent and overflow when the code for the dynamical system is run. For most of the chaotic system, infinite periodic orbits are combined and connected in enough transient period no matter whether equilibrium points exist or not.

Manuscript received: 22 June 2021,
Accepted: 23 June 2021.

[1] hyperchaos@lut.edu.cn (**Corresponding author**)

Intermittent and discontinuous control benefit from intrinsic self-adaption of the chaotic systems. For synchronization control of chaotic systems, the orbits become self-leading to reach the target orbits within certain transient period and thus external control and energy consumption become non-necessary. For chaotic systems, any external control from additive branch circuit will cost certain energy when the controller is activated. For synchronization stabilization, continuous coupling will consume energy in the coupling channel when resistor is used to connect the chaotic circuits because of cost in Joule heat in the coupling resistor. Therefore, discontinuous or intermittent coupling decreases certain energy costs in the coupling channels and controllers, and period for switch on-off for the controllers becomes worthy of investigation.

Intrinsic response time delay and propagation time delay depend on the local property and coupling channels. Some electric components can be activated only when the driving voltage or channel current are beyond the threshold, for example photocurrent can be generate in the phototube only when the frequency in the illumination is beyond the threshold even the illumination intensity is much large for the phototube. For an engine or motor, it needs certain transient period to reach a high speed and rotation rate. For some interneurons, autapse develops a close loop to connect the synapse and the body or muscle, and intrinsic time delay is considered and estimated by using the autaptic current.

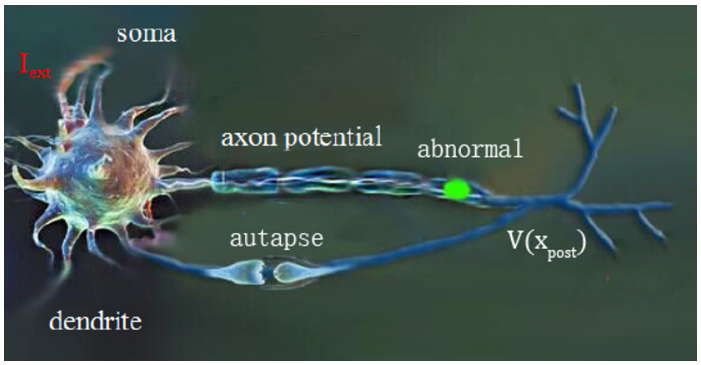

Figure 1 Schematic diagram for autapse to neuron

In generic way, time delay τ and feedback gain k are involved in the oscillator model to describe the response time delay as follows,

$$\frac{dx}{dt} = f(x,\mu) \pm kx(t-\tau) \tag{1}$$

The autaptic current or driving can be inhibitory or excitatory, and the firing modes of the nonlinear oscillator can be controlled effectively. For collective behaviors in spatiotemporal systems, distributed time delay can be introduced to estimate the effect of different links and coupling channels, it is obtained by,

$$\frac{dx_i}{dt} = f(x,\mu) + D\sum_{j=1,i\neq j}^{N} \varepsilon_{ij} x(t-\tau_j) \tag{2}$$

Where the connection matrix $\varepsilon_{ij} = 1$ indicates complete connection between the node i and node j, otherwise, it is set as 0, the gain D measure the connection intensity between two nodes, the time delay τ_j estimates the propagation period along the connection channel or link.

Except the electromagnetic field, signal propagation along the coupling channels and links in the network often require finite period, and thus time delay becomes important. In a non-uniform network, distributed time delay should be applied for different links and coupling channels (Wang and Ma 2018).

Controllability and standard criterion for controllers are useful in practice. From mathematical viewpoint, a variety of controllers and control schemes can be applied for all the dynamical systems and networks. In fact, the controller can be in simple form, lower energy consumption, finite and shorter transient period before reaching target orbits. In particular, fewer controllers are appreciated, for example, local pinning control is more effective than global control because control all the nodes becomes much difficult.

Dimensional homogeneity and scale transformation are critical for dynamical analysis and control. For some realistic systems, dynamical equations can be obtained to estimate the correlation between different physical variables. For nonlinear circuit, Kirchhoff's law is often used to obtain the circuit equations composed of physical variables (voltage, current, magnetic flux, charges) with different physical units. Therefore, standard scale transformation (Wang *et al.* 2019) should be applied for the physical parameters, variables, field energy, and thus dimensionless dynamical system and Hamilton energy can be obtained for finding numerical solutions via reliable algorithm. For example, the sampled time units from nonlinear oscillator or dimensionless dynamical systems should be discerned by using time units than seconds or milliseconds. For example, the common known physical variables (voltage V, current i, magnetic flux φ, charge q, time t) can be mapped into dimensionless variables (Wang *et al.* 2019)

as follows,

$$x = \frac{V}{V_0};\ y = \frac{iR}{V_0}[or, y = \frac{i}{I_0}];$$
$$w = \frac{\varphi}{LI_0} = \frac{\varphi R}{LV_0}, z = \frac{q}{CV_0};\ \tau = \frac{t}{\sqrt{LC}} = \frac{t}{RC} \quad (3)$$

Where L, C, R represents the inductance, capacitance, resistance of electric components of the nonlinear circuit, and V_0, I_0 denote the scale value, for example, V_0, I_0 can be selected from the amplitudes from external realistic signal or intrinsic value of nonlinear electric components.

Hamilton energy function meets the most suitable Lyapunov function. For any dynamical systems, continuous energy pumping and exchange are critical to keep and change the dynamics and firing modes. The Helmholtz theorem provides helpful guidance to estimate the sole Hamilton energy function and then guides how the dynamical system can be controlled in reliable scheme. Lyapunon function scheme seems to confirm the controllability of any chaotic systems and networks, however, the most suitable Lyapunov function (Zhou *et al.* 2021) must be the Hamilton energy function and any arbitrary setting for gains in the Lyapunov function and the controllers just regulate a damaged system than the original dynamical system. For generic dynamical system, the Hamilton energy function H can be obtained from the following criterion,

$$\frac{dX}{dt} = F_c(X) + F_d(X);\ \nabla H^T F_c(X) = 0;$$
$$\frac{dH}{dt} = \nabla H^T F_d(X) \quad (4)$$

Where the vector X describes the variable of the system, $F_c(X)$ represents the conservative field containing the full rotation and $F_d(X)$ is the dissipative field containing the divergence. Indeed, the Hamilton energy function is composed of all system variables and some intrinsic parameters, and effective control of the energy flow will control the stability and firing modes completely (Ma *et al.* 2017).

Memristive and boundary effect, fractional order calculation are relative to the intrinsic property of the dynamical systems. The nonlinear circuits involved with any memristor can be mapped into memristive system and becomes dependent on the initial value for memristive variable such as magnetic flux, and thus the dynamics is switched between different modes when any slight changes occur for initial values. For spatiotemporal systems with finite size, no-flux boundary condition is applied while periodic boundary condition is more suitable for networks with infinite size or system with globular, ring types. Local memory, boundary value and non-uniform diffusive effect require fractional calculation and approach (Zhou *et al.* 2020). Indeed, more electric components such as phototube, Josephson junction, piezoelectric ceramic can be incorporated into the nonlinear circuits for enhancing more specific biophysical functions in neural circuits.

LITERATURE CITED

Ma, J., F. Wu, W. Jin, P. Zhou, and T. Hayat, 2017 Calculation of hamilton energy and control of dynamical systems with different types of attractors. Chaos: An Interdisciplinary Journal of Nonlinear Science **27**: 053108.

Ma, J., Z.-q. Yang, L.-j. Yang, and J. Tang, 2019 A physical view of computational neurodynamics. Journal of Zhejiang University-Science A **20**: 639–659.

Wang, C. and J. Ma, 2018 A review and guidance for pattern selection in spatiotemporal system. International Journal of Modern Physics B **32**: 1830003.

Wang, C., J. Tang, and J. Ma, 2019 Minireview on signal exchange between nonlinear circuits and neurons via field coupling. The European Physical Journal Special Topics **228**: 1907–1924.

Zhou, P., X. Hu, Z. Zhu, and J. Ma, 2021 What is the most suitable lyapunov function? Chaos, Solitons & Fractals **150**: 111154.

Zhou, P., J. Ma, and J. Tang, 2020 Clarify the physical process for fractional dynamical systems. Nonlinear Dynamics **100**: 2353–2364.

How to cite this article: Ma, J. *Chaos Theory and Applications: The Physical Evidence, Mechanism are Important in Chaotic Systems*. Chaos Theory and Applications, 4(1), 1-3, 2022.

CHAOS
Theory and Applications
in Applied Sciences and Engineering

e-ISSN: 2687-4539
RESEARCH ARTICLE
Vol.4 / No.1 / 2022 / pp.4-9
https://doi.org/10.51537/chaos.976593

Circuit Implementation and PRNG Applications of Time Delayed Lorenz System

Burak Arıcıoğlu *,[1] **and Sezgin Kaçar** *
*Sakarya University of Applied Sciences, Department of Electrical and Electronics Engineering, 54050, Sakarya, Turkey.

ABSTRACT In this study, time delayed form of Lorenz system is introduced, and exemplary applications of the time delayed Lorenz system are performed. Firstly, the time delayed Lorenz system is numerically solved by considering the Lorenz system as a system of time delayed differential equations. Then, time series and phase portraits of the state variables of the time delayed system are obtained. After then, circuit implementation of the time delayed system is carried out with discrete analog components. Finally, a random number generator application is carried out by selecting different number of bits obtained from the state variables of the time delayed system. The results of all the applications are sufficiently good that the time delayed system can be used in engineering applications.

KEYWORDS
Time delayed chaotic systems
Lorenz System
Time delayed differential equations
Circuit implementation
Random number generator

INTRODUCTION

There are many new chaotic systems proposed in the literature after chaos phenomenon and chaotic systems are emerged as a field of study. However, the Lorenz system, one of the most popular chaotic system, has been still studied (Lorenz 1963). Although the Lorenz system retains its popularity, the use of the Lorenz chaotic system in engineering applications like circuit implementation is not very easy. Moreover, the introduction of different time delay for each state variable will make harder to solve the system numerically and to implement as a circuit. In this study, different amount of time delays for each state variable is considered.

Time delayed differential equations are very important for chaotic systems and their engineering applications (Hale and Lunel 2013). Hence, there are many different studies of time delayed chaotic systems in the literature. For example, stability analyses of time delayed differential equations were discussed (Deng *et al.* 2006). There are also studies of synchronization of such time delayed systems (Cheng *et al.* 2008). In another study, a time delayed chaotic system was obtained from Logistic-map system (Acho 2017). In (Qin-Qin 2015), a parameter defining problem was considered for a general time delayed chaotic system and its analyses were performed. In (Pham *et al.* 2016), a novel time delayed chaotic system with hidden attractors was proposed. A parameter defining problem was investigated in (Tang *et al.* 2009) to determine unknown parameters of a time delayed chaotic system. There are also studies in which applications of time delayed systems were realized for sliding-mod (Liu and Yang 2015) and active control (Tang 2014).

If the realized engineering applications of the chaotic systems are investigated, the most of these applications are focused on circuit implementation (Pehlivan *et al.* 2019; Adiyaman *et al.* 2020; Kacar *et al.* 2018; Jahanshahi *et al.* 2018; Liu *et al.* 2020) and random number generator (RNG) (Akgul *et al.* 2019; Moysis *et al.* 2020; Alcin *et al.* 2021; Agarwal 2021; Kaçar 2016; Vaidyanathan *et al.* 2018). Accordingly, it will be sufficient to realize these two applications of a proposed chaotic system to show the usability of the chaotic system in engineering applications. Hence, a circuit implementation and RNG applications of the proposed Time Delayed Lorenz System (TDLS) are realized in this study. The contribution of this study to the literature can be explained as follows. In this study, the different time delays are used for each state variable simultaneously and chaotic behaviour is observed after solving the time delayed differential equations numerically. Then, to the best of the authors' knowledge, a time delayed chaotic system is modelled using discrete circuit components for the first time in the literature. Finally, four different pseudo random number generator (PRNG) applications are realized by selecting different bits of the state variables.

Manuscript received: 30 July 2021,
Revised: 20 September 2021,
Accepted: 29 September 2021.

[1]baricioglu@subu.edu.tr (**Corresponding Author**)

The organization of the article is as follows. In the second section, the proposed TDLS is introduced. In the third section, circuit implementation of the TDLS is given. In the fourth section, the PRNG applications of the TDLS are presented. Finally, conclusion is given in the fifth section.

TIME DELAYED LORENZ SYSTEM

In this section, the time delayed form of Lorenz chaotic system is presented. The time delayed Lorenz system (TDLS) is given in Equation 1. The most important aspect of the proposed system is that each state variable has a different amount of time delay.

$$\begin{aligned} \dot{x} &= a(y(t-\tau_y) - x(t-\tau_x)) \\ \dot{y} &= x(t-\tau_x)(b - z(t-\tau_z)) - y(t-\tau_y) \\ \dot{z} &= x(t-\tau_x)y(t-\tau_y) - cz(t-\tau_z) \end{aligned} \tag{1}$$

Equation 1, the system parameters are $a = 10$, $b = 28$, and $c = 8/3$, the initial conditions are $x(0) = 10$, $y(0) = -10$, and $y(0) = 15$, the time delays are $\tau_x = 0.0014$, $\tau_y = 0.01$, and $\tau_z = 0.05$. The obtained time series and phase of the TDLS when numerically solved for these given values are given in Figure 1 and 2, respectively. The used algorithm for numerical solution of Equation 1 tracks discontinuities and integrates with the explicit Runge-Kutta (2,3) pair and interpolant (Shampine and Thompson 2001; Jacek Kierzenka and Thompson 2021). Also, in the used numerical solution, the step intervals are selected longer than the (Shampine and Thompson 2001; Jacek Kierzenka and Thompson 2021).

When Figure 1 is examined, it can be said that the obtained time series of the TDLS are varied randomly and nonperiodically. When Figure 2 is examined, it can be said that the orbits of the phase portraits in accordance with chaotic behaviour and the phase portraits of TDLS are very different from the original Lorenz system. Accordingly, the system exhibits chaotic behaviour for the given parameters, initial conditions, and time delay values and it is understood that the time delays introduce differences in the dynamical behaviour of the system.

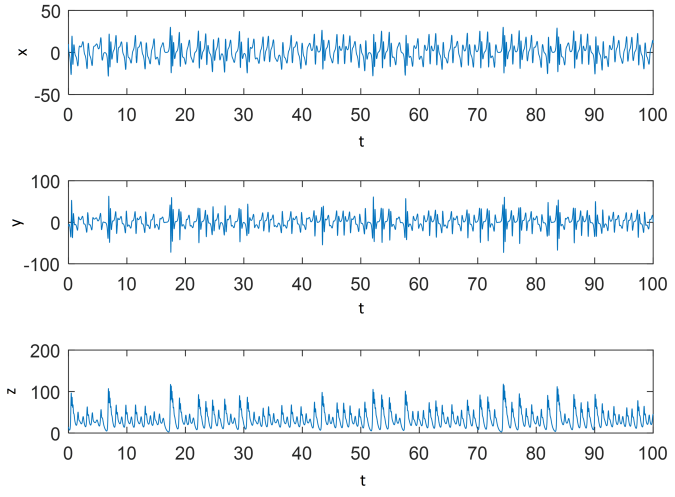

Figure 1 Time series of the state variables

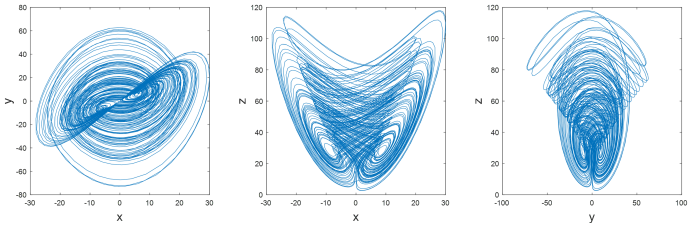

Figure 2 Phase portraits of the state variables

CIRCUIT IMPLEMENTATION

In this section, circuit implementation of the TDLS is given. In the literature, there are many studies in which the chaotic systems were realized with electronic circuits (Pehlivan *et al.* 2019; Adiyaman *et al.* 2020; Kacar *et al.* 2018; Jahanshahi *et al.* 2018; Liu *et al.* 2020). However, to the best of the authors' knowledge, there are no circuit implementation of time delayed chaotic systems in the literature. In this paper, electronic circuit implementation of the time delayed circuit is achieved.

The circuit for the time delay is given in Figure 3. Time delay is realized with a source follower and an LC circuit as shown in Figure 3. In the figure $x(t)$ is the state variable and $x(t-d)$ is the time delayed form of $x(t)$ by d seconds.

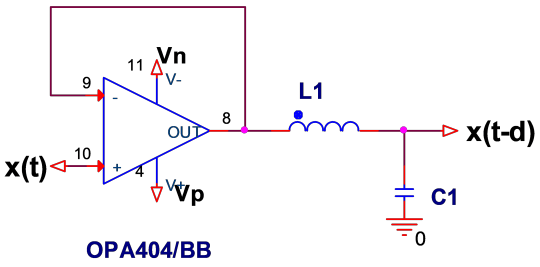

Figure 3 Time delay circuit

In the circuit, the time delay in seconds is

$$d = \sqrt{L_1 C_1} \tag{2}$$

and the time delay must be lesser than or equal to one over the bandwidth of the signal $x(t)$ since the LC circuit will suppress higher frequency terms greater than $\frac{1}{\sqrt{L_1 C_1}}$.

$$d \leq 1/B_{x(t)} \tag{3}$$

Here $B_{x(t)}$ is bandwidth of the signal in rad/s.

Before the circuit implementation of the TDLS, the state variables of the TDLS must be scaled as it is seen in Figure 1 that the amplitude of the state variables are quite high. The state variable x,y, and z are scaled down by the factor of 5,10, and 20, respectively. Since the state variables are scaled down, the initial values are also scaled down by the same factors. Hence, the initial conditions are $x(0) = 2$, $y(0) = -1$, and $y(0) = 0.75$ for the circuit implementation.

For the scaling process of the state variables, let $X = x/5$, $Y = y/10$, and $Z = z/20$. Then, the time derivatives are $\dot{X} = \dot{x}/5$, $\dot{Y} = \dot{y}/10$, and $\dot{Z} = \dot{z}/20$. By inserting these new state variables into Equation 1, the system becomes

$$\begin{aligned} 5\dot{X} &= a(10Y(t-\tau_y) - 5X(t-\tau_x)) \\ 10\dot{Y} &= 5X(t-\tau_x)(b - 20Z(t-\tau_z)) - 10Y(t-\tau_y) \\ 20\dot{Z} &= 5X(t-\tau_x)10Y(t-\tau_y) - c20Z(t-\tau_z) \end{aligned} \tag{4}$$

By rearranging Equation 4, the scaled TDLS becomes

$$\begin{aligned} \dot{X} &= a(2Y(t-\tau_y) - X(t-\tau_x)) \\ \dot{Y} &= 0.5X(t-\tau_x)(b - 2Z(t-\tau_z)) - Y(t-\tau_y) \\ \dot{Z} &= 0.125X(t-\tau_x)Y(t-\tau_y) - cZ(t-\tau_z) \end{aligned} \tag{5}$$

After scaling process of the state variables, the system is scaled up in the frequency domain by the factor of 2500 to increase bandwidth of the state variables and to decrease the run time of the circuit. Since the frequency spectrum of the state variables are scaled up by the factor of 2500, the time delays are scaled down by the same factor. The circuit realization of system in Equation 5 is realized for the system parameters values $a = 10$, $b = 28$, and $c = 8/3$, the initial conditions are $x(0) = 2$, $y(0) = -1$, and $y(0) = 0.75$, the time delays are $\tau_x = 0.4\mu s$, $\tau_y = 4\mu s$, and $\tau_z = 20\mu s$. The complete circuit realization of the system is given in Figure 4.

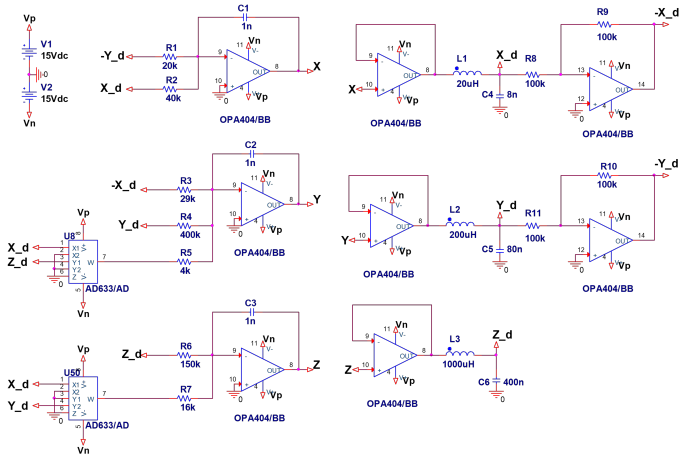

Figure 4 Circuit implementation of the time delayed Lorenz system for the system parameters values $a = 10$, $b = 28$, and $c = 8/3$, the initial conditions are $x(0) = 2$, $y(0) = -1$, and $y(0) = 0.75$, the time delays are $\tau_x = 0.4\mu s$, $\tau_y = 4\mu s$, and $\tau_z = 20\mu s$s

In the circuit, $R_1 = 20k\Omega, R_2 = 40k\Omega, R_3 = 29k\Omega, R_4 = 400k\Omega, R_5 = 4k\Omega, R_6 = 150k\Omega, R_7 = 16k\Omega, R_8 = R_9 = R_10 = R_11 = 100k\Omega, L_1 = 20\mu H, L_2 = 200\mu H, L_3 = 1000\mu H, C_1 = C_2 = C_3 = 1nF, C_4 = 8nF, C_5 = 80nF, C_6 = 400nF$.

The time series and phase portraits obtained from the simulation of the circuit in Figure 4 are given in Figure 5 and 6, respectively. The simulation is performed on ORCAD-PSpice platform.

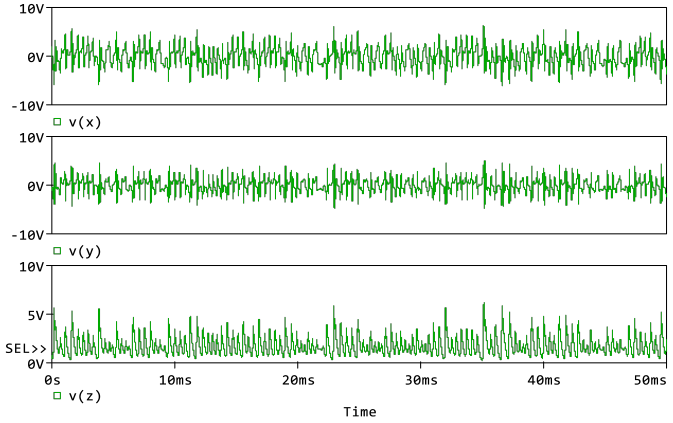

Figure 5 The time series of the delayed Lorenz system for the system parameters values $a = 10$, $b = 28$, and $c = 8/3$, the initial conditions are $x(0) = 2$, $y(0) = -1$, and $y(0) = 0.75$, the time delays are $\tau_x = 0.4\mu s$, $\tau_y = 4\mu s$, and $\tau_z = 20\mu s$s

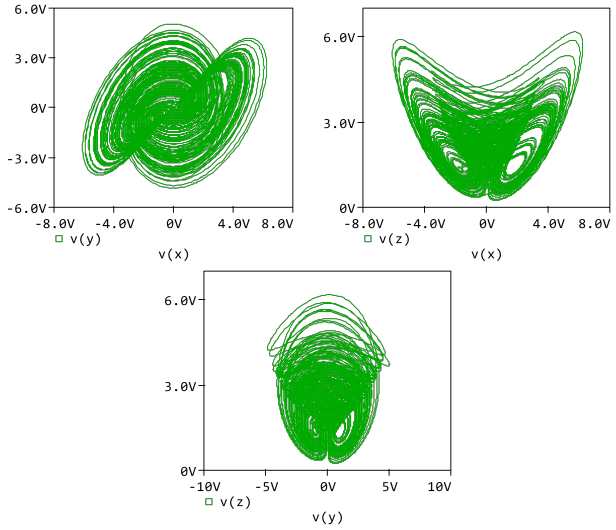

Figure 6 The phase portraits of the delayed Lorenz system for the system parameters values $a = 10$, $b = 28$, and $c = 8/3$, the initial conditions are $x(0) = 2$, $y(0) = -1$, and $y(0) = 0.75$, the time delays are $\tau_x = 0.4\mu s$, $\tau_y = 4\mu s$, and $\tau_z = 20\mu s$s

If the time series and phase portraits obtained from the spice simulation are compared with the time series and the phase portraits obtained from solving the TDLS numerically, it can be said that the circuit implementation of the TDLS is realized accurately.

PRNG APPLICATIONS

In this section, the realization of four different PRNG designs are given. The PRNGs are obtained by solving the TDLS given in Equation 1 numerically. In each designed PRNG, different bit series obtained from the state variables of the TDLS are used. The flowchart of the PRNG designs is given in Figure 7. As it is seen in Figure 7, the state variables are obtained by solving the system numerically, after setting the system parameters, initial conditions, and time delays values. The state variables obtained by numerical calculations are in floating point format are converted into 32 bits binary format. Then, the random number bit series are obtained by selecting certain appropriate number of least significant bits (LSBs). Here, each PRNG is designed from different state variables and with selecting different number of LSBs. In this study, four different PRNGs are designed with this approach. For the design of PRNG-1, a random bit series is generated by selecting the first LSB from each state variable (x,y,z). For the design of PRNG-2, PRNG-3, and PRNG-4, a random bit series is generated by selecting the first four LSBs from each state variables x,y, and z, respectively. For every PRNG, NIST-800-22 statistical tests (Bassham *et al.* 2010) are performed when the size of the generated bit series are reached 1000000 bits which is required by the NIST tests.

The NIST test results for all the generated PRNGs are given in Table 1. For a bit series to pass successfully from each NIST test, the P-value obtained in each test must be between 0.001 and 1 ($1 > P$-value> 0.001). Here P-value is the probability that a perfect RNG would have generated a sequence less random than the sequence that was tested. The P-value equals to 1 indicates that the sequence has perfect randomness, whereas P-value equals to 0 indicates that the sequence is completely non-random. Furthermore, when the P-value ≥ 0.001, the sequence is considered as random with a confidence of 99.9%(Bassham *et al.* 2010). All the NIST tests are performed on MATLAB environment.

If the results given in Table 1. are examined, it can be said that all the designed PRNGs pass all the NIST tests successfully. Accordingly, the proposed TDLS in Equation 1. has sufficient randomness that it can be used in data security applications.

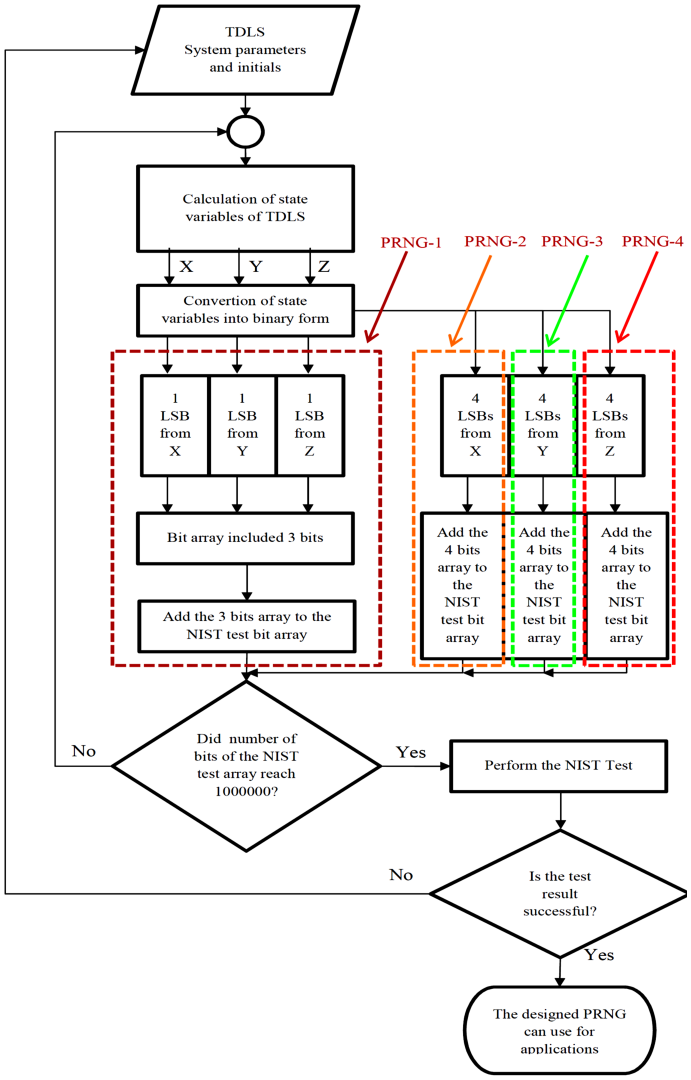

Figure 7 Flow diagram of the designed PRNGs

Table 1 NIST-800-22 test results of TDLS based PRNGs

Statistical Tests	PRNG -1	PRNG -2	PRNG -3	PRNG -4	Results
Frequency (Monobit) Test	0.227047262346928	0.939419098199487	0.452051058788007	0.74896833055336	Successful
Block-Frequency Test	0.420199408706029	0.12683780891	0.25828539912	0.18496247976	Successful
Cumulative-Sums Test	0.40154501916006	0.954262689644538	0.657794646611129	0.580632315828042	Successful
Runs Test	0.809910815227043	0.78561757692	0.45239095310	0.20333669229	Successful
Longest-Run Test	0.699072314072508	0.0593326790453765	0.071698278949431	0.581605726274521	Successful
Binary Matrix Rank Test	0.567418552088598	0.29417664507	0.36806531540	0.49848122628	Successful
Discrete Fourier Transform Test	0.0183542134338342	0.186356486587195	0.0310440276996156	0.659590791427404	Successful
Non-Overlapping Templates Test	0.0910820098687739	0.04581818944	0.00265744608	0.03188609869	Successful
Overlapping Templates Test	0.554865280067303	0.669055771344141	0.532900762615005	0.247345441097719	Successful
Maurer's Universal Statistical Test	0.679570957855461	0.80734843081	0.08350574528	0.92319905938	Successful
Approximate Entropy Test	0.639684970544748	0.106378560917655	0.650943909676795	0.117260917143001	Successful
Random-Excursions Test (x = -4)	0.703450581514076	0.37281099664	0.16507680806	0.28180552081	Successful
Random-Excursions Variant Test (x = -9)	0.900334238396749	0.301103909474349	0.274949621155743	0.26897769139	Successful
Serial Test-1	0.498246191923405	0.13739086594	0.24094191226	0.51233919246	Successful
Serial Test-2	0.703867335568016	0.172244663440799	0.324188206506017	0.539500232899045	Successful
Linear-Complexity Test	0.1748830988160720	0.98952603429	0.91278048851	0.46910323363	Successful

CONCLUSIONS

In this study, the time delay form of Lorenz system which is one of the most known and popular chaotic system is presented. The most important aspect of the proposed time delayed system in here is that the system still exhibits chaotic behaviour with different dynamical properties after introducing different time delay to each state variable. The first important result of this study is that observing chaotic behaviour of the time delayed system by solving numerically.

The most important contribution of this study to the literature is successful analog circuit realization of time delayed system with three different time delays. As it can be seen from the obtained time series and phase portraits in MATLAB and PSpice environments, the circuit realization of the time delayed chaotic system is successful. Another important application realized in this study is designing four different PRNGs by selecting different number of LSBs of the state variables. Moreover, all the designed PRNGs pass the NIST tests successfully. According to the NIST tests results all the generated bit series have considered to be random with a confidence of 99.9%. This shows that, the designed RNGs are suitable for multimedia security applications. As a result, the exhibition of the chaotic behaviour of the proposed system is proved with all the successfully realized applications and this shows that the proposed system can be used in engineering applications.

Conflicts of interest

The authors declare that there is no conflict of interest regarding the publication of this paper.

Availability of data and material

Not applicable.

LITERATURE CITED

Acho, L., 2017 A continuous-time delay chaotic system obtained from a chaotic logistic map. In *IASTED International Conference Modelling, Identification and Control."Modelling, Identification and Control (MIC 2017)", ACTA Press, Innsbruck*, p. 147.

Adiyaman, Y., S. Emiroglu, M. K. Ucar, and M. Yildiz, 2020 Dynamical analysis, electronic circuit design and control application of a different chaotic system. Chaos Theory and Applications **2**: 10–16.

Agarwal, S., 2021 Designing a pseudo-random bit generator using generalized cascade fractal function. Chaos Theory and Applications **3**: 11–19.

Akgul, A., C. Arslan, and B. Aricioglu, 2019 Design of an interface for random number generators based on integer and fractional order chaotic systems. Chaos Theory and Applications **1**: 1–18.

Alcin, M., T. Murat, P. ERDOĞMUŞ, and I. Koyuncu, 2021 Fpga-based dual core trng design using ring and runge-kutta-butcher based on chaotic oscillator. Chaos Theory and Applications **3**: 20–28.

Bassham, L., A. Rukhin, J. Soto, J. Nechvatal, M. Smid, *et al.*, 2010 A statistical test suite for random and pseudorandom number generators for cryptographic applications.

Cheng, C.-K., H.-H. Kuo, Y.-Y. Hou, C.-C. Hwang, and T.-L. Liao, 2008 Robust chaos synchronization of noise-perturbed chaotic systems with multiple time-delays. Physica A: Statistical Mechanics and its Applications **387**: 3093–3102.

Deng, W., Y. Wu, and C. Li, 2006 Stability analysis of differential equations with time-dependent delay. International Journal of Bifurcation and Chaos **16**: 465–472.

Hale, J. K. and S. M. V. Lunel, 2013 *Introduction to functional differential equations*, volume 99. Springer Science & Business Media.

Jacek Kierzenka, L. F., Shampine and S. Thompson, 2021 Tutorial on solving ddes with dde23.

Jahanshahi, H., K. Rajagopal, A. Akgul, N. N. Sari, H. Namazi, *et al.*, 2018 Complete analysis and engineering applications of a megastable nonlinear oscillator. International Journal of Non-Linear Mechanics **107**: 126–136.

Kaçar, S., 2016 Analog circuit and microcontroller based rng application of a new easy realizable 4d chaotic system. Optik **127**: 9551–9561.

Kacar, S., Z. Wei, A. Akgul, and B. Aricioglu, 2018 A novel 4d chaotic system based on two degrees of freedom nonlinear mechanical system. Zeitschrift für Naturforschung A **73**: 595–607.

Liu, H. and J. Yang, 2015 Sliding-mode synchronization control for uncertain fractional-order chaotic systems with time delay. Entropy **17**: 4202–4214.

Liu, J., K. Rajagopal, T. Lei, S. Kaçar, B. Arıcıoğlu, *et al.*, 2020 A novel hypogenetic chaotic jerk system: Modeling, circuit implementation, and its application. Mathematical Problems in Engineering **2020**.

Lorenz, E. N., 1963 Deterministic nonperiodic flow. Journal of atmospheric sciences **20**: 130–141.

Moysis, L., A. Tutueva, K. Christos, and D. Butusov, 2020 A chaos based pseudo-random bit generator using multiple digits comparison. Chaos Theory and Applications **2**: 58–68.

Pehlivan, İ., K. Ersin, L. Qiang, A. Basaran, and M. Kutlu, 2019 A multiscroll chaotic attractor and its electronic circuit implementation. Chaos Theory and Applications **1**: 29–37.

Pham, V.-T., S. Vaidyanathan, C. Volos, S. Jafari, N. Kuznetsov, *et al.*, 2016 A novel memristive time–delay chaotic system without equilibrium points. The European Physical Journal Special Topics **225**: 127–136.

Qin-Qin, C., 2015 A method of identifying parameters of a time-varying time-delay chaotic system. Acta Phys. Sinica **64**.

Shampine, L. F. and S. Thompson, 2001 Solving ddes in matlab. Applied Numerical Mathematics **37**: 441–458.

Tang, J., 2014 Synchronization of different fractional order time-delay chaotic systems using active control. Mathematical problems in Engineering **2014**.

Tang, Y., M. Cui, L. Li, H. Peng, and X. Guan, 2009 Parameter identification of time-delay chaotic system using chaotic ant swarm. Chaos, Solitons & Fractals **41**: 2097–2102.

Vaidyanathan, S., A. Akgul, S. Kaçar, and U. Çavuşoğlu, 2018 A new 4-d chaotic hyperjerk system, its synchronization, circuit design and applications in rng, image encryption and chaos-based steganography. The European Physical Journal Plus **133**: 1–18.

How to cite this article: Arıcıoğlu, B, and Kaçar, S. Circuit Implementation and PRNG Applications of Time Delayed Lorenz System. Chaos Theory and Applications, 4(1), 4-9, 2022.

CHAOS
Theory and Applications
in Applied Sciences and Engineering

e-ISSN: 2687-4539
RESEARCH ARTICLE
Vol.4 / No.1 / 2022 / pp.10-18
https://doi.org/10.51537/chaos.988758

Analysis of a Fractional-order Glucose-Insulin Biological System with Time Delay

B. Fernández-Carreón [*,1], **J.M. Munoz-Pacheco** [*,2], **E. Zambrano-Serrano** [β,3] **and O.G. Félix-Beltrán** [*,4]

*Faculty of Electronics Sciences, Benemérita Universidad Autonóma de Puebla, Puebla 72570, Mexico, βFacultad de Ingeniería Mecánica y Eléctrica, Universidad Autonóma de Nuevo León, N.L. 66455, Mexico.

ABSTRACT In the human glucose-insulin regulatory system, diverse metabolic issues can arise, including diabetes type I and type II, hyperinsulinemia, hypoglycemia, etc. Therefore, the analysis and characterization of such a biological system is a must. It is well known that mathematical models are an excellent option to study and predict natural phenomena to some extent. In this way, fractional-order theory provides generalizations for derivatives and integrals to arbitrary orders giving us a framework to add memory properties and an additional dimension to the mathematical models to approximate real-world phenomena with higher accuracy. In this work, we study the glucose and insulin governing mechanisms using a fractional-order version of a mathematical model. Applying the fractional-order Caputo derivative, we can investigate different concentration rates among insulin, glucose, and healthy beta cells. Additionally, the model incorporates two time-lags to represent the elapsed time of two processes, i.e., the delay in secrete insulin for a blood glucose increment and the lag to get a glucose reduction caused by raised insulin level. Analytical results of the equilibrium points and their corresponding stability are given. Numerical results, including phase portraits and bifurcation diagrams, reveal that the fractional-order increases the chaotic regions, leading to potential metabolic problems. Vice versa, the system seems to work correctly when the behavior evolves to periodic windows.

KEYWORDS
Chaos
Chaotic systems
Fractional-orders
Glucose-insulin
Time-delay

INTRODUCTION

One of the most known metabolic issues is called diabetes mellitus, in which the blood sugar control mechanism is disrupted. As a result, insulin, the main control factor is not released at proper times, or the body cells are unaware of its presence (ADA 2020; Shabestari *et al.* 2018; Lozano 2006; Emerging Risk Factors Collaboration *et al.* 2010). Various pathological processes are involved in the development of diabetes mellitus, although the vast majority of cases can be included in two categories. In the first one, type 1 diabetes mellitus, where the cause is an absolute deficiency in insulin secretion, often with evidence of autoimmune destruction of pancreatic cells. The second and most typical case is type 2 diabetes mellitus, which is provoked by two factors: insulin resistance (generally associated with obesity), and an inadequate compensatory secretory response (Lozano 2006; R.Rosalba *et al.* 2018; Shabestari *et al.* 2018; ADA 2020; Bertram and Pernarowski 1998). Other disorders include hyperglycemia which is characterized by high blood sugar levels. In contrast, hypoglycemia, also known as low blood glucose or sugar, occurs when the level of glucose in the blood falls below normal. Hypoglycemia can be a side effect of insulin and other types of diabetes medicines that help the body produce more insulin.

Those metabolic disorders are a world problem according to World Health Organization (WHO). For instance, Mexico is the sixth country with diabetic patients and the seventh in obesity (Statista 2019) in the world, therefore, the prevalence of diabetes due to a previous diagnosis has increased with a positive annual trend of 2.7%. In 2016, the prevalence of diabetes was 9.4% higher than in 2012 and at least in Mexico until 2016 there were just over 6.4 million people diagnosed with diabetes, about 60,000 more than in 2012. 48.1% of people with diabetes also have a previous diagnosis of hypertension. This prevalence increases to 50.4%, if they live in urban areas, and to 60%, if they are 60 years

Manuscript received: 1 September 2021,
Revised: 2 December 2021,
Accepted: 14 December 2021.

[1] bere.fc.03@gmail.com
[2] jesusm.pacheco@correo.buap.mx (**Corresponding Author**)
[3] erneszambrano@gmail.com
[4] olga.felix@correo.buap.mx

old or older. 50.4% of people with diabetes also have a previous medical diagnosis of high cholesterol, which increases to 52.6% if they live in rural areas, and 55.5% if they are between 40 and 59 years old. 40.4% of people with diabetes also have obesity; this prevalence increases by 49.7% if they are between 40 and 59 years old (R.Rosalba *et al.* 2018; Statista 2019).

As can be noted, people with obesity and hypertension, who are prone to suffer metabolic disorders related to the proper regulation of insulin and glucose, are rapidly increasing each year (Shabestari *et al.* 2018; ADA 2020). Thus, many scientific areas are facing this problem from diverse points of view. It is well known that mathematical models are a proved option to understand the nonlinear dynamics of biological systems to some extent. *The goal is to get a more realistic model that covers all potential scenarios of the metabolic disorders in the glucose-insulin system*. In this manner, we may predict with a better approximation the health issues associated with insulin levels and how it affects glucose metabolism. Additionally, novel medical treatments could be carried on for better control of diabetes mellitus. Some pioneering works on this subject are those described by (Bajaj *et al.* 1987; Sarika *et al.* 2008; Lenbury *et al.* 2001; Chuedoung *et al.* 2009).

As first attempt to improve the precision of the models, many published works have included time-delays (Al-Hussein *et al.* 2020; Shabestari *et al.* 2018; Sarika *et al.* 2008; Palumbo *et al.* 2007; Chuedoung *et al.* 2009; Rajagopal *et al.* 2018). For instance, (Shabestari *et al.* 2018) analyzed the impact of different time lags in the behavior of insulin level that needs some time instants for having presence in plasma; and the lapsed time for an adequate glucose stimulation. In Ref. (Al-Hussein *et al.* 2020), they added an extra term to represent the insulin decline due to glucose interchange. The impact of the partial time lags in an electrically coupled Izhikevich neuron model was examined by (Shafiei *et al.* (2019)). There, it was shown that if the probability of partial time delays increases may imply the emergence of complex dynamical behaviors. A graphical representation of the time-delay effect for equations given by $\dot{X} = F(t, X(t), X(t-\tau))$ is shown in Fig. 1.

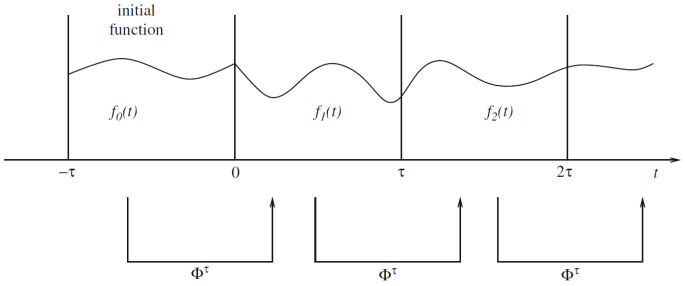

Figure 1 Implication of time-dependent delay in the solution of Delay Differential Equations (DDEs) (Lakshmanan and Senthilkumar 2010).

We observe that the solution is approximated mapping a initial function onto other subsequent functions in time intervals τ.

Moreover, the fractional calculus is recognized as one suitable option to increase the accuracy of the biological mathematical models because it permits the inclusion of arbitrary orders for the derivative operators in the differential equations of the underlying system (Ionescu *et al.* 2017; Rihan 2013; Teka *et al.* 2018; Assadi *et al.* 2017). Therefore, the biological system can have an extra degree of freedom, i.e., a real parameter given by the fractional order, to represent distinct behaviors. Additionally, the fractional-order provides a memory effect into the time evolution of the system, since its future solutions will depend on all past times and not only from recent events. A graphical representation of the memory could be given in a numerical fashion. Fig. 2 presents the fading memory in fractional-order systems as a function of binomial coefficients $c_j^{(q)}$. To compute the solution w_k, is necessary the whole vector of previous solutions, i.e., w_{k-1}, w_{k-2} , . . . , w_0. However, those previous solutions are weighted by the binomial coefficients. It means that the initial condition is always affected by a lower value than the former solutions. Because of that, we mention that past events contribute lesser than recent events to the current state.

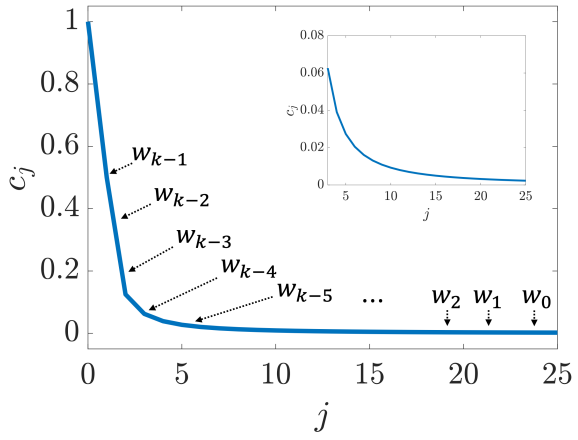

Figure 2 Numerical point of view of the fading memory of fractional-order systems according binomial coefficients $c_0^{(q)} = 1$, and $c_j^{(q)} = \left(1 - \frac{1+q}{j}\right) c_{j-1}^{(q)}$ with $q = 0.5$.

As a result, various works focusing on examining time lags for describing biological systems defined by fractional derivatives have been lately published. (Chinnathambi *et al.* 2021; Rihan *et al.* 2021; Singh and Pandey 2021; Yao and Tang 2021). Regarding fractional-order glucose-insulin models, (Zambrano-Serrano *et al.* 2018) analyzed the synchronized behavior between two β-cells-based fractional-order models under various cases of bursting signals. (Munoz-Pacheco *et al.* 2020) studied the estimation of metabolic disorders such as diabetes mellitus, hypoglycemia, and hyperinsulinemia using arbitrary order derivatives represented by a singular kernel.

In this framework, the fractional calculus-based models are essential to accurately capture the biological behaviors, including diabetes's related problems, and necessary to understanding this open topic. This work reports a time-delay chaotic glucose-insulin system with fractional differential equations. Our model incorporates Caputo derivatives to investigate the implications of the power-law memory kernel with the glucose-insulin interplay. Additionally, a pair of time delays define the lag between glucose detection and insulin secretion. Using the fractional calculus theory, we demonstrate the equilibrium points' stability and determine the fractional-order value where the system may present chaotic oscillations. We also derive numerical observations such as phase portraits and bifurcation diagrams to compare the integer and fractional-order models. The obtained results are consistent with the theoretical deductions and agree with previous findings in the area.

The paper outline is as follows. Section II introduces the proposed biological model along with its system parameters. Section III demonstrates the stability of the model for both equilibrium points and fractional-order. Section IV gives the results of the numerical simulations, and finally, Section V presents the conclusion.

FRACTIONAL-ORDER GLUCOSE-INSULIN METABOLIC SYSTEM WITH TIME LAGS

This section presents the proposed fractional-order glucose-insulin metabolic regulatory system with time delay inspired by the work reported in (Shabestari *et al.* 2018). They introduced an integer-order model with time lags to describe the primary control of insulin secretion, and glucose metabolism by the pancreatic beta cells in a feedback operation.

The model can represent the following phases. Typically, during meal consumption, the level of glucose increases considerably. Then, those levels are detected by the regulatory system, which promotes the generation and liberation of insulin by beta-cells. Next, the glucose concentration minimizes by the action of high levels of insulin, provoking that the human body burns and preserves nutrients. The second phase explains how insulin production reduces as a function of the average glucose level, for instance, when the organism does not receive any meal for a long time interval. As a result, the regulatory system changes from absorption to the post-absorption stage. One can see that this simple oscillatory process with negative feedback sustains a proper glucose level for the whole body, including organs and tissues. The reported integer-order model by (Shabestari *et al.* 2018) is:

$$\begin{aligned}
\frac{dx}{dt} &= r_1 y(t-\tau_g)z(t-\tau_g) - r_2 x + c_1 z(t-\tau_g),\\
\frac{dy}{dt} &= \frac{R_3 N}{z} - R_4 x(t-\tau_i) + C_2,\\
\frac{dz}{dt} &= R_5(y-\hat{y})(T-z) + R_6 z(T-z) - R_7 z,
\end{aligned} \tag{1}$$

where $x(t)$, $y(t)$, $z(t)$, and $\hat{y}$ represent the insulin level, glucose level, beta-cells number and the glucose metabolism considering its basal state, respectively. According to clinical experiments by (Palumbo *et al.* 2007), the delay for the insulin production, as a result of blood glucose level rising, could be set $\tau_g = 0.56$. The delay between augmented insulin level and glucose reduction is $\tau_i = 0.05$ as suggested (Prager *et al.* 1986).

Table 1 System parameters for fractional-order glucose-insulin metabolic regulatory system.

Parameter	Value	Parameter	Value	Parameter	Value
r_1	0.472	r_2	0.25	R_3	0.82
R_4	0.6	R_5	0.3	R_6	0.3
R_7	0.2	$\hat{y}$	1.42	N	1.27
T	1.5	c_1	0.1	C_2	0.8

Indeed, certain metabolic disorders, such as hyperglycemia (extremely high glucose) and hypoglycemia (low glucose), are associated with inaccurate time delay values. $r_1 y(t-\tau_g)z(t-\tau_g)$ explains the increments both insulin and glucose as a function of the time delay τ_g; $r_2 x$ means the speed of insulin reduction unassociated with glucose; $c_1 z(t-\tau_g)$ s the insulin raising rate as a function of the beta-cells, which does not depend on any other element. Additionally, the average number of beta-cells is represented as N; while the glucose decreasing cadence when the insulin is secreted with τ_i is given by $R_4 x(t-\tau_i)$. T is the entire population of beta-cells; $R_5(y-\hat{y})(T-z)$ denotes the increment of dividing beta-cells against the non-dividing ones that are induced by the interaction between glucose and the starving stage. $R_6 z(T-z)$ means raise of z because of synergy relating to dividing and nondividing beta-cells, whereas $R_7 z$ is its diminution. (Prager *et al.* 1986; Chuedoung *et al.* 2009; Shabestari *et al.* 2018).

The behavior of the *integer-order* glucose-insulin system (1), with delays $\tau_g = 0.56$ $\tau_i = 0.05$, initial conditions $[x(0), y(0), z(0)] = [6.03, 1.79, 0.82]$, and parameters in Table 1 is shown in Fig. 3. We observe that the system behaves periodically, presumably having a healthy behavior, i.e., the interaction between glucose and insulin is correct.

Fractional-order model derivation

Motivated by the memory characteristics of the arbitrary-order derivatives, we derive herein a fractional-order version of the glucose-insulin system (1). By using the Caputo derivative, we obtain

$$\begin{aligned}
{}_{t_0}^{C}D_t^q x(t) &= r_1 y(t-\tau_g)z(t-\tau_g) - r_2 x + c_1 z(t-\tau_g),\\
{}_{t_0}^{C}D_t^q y(t) &= \frac{R_3 N}{z} - R_4 x(t-\tau_i) + C_2,\\
{}_{t_0}^{C}D_t^q z(t) &= R_5(y-\hat{y})(T-z) + R_6 z(T-z) - R_7 z.
\end{aligned} \tag{2}$$

where q represents the fractional-order and ${}_{t_0}^{C}D_t^q(\cdot)$ is defined by

Definition 1 *Consider $f : [0, +\infty] \to \mathbb{R}$ as a function with order $n-1 \leq q < n$, thus, it can be denoted by the fractional-order derivative in the Caputo sense as*

$${}_{t_0}^{C}D_t^q g(t) = \Delta \int_{t_0}^{t} \frac{g^{(n)}(\tau)}{(t-\tau)^{q+1-n}} d\tau, \quad t > 0, \tag{3}$$

where Δ is the Gamma function of $\frac{1}{\Gamma(n-q)}$ and $n-1 \leq q < n$.

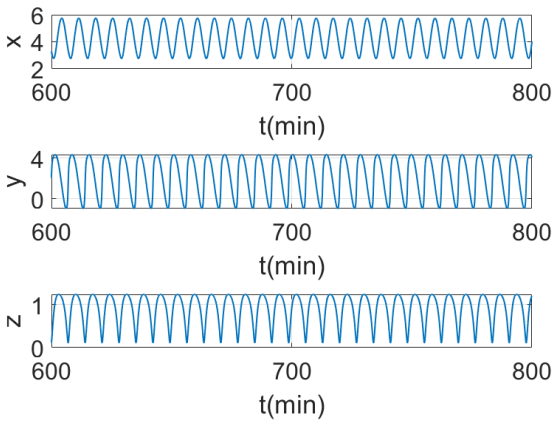

(a)

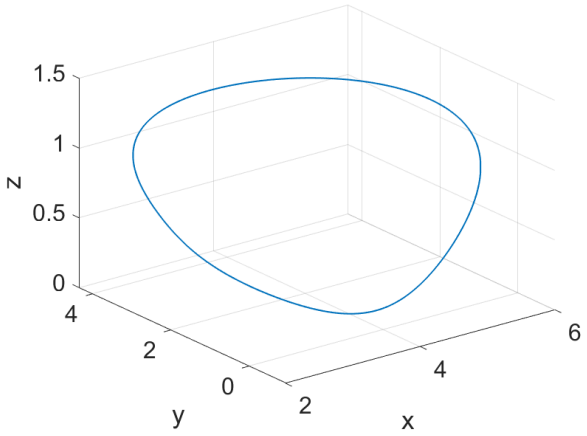

(b)

Figure 3 (a) Time evolution and (b) phase portrait of the integer-order glucose-insulin system (1) under $\tau_i = 0.05$ and $\tau_g = 0.56$. $[x, y, z]$ represent the glucose, insulin, and beta-cells, respectively.

According to (Diethelm 2010), the Caputo and Riemann-Liouville (RL) derivatives are equivalent for initial value problems (IVP) with similar initial conditions. Moreover, the Caputo derivative interpretation (3) generalizes formally the integer-order derivative using Laplace transformation. Finally, it is well known that Caputo derivative can be the left inverse of the fractional integral given by RL.

Theorem 1 *Diethelm (2010) For $n \geq 0$ and g being a continuous function, then*

$$ {}_{t_0}^{C}D_t^{qRL}J^q g(x) = g(x), \tag{4} $$

but not its right inverse:

Theorem 2 *Diethelm (2010) Being $n \geq 0$, $m = \lceil n \rceil$ with $g \in \Theta^m[a_1, a_2]$. Thus*

$$ {}^{RL}J_{t_0}^{qC}D_t^q g(x) = g(x) - \sum_{k=0}^{m-1} \frac{D^k g(a_1)}{k!}(x-a_1)^k, \tag{5} $$

where ${}^{RL}J^q$ means the RL integral. We choose the Caputo derivative because the IVP in the fractional-order domain can be stated analogously to the integer-order case, which gives us a physical interpretation of the fractional derivative (Petráš 2011). Additionally, we can represent the memory characteristics of the power-law kernel in the dynamical evolution of biological systems (Munoz-Pacheco *et al.* 2020).

STABILITY ANALYSIS

Equilibrium points

As the first step, we should analyze the stability of the equilibrium points under the related theory of delay-time systems (Lakshmanan and Senthilkumar 2010; Lazarević 2011; Naifar *et al.* 2019). By selecting $f(x, y, z) = 0$ and system parameters of Table 1 for the fractional-order glucose-insulin system (2), we obtain the following equilibrium points, $E_1 = (-1.97, 1.77, -0.53)$ and $E_2 = (3.19, 1.59, 0.94)$. By computing the Jacobian matrix, we can study the local asymptotic stability at each one of the equilibrium points. Thus, we have

$$ J_E = \begin{pmatrix} J_{11} & J_{12} & J_{13} \\ J_{21} & 0 & J_{23} \\ 0 & J_{32} & J_{33} \end{pmatrix}. \tag{6} $$

$$ |J_E - \lambda I| = 0, \tag{7} $$

where $J_E = J_0 + e^{-\lambda\tau}J_{\tau_g,\tau_i}$. J_0 is the Jacobian matrix of system (2) without delay ($\tau = 0$), whereas J_{τ_g,τ_i} is the Jacobian matrix under the delays τ_g and τ_i, respectively. I indicates an identity matrix whereas λ the corresponding eigenvalues.

Using the parameters in Table 1, we obtain

$$ J_{11} = -\tfrac{1}{4}, \quad J_{12} = \tfrac{59z^*e^{-\lambda\tau_g}}{125}, \quad J_{13} = e^{-\lambda\tau_g}\left(\tfrac{59y^*}{125} + \tfrac{1}{10}\right), $$
$$ J_{21} = -\tfrac{3e^{-\lambda\tau_i}}{5}, \quad J_{23} = -\tfrac{5207}{5000z^{*2}}, $$
$$ J_{32} = \tfrac{9}{20} - \tfrac{3z^*}{10}, \quad J_{33} = \tfrac{169}{250} - \tfrac{3z^*}{5} - \tfrac{3y^*}{10}. $$

Evaluating $E^* = (x^*, y^*, z^*)$ in Jacobian matrix (6), the pseudo-characteristic equations for E_1 and E_2 are, respectively.

$$ \begin{aligned} \lambda^3 - 0.2096\lambda^2 - 0.4099e^{-\lambda\tau} + 2.176\lambda \\ +0.1488\lambda e^{-\lambda\tau} + 0.5728 \quad = 0. \end{aligned} \tag{8} $$

$$ \begin{aligned} \lambda^3 + 0.6131\lambda^2 - 0.1826e^{-\lambda\tau} + 0.2917\lambda \\ -0.2652\lambda e^{-\lambda\tau} + 0.05022 \quad = 0. \end{aligned} \tag{9} $$

with $\tau = \tau_g + \tau_i$. We observe that both equilibrium points are saddle points as shown in Table 2. E_1 is index-2 since has one real negative eigenvalue and a complex conjugate pair with a positive real part. On the other hand, E_2 is index-1 because has three real eigenvalues with two negative and one positive (Sprott 2015). It is worthy to note that the stability of equilibrium points depends on the time lags.

Table 2 Stability type of the equilibrium points for the proposed fractional-order time-delay glucose-insulin system with $\tau_g = 0.56$ and $\tau_i = 2.55$.

Equilibrium points	Eigenvalues	Stability
$E_1 = (-1.97, 1.77, -0.53)$	$\lambda_1 = -0.044,$ $\lambda_{2,3} = 0.230 \pm 1.449i,$	index-2 saddle point
$E_2 = (3.19, 1.59, 0.94)$	$\lambda_1 = 1.697,$ $\lambda_2 = -0.782$ $\lambda_3 = -1.528$	index-1 saddle point

Now, the next step is focusing on the positive equilibrium point E_2 to examine its repercussions in the system dynamics since it is associated profoundly with the discrete-time lags. For time delay τ, we may denote the characteristic equation as

$$\eta_1(\lambda) + \eta_2(\lambda)e^{-\lambda\tau} = 0, \tag{10}$$

that is the linearized case, i.e. evaluated at $E^* = (x^*, y^*, z^*)$, with

$$\begin{aligned} \eta_1(\lambda) &= \lambda^3 + \eta_{1,1}\lambda^2 + \eta_{1,2}\lambda + \eta_{1,3}, \\ \eta_2(\lambda) &= \eta_{2,1}\lambda^2 + \eta_{2,2}\lambda + \eta_{2,3}, \end{aligned} \tag{11}$$

Without any loss of generality, the characteristic eq. (10) when the positive equilibrium point E_2 is not affected by the time delays ($\tau_g = 0$ and $\tau_i = 0$), becomes

$$\lambda^3 + (\eta_{1,1} + \eta_{2,1})\lambda^2 + (\eta_{1,2} + \eta_{2,2})\lambda + (\eta_{1,3} + \eta_{2,3}) = 0, \tag{12}$$

Using Routh-Hurwitz criterion, the roots of (6) have non-positive real parts, that is, E^* is asymptotically stable for $P_1 = \eta_{1,1} + \eta_{2,1} > 0$, $P_2 = \eta_{1,3} + \eta_{2,3} > 0$, and $P_3 = (\eta_{1,1} + \eta_{2,1})(\eta_{1,2} + \eta_{2,2}) - (\eta_{1,3} + \eta_{2,3}) > 0$. Due to $P1 = 0.6131$, $P_2 = -0.132$, and $P_3 = 0.148$, E_2 is unstable when $\tau = 0$.

Minimum fractional-order

As well known, the stability region for fractional-order systems extends beyond the left-half plane in the complex plane to the positive one also (Petráš 2011), as shown in Fig. 4.

Let us consider the standard form of a nonlinear dynamical system in the fractional-order domain as

$${}_{t_0}^{C}D_t^q x = Ax + Bu, \tag{13}$$

where $x \in \mathbb{R}^n$, $u \in \mathbb{R}^m$,, $A \in \mathbb{R}^{n\times n}$, and $B \in \mathbb{R}^{n\times m}$; and ${}_{t_0}^{C}D_t^q x = [{}_{t_0}^{C}D_t^q x_1, \ldots, {}_{t_0}^{C}D_t^q x_n]^T$ denotes Caputo derivative while q is the fractional-order. For the autonomous scenario, system (13) can be expressed by ${}_{t_0}^{C}D_t^q x = Ax$, being $x(0) = x_0 and\ 0 < q < 1$. In this manner, its stability conditions are analyzed by the next postulates (Petráš 2011; Munoz-Pacheco *et al.* 2020):

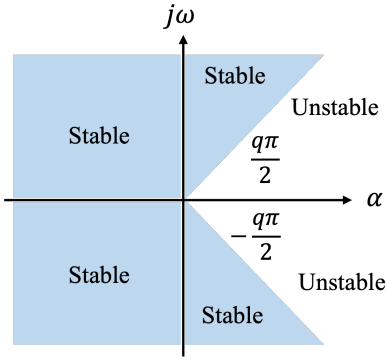

Figure 4 Stability region of fractional order linear time invariant systems with order $0 < q < 1$.

- A system in the form of ${}_{t_0}^{C}D_t^q x = Ax$ is considered *asymptotically stable* as long as the whole set of eigenvalues, λ, satisfies $|\arg(\lambda)| > \frac{q\pi}{2}$, which indicates the evolution $x(t)$ converges to 0 as t^{-q}.
- A system in the form of ${}_{t_0}^{C}D_t^q x = Ax$ is considered *stable* as long as the whole set of eigenvalues, λ, satisfies $|\arg(\lambda)| > \frac{q\pi}{2}$ whereas the critical eigenvalues fulfills with $|\arg(\lambda)| = \frac{q\pi}{2}$ having a geometric multiplicity of one.

Therefore, for a certain fractional-order q, system ${}_{t_0}^{C}D_t^q x = Ax + Bu$, is unstable when at least one of their eigenvalues at equilibrium point E^*, yields (Petráš 2011)

$$q > \frac{2}{\pi}\arctan\frac{|Im(\lambda)|}{|Re(\lambda)|}. \tag{14}$$

For the fractional-order delay-time glucose-insulin system (2), the small value of the fractional-order where the system becomes unstable is $q \geq 0.9$ under the eigenvalues from equilibrium point E_2. This result suggest that chaos behavior, which may be related to an metabolic disorder of the glucose-insulin biological system, can be observed at interval $0.9 \leq q \leq 1$.

Lemma 1 *An index-2 saddle point is an equilibrium point that preserves the next conditions for their eigenvalues. It must have a negative real eigenvalue $\lambda_1 < 0$, and a pair of complex eigenvalues that satisfies $|arg(\lambda_2)| = |arg(\lambda_3)| < q\pi/2$. Viceversa, when $\lambda_1 > 0$ and $|arg(\lambda_2)| = |arg(\lambda_3)| > q\pi/2$, we have an index-1 saddle point.*

From Lemma 1, we confirm that equilibrium points E_1 and E_2 are index-2 and index-1 saddle points respectively. In next section, we explore the effect of the fractional-order in the dynamical behavior of time-delay glucose-insulin system (2).

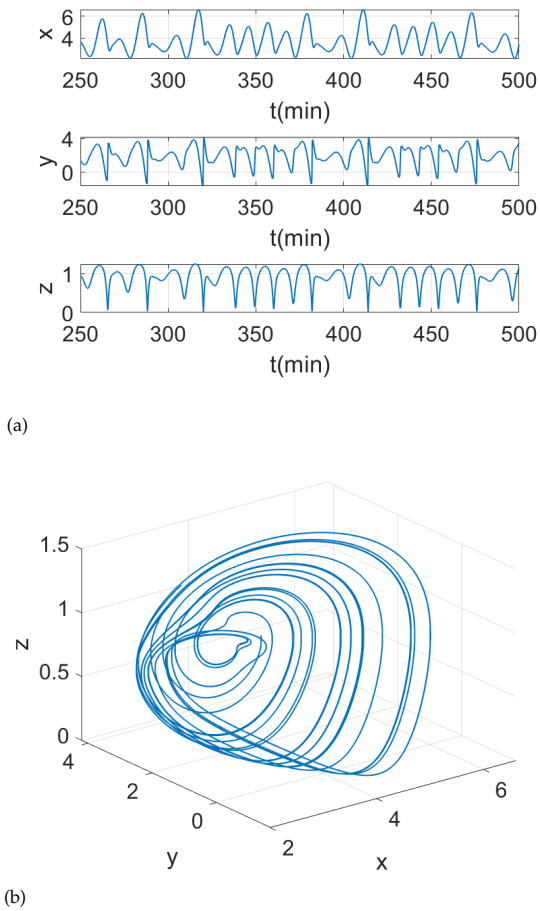

Figure 5 (a) Time evolution and (b) phase portrait of the fractional order time-delay glucose-insulin system (2) with $q = 0.95$, $\tau_i = 2.55$, and $\tau_g = 0.56$. $[x, y, z]$ represent the glucose, insulin, and beta-cells, respectively. 50% of iterations were discard to avoid transient effects.

NUMERICAL RESULTS AND DISCUSSION

To compute the solutions of system (2), we apply the numerical algorithm proposed by (Petráš 2011) which claims that the general numerical solution of the fractional differential equation

$$ {}_aD_t^q w(t) = f(w(t), t), $$

can be expressed as

$$ w(t_k) = f\left(w(t_{k-1}), t_{k-1}\right) h^q - \sum_{j=1}^{k} c_j^{(q)} w(t_{k-j}), \qquad (15) $$

with $k = 1, 2, \ldots, n$, $n = \frac{T_f}{h}$, h the time step, and $c_j^{(q)}$ are binomial coefficients given by $c_0^{(q)} = 1$, and $c_j^{(q)} = \left(1 - \frac{1+q}{j}\right) c_{j-1}^{(q)}$.

This approach is based on the fact that for a wide class of functions, the three definitions, Caputo, Riemann-Liouville and Grünwald-Letnikov, are equivalent. In this manner, the numerical solution of fraction-order time-delay glucose-insulin system (2) applying algorithm (15) can be obtained with

$$ \begin{aligned} x_k &= \left(r_1 y_{k-1-m_1} z_{k-1-m_1} - r_2 x_{k-1} + c_1 z_{k-1-m_1}\right) h^q - \sum_{j=1}^{k} c_j^{(q)} x_{k-j}, \\ y_k &= \left(\frac{R_3 N}{z_{k-1}} - R_4 x_{k-1-m_2} + C_2\right) h^q - \sum_{j=1}^{k} c_j^{(q)} y_{k-j}, \\ z_k &= \left(R_5 (y_{k-1} - \hat{y})(T - z_{k-1}) + R_6 z_{k-1}(T - z_{k-1}) - R_7 z_{k-1}\right) h^q \\ &\quad - \sum_{j=1}^{k} c_j^{(q)} z_{k-j}, \end{aligned} \qquad (16) $$

where $m_1 = \frac{\tau_g}{h}$ and $m_2 = \frac{\tau_i}{h} \in \mathbb{Z}^+$. With $h = 0.01$, $q = 0.95$, initial conditions $[x(t), y(t), z(t)] = [6.03, 1.79, 0.82]$ for $-\tau_g \leq t \leq 0$, and parameters in Table 1, the fractional-order time-delay glucose-insulin system (2) leads to a chaos behavior as given in Fig. 5. The revealed results agree well with the literature in the area (Baghdadi *et al.* 2015; Al-Hussein *et al.* 2020; Kroll 1999; Aram *et al.* 2017), where a chaotic behavior in the biological system is stated as indication of a probable health issue (metabolic dysfunction).

Due to the importance of analyzing the glucose-insulin system under several conditions (Chuedoung *et al.* 2009), we compute the bifurcation diagrams for two cases. First, we discover the relation between the fractional-order and dynamical behaviors of the glucose-insulin regulatory system.

To do that, we have chosen $\tau_g = 0.56$, and $\tau_i = 2.55$ because they coincide with those lags seen in tests carried out on healthy human beings, where there is usually 1 or 2 minutes delay for insulin to be secreted. Additionally, the delay increases up to 10 minutes in children with malnutrition (Bertram and Pernarowski 1998; Forrest and Payne Robinson 1925).

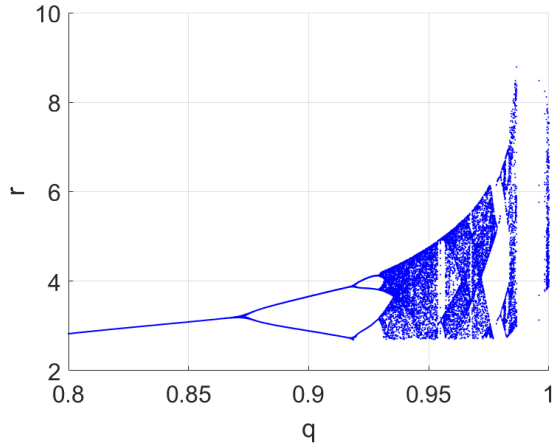

Figure 6 Bifurcation diagram for q with $\tau_g = 0.56$ y $\tau_i = 2.55$.

The bifurcation diagram for the fractional-order $q = 0.95$ is illustrated in Fig. 6. Herein, r defines glucose-insulin behavior as $r = \sqrt{x(t_k)^2 + y(t_k)^2}$ (Muñoz-Pacheco 2019; Munoz-Pacheco *et al.* 2020). We also follow the suggestions given in (Jafari *et al.* 2021) for getting a correct bifurcation diagram.

The extra parameter q permits us to gain insights into the glucose-insulin regulatory system because the memory effects can be taken into account in the process of secreted insulin in response to glucose concentrations. Figure 6 shows the bifurcation diagram for the case $0.93 \leq q \leq 1$. One can observe a chaotic behavior as was predicted by Eq. 14 and Lemma 1. It is worthy to note that not only the chaotic behavior is observed for integer-order $q = 1$ but also for fractional-orders. This result suggest that the regulation of

the glucose trough insulin is highly complex when a power-law kernel is considered to describe the long memory effects. For a fractional-order $q < 0.93$, the glucose-insulin system evolves to regular oscillations, which could be associated to a healthy state. A similar periodic behavior has been observed for typical results in the human metabolic system (Tasaka *et al.* 1994; Li *et al.* 2006).

As second scenario, we study the implications of the time-delay on the fractional-order system (2). As first step, we compute the bifurcation diagram of the lags related to insulin (τ_i) and glucose (τ_g) but using an integer-order, i.e. *no memory*. The chaotic regions are confined to an small sections about $\tau_i = 2.5$, and $\tau_g = 0.5$ and $\tau_g = 2.5$ as given in Fig. (7). When memory is not considered, the influence of delays may not be so decisive for the proper operation of the glucose-insulin feedback mechanism.

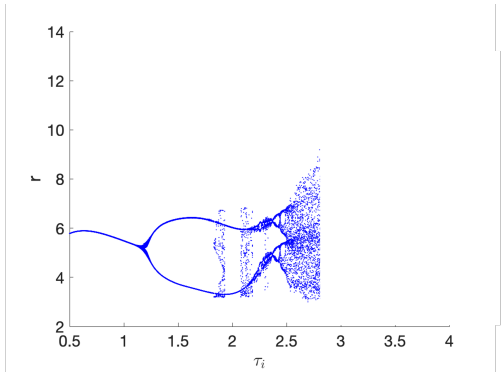

(a)

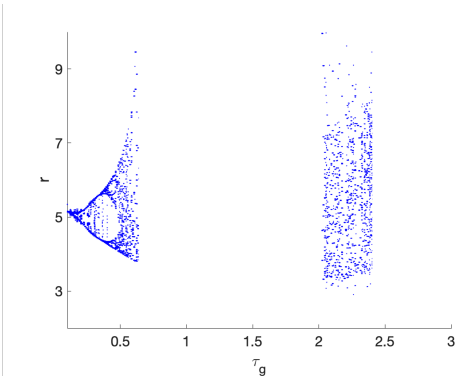

(b)

Figure 7 Bifurcation diagram for the integer-order time-delay glucose-insulin system (2). (a) τ_i with $\tau_g = 0.56$ y $q = 1$; and (b) τ_g with $\tau_i = 2.55$ y $q = 1$.

In our last case, we now compute the bifurcation diagram of the glucose-insulin regulatory system (2) with a fractional-order $q = 0.95$, i.e., with a *power-law-type memory*, as displayed in Fig. 8. We found that the chaotic regions are broader than the integer-order case.

For both delays a period-doubling cascade leads to chaotic states about $\tau_i \approx 2.1$ and $\tau_g \approx 0.2$. Next, the chaotic behavior is disrupted by a crisis scenario ($\tau_i \approx 3.5$ and $\tau_g \approx 1.5$), and the system shifts to one- or two-period oscillations but only to converge to chaos again under the same mechanism at $\tau_i \approx 3.9$ and $\tau_g \approx 1.8$.

For both delays a period-doubling cascade leads to chaotic states about $\tau_i \approx 2.1$ and $\tau_g \approx 0.2$. Next, the chaotic behavior is disrupted by a crisis scenario ($\tau_i \approx 3.5$ and $\tau_g \approx 1.5$), and the system shifts to one- or two-period oscillations but only to converge to chaos again under the same mechanism at $\tau_i \approx 3.9$ and $\tau_g \approx 1.8$.

Besides, the spectrum of Lyapunov exponents for two different values of q are computed and showed in Table 3. They were calculated employing the approach proposed in (Sano and Sawada 1985). These results display a positive Lyapunov exponent implying that chaotic behavior is observed due to sensitivity to initial conditions.

Table 3 Lyapunov exponents for different values of q.

Fractional-order	Spectrum of Lyapunov exponents		
$q = 0.97$	$LE_1 = 0.434$	$LE_2 = 0$	$LE_3 = -3.25$
$q = 0.95$	$LE_1 = 0.368$	$LE_2 = 0$	$LE_3 = -2.758$

From these observations, the memory of fractional-order derivatives described by Caputo in eq. (2) elucidates new insights about the glucose-insulin regulatory system since the memory and time-delay are vital for the onset of chaos where the pancreas might not supply an adequate quantity of insulin to regulate the glucose level. Finally, the system exhibits a stable periodic state (i.e., without any reasonable condition of metabolic disruptions) when the insulin lag is lower than two minutes and fractional-order $q < 0.9$.

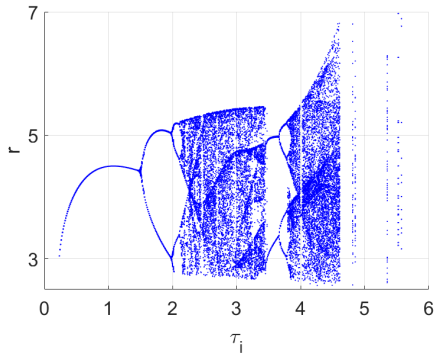

(a)

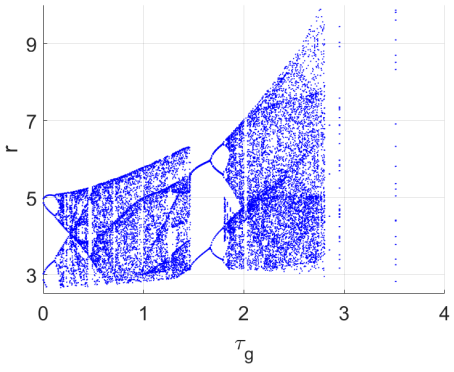

(b)

Figure 8 Bifurcation diagram for the fractional-order time-delay glucose-insulin system (2). (a) τ_i with $\tau_g = 0.56$ y $q = 0.95$; and (b) τ_g with $\tau_i = 2.55$ y $q = 0.95$.

CONCLUSION

The dynamical analysis of a fractional-order time-delay glucose-insulin system was performed applying the Caputo derivative. In particular, we studied the implications between the common disorders represented as chaotic states and a power-law memory kernel. It was observed that the fractional-order biological system alternates between a chaotic behavior (a health disorder) and a disorder-free state, as a function of not only time-delay but also fractional-order. We computed phase portraits and bifurcations diagrams to understand that regulatory mechanism, which confirmed that the fractional-order operator, i.e., a memory profile, provides improved accuracy of the underlying glucose-insulin disorders. Numerical simulations were in good agreement with the theoretical findings. Researchers from many scientific areas can also extend this work to other biological systems, which require considering the memory of past events in a non-Markovian approach. In future work, we will investigate a control scheme to drive the glucose-insulin system to stable behavior.

Acknowledgments

This work was supported by 2021 VIEP-BUAP project.

Conflicts of interest

The authors declare that there is no conflict of interest regarding the publication of this paper.

Availability of data and material

Not applicable.

LITERATURE CITED

ADA, A. D. A., 2020 Classification and diagnosis of diabetes: Standards of medical care in diabetes. Diabetes Care **43**: S14–S31.

Al-Hussein, A.-B. A., F. Rahma, L. Fortuna, M. Bucolo, M. Frasca, *et al.*, 2020 A new time-delay model for chaotic glucose-insulin regulatory system. International Journal of Bifurcation and Chaos **30**: 2050178.

Aram, Z., S. Jafari, J. Ma, J. C. Sprott, S. Zendehrouh, *et al.*, 2017 Using chaotic artificial neural networks to model memory in the brain. Communications in Nonlinear Science and Numerical Simulation **44**: 449–459.

Assadi, I., A. Charef, D. Copot, R. D. Keyser, T. Bensouici, *et al.*, 2017 Evaluation of respiratory properties by means of fractional order models. Biomedical Signal Processing and Control **34**: 206 – 213.

Baghdadi, G., S. Jafari, J. C. Sprott, F. Towhidkhah, and M. H. Golpayegani, 2015 A chaotic model of sustaining attention problem in attention deficit disorder. Communications in Nonlinear Science and Numerical Simulation **20**: 174–185.

Bajaj, J., G. S. Rao, J. S. Rao, and R. Khardori, 1987 A mathematical model for insulin kinetics and its application to protein-deficient (malnutrition-related) diabetes mellitus (PDDM). Journal of Theoretical Biology **126**: 491 – 503.

Bertram, R. and M. Pernarowski, 1998 Glucose diffusion in pancreatic islets of langerhans. Biophysical Journal **74**: 1722 – 1731.

Chinnathambi, R., F. A. Rihan, and H. J. Alsakaji, 2021 A fractional-order model with time delay for tuberculosis with endogenous reactivation and exogenous reinfections. Mathematical Methods in the Applied Sciences **44**: 8011–8025.

Chuedoung, M., W. Sarika, and Y. Lenbury, 2009 Dynamical analysis of a nonlinear model for glucose–insulin system incorporating delays and β -cells compartment. Nonlinear Analysis: Theory, Methods & Applications **71**: e1048 – e1058.

Diethelm, K., 2010 *The analysis of fractional differential equations: An application-oriented exposition using differential operators of Caputo type*. Springer Science & Business Media.

Emerging Risk Factors Collaboration *et al.*, 2010 Diabetes mellitus, fasting blood glucose concentration, and risk of vascular disease: a collaborative meta-analysis of 102 prospective studies. Lancet **375**: 2215–22.

Forrest, E. and H. M. Payne Robinson, 1925 Insulin, growth hormone and carbohydrate tolerance in jamaican children rehabilitated from severe malnutrition .

Ionescu, C., A. Lopes, D. Copot, J. Machado, and J. Bates, 2017 The role of fractional calculus in modeling biological phenomena: A review. Communications in Nonlinear Science and Numerical Simulation **51**: 141 – 159.

Jafari, A., I. Hussain, F. Nazarimehr, S. M. R. H. Golpayegani, and S. Jafari, 2021 A simple guide for plotting a proper bifurcation diagram. International Journal of Bifurcation and Chaos **31**: 2150011.

Kroll, M. H., 1999 Biological variation of glucose and insulin includes a deterministic chaotic component. Biosystems **50**: 189–201.

Lakshmanan, M. and D. Senthilkumar, 2010 *Dynamics of Nonlinear Time-Delay Systems*. Springer-Verlag Berlin Heidelberg.

Lazarević, M., 2011 Stability and stabilization of fractional order time delay systems. Scientific Technical Review **61**: 31–45.

Lenbury, Y., S. Ruktamatakul, and S. Amornsamarnkul, 2001 Modeling insulin kinetics: responses to a single oral glucose administration or ambulatory-fed conditions. Biosystems **59**: 15 – 25.

Li, J., Y. Kuang, and C. C. Mason, 2006 Modeling the glucose–insulin regulatory system and ultradian insulin secretory oscillations with two explicit time delays. Journal of theoretical biology **242**: 722–735.

Lozano, J. A., 2006 Diabetes mellitus. Offarm **25 (10)**: 66–78.

Muñoz-Pacheco, J. M., 2019 Infinitely many hidden attractors in a new fractional-order chaotic system based on a fracmemristor. The European Physical Journal Special Topics **228**: 2185–2196.

Munoz-Pacheco, J. M., C. Posadas-Castillo, and E. Zambrano-Serrano, 2020 The effect of a non-local fractional operator in an asymmetrical glucose-insulin regulatory system: Analysis, synchronization and electronic implementation. Symmetry **12**: 1395.

Naifar, O., A. M. Nagy, A. B. Makhlouf, M. Kharrat, and M. A. Hammami, 2019 Finite-time stability of linear fractional-order time-delay systems. International Journal of Robust and Nonlinear Control **29**: 180–187.

Palumbo, P., S. Panunzi, and A. De Gaetano, 2007 Qualitative behavior of a family of delay-differential models of the glucose-insulin system. Discrete and Continuous Dynamical Systems. Series B **2**.

Petráš, I., 2011 *Fractional-Order Nonlinear Systems*. Springer.

Prager, R., P. Wallace, and J. M. Olefsky, 1986 In vivo kinetics of insulin action on peripheral glucose disposal and hepatic glucose output in normal and obese subjects. The Journal of Clinical Investigation **78**: 472–481.

Rajagopal, K., V.-T. Pham, F. R. Tahir, A. Akgul, H. R. Abdolmohammadi, *et al.*, 2018 A chaotic jerk system with non-hyperbolic equilibrium: Dynamics, effect of time delay and circuit realisation. Pramana **90**: 1–8.

Rihan, F., A. Arafa, R. Rakkiyappan, C. Rajivganthi, and Y. Xu, 2021 Fractional-order delay differential equations for the dynamics of hepatitis c virus infection with ifn-α treatment. Alexandria Engineering Journal **60**: 4761–4774.

Rihan, F. A., 2013 Numerical modeling of fractional-order biological systems. Abstract and Applied Analysis **2013**: 11.

R.Rosalba, B.Ana, A.Carlos, Z.Emiliano, V.Salvador, *et al.*, 2018 Prevalencia de diabetes por diagnóstico médico previo en méxico. Salud Pública de México **60**: 1–9.

Sano, M. and Y. Sawada, 1985 Measurement of the lyapunov spectrum from a chaotic time series. Physical review letters **55**: 1082.

Sarika, W., Y. Lenburya, K. Kumnungkit, and W. Kunphasuruang, 2008 Modelling glucose-insulin feedback signal interchanges involving β-cells with delays. ScienceAsia **34**: 77–86.

Shabestari, P. S., K. Rajagopal, B. Safarbali, S. Jafari, and P. Duraisamy, 2018 A novel approach to numerical modeling of metabolic system: Investigation of chaotic behavior in diabetes mellitus. Complexity **2018**.

Shafiei, M., F. Parastesh, M. Jalili, S. Jafari, M. Perc, *et al.*, 2019 Effects of partial time delays on synchronization patterns in izhikevich neuronal networks. The European Physical Journal B **92**: 1–7.

Singh, H. K. and D. N. Pandey, 2021 Stability analysis of a fractional-order delay dynamical model on oncolytic virotherapy. Mathematical Methods in the Applied Sciences **44**: 1377–1393.

Sprott, J. C., 2015 Strange attractors with various equilibrium types. The European Physical Journal Special Topics **224**: 1409–1419.

Statista, 2019 Countries with the highest number of diabetics worldwide in 2019. https://www.statista.com/statistics/281082/countries-with-highest-number-of-diabetics/, Accessed: 2021-07-30.

Tasaka, Y., F. Nakaya, H. Matsumoto, and Y. Omori, 1994 Effects of aminoguanidine on insulin release from pancreatic islets. Endocrine journal **41**: 309–313.

Teka, W. W., R. K. Upadhyay, and A. Mondal, 2018 Spiking and bursting patterns of fractional-order izhikevich model", journal = "communications in nonlinear science and numerical simulation **56**: 161 – 176.

Yao, Z. and B. Tang, 2021 Further results on bifurcation for a fractional-order predator-prey system concerning mixed time delays. Discrete Dynamics in Nature and Society **2021**.

Zambrano-Serrano, E., J. M. Munoz-Pacheco, L. C. Gómez-Pavón, A. Luis-Ramos, and G. Chen, 2018 Synchronization in a fractional-order model of pancreatic β -cells. The European Physical Journal Special Topics **227**: 907–919.

How to cite this article: Fernández-Carreón, B., Munoz-Pacheco, J.M., Zambrano-Serrano, E., Felix-Beltrán, O.G. Analysis of a Fractional-Order Glucose-Insulin Biological System with Time Delay. Chaos Theory and Applications, 4(1), 10-18, 2022.

CHAOS
Theory and Applications
in Applied Sciences and Engineering

e-ISSN: 2687-4539
RESEARCH ARTICLE
Vol.4 / No.1 / 2022 / pp.19-25
https://doi.org/10.51537/chaos.998110

A Comparative Proposal on Learning the Chaos to Understand the Environment

Mustafa Atilla Arıcıoğlu *,1 **and Osman Nurullah Berk** β,2

*Department of Business, Faculty of Political Science, Necmettin Erbakan University, 42090, Konya, Turkey, βDepartment of Business, Beysehir Ali Akkanat Faculty of Business Administration, Selcuk University, 42130, Konya, Turkey.

ABSTRACT Towards the end of the twentieth century, radical changes have taken place within the framework of strategic management and organization-environment relationship. Technology, speed, competition and globalization factors have rapidly modified the environmental dynamics in the organization-environment relationship. In today's chaotic world, the effects of the crisis and environmental uncertainties have spread rapidly and widely not only in narrow area but all over the world. This situation makes it difficult for organizations aiming to live an eternal life to continue their lives and accelerates the occurrence of organizational death. In this context, Organizational Ecology and Chaos Theories have been emerging as guides in ensuring the sustainability of organizations. This study, it is aimed to draw a road map for organizations by making a comparison based on the suggestions and arguments of Organizational Ecology and Chaos Theories in order for organizations to have a more sustainable life. As a result of the evaluation, recommendations were made for learning to live with uncertainties and a correct action plan by developing sensors on the way to becoming a sustainable organization, based on the dynamics of the future. At this point, organizations need to have a flexible and agile structure and develop early warning systems so that they can leave the foggy and unpredictable environment created by the chaotic atmosphere with minimum damage and seize the new opportunities that arise. In addition, they should determine strategies by developing various scenarios against unforeseen threats, and they should consider environmental factors while doing these.

KEYWORDS
Chaos
Organizational ecology
Environment
Sustainability

INTRODUCTION

Discussions on the existence and sustainability of organizations have been one of the most significant areas for organizational theories. Identifying the organization by themselves or describing the notions of competition, environment, employees and processes by the administrators on the basis of the organization have been reviewed in the context of the environment in post-modernist approaches in addition to the modern organizational theory approaches. This ancient relationship between the organization and the environment has become even more striking since the end of the 1980s.

As a matter of fact, the shaping of the new world by globalization indicates the existence of a process that needs to be followed more carefully for organizations. Economic, political and legal changes deal with new actors, new dynamism and new/re-emerging concepts within this process.

In other words, it will be possible for organizations to understand the environment by learning these changes. The vision of the manager and the internal dynamics of the organizations become more important in this effort to make sense. Because the world has become more interconnected and dependent than ever before by adapting to technology with its contents. The reason for the mutual fragilities in the international arena to gain a new dimension is based on global and technological developments (Kotler and Caslione 2009). However, the developments experienced have led to some negative changes in people's lives as well as positive developments. Increasing interaction between countries and people, the changing permeability between societies, the increasing importance of companies in world management, companies' competitive tools becoming insufficient for consumers/customers, the continuation of discussions about what the existence of humans is

Manuscript received: 20 September 2021,
Revised: 8 November 2021,
Accepted: 31 December 2021.

[1] maaricioglu@erbakan.edu.tr
[2] osman.berk@selcuk.edu.tr (**Corresponding Author**)

or how affect the environment makes it difficult for organizations to understand the environment and even more their impacts on the environment.

These waves of change and transformation affect organizations significantly and lead to unexpected results. In today's world, sudden and rapid changes can occur in a short time that can lead to unexpected results. This situation can unexpectedly change the value phenomenon of organizations that are in constant interaction with their environment, and can overturn the advantages of the market. All these developments have revealed the necessity for organizations to adapt to a complex, chaotic and dynamic environment in order to maintain their sustainability and gain a competitive advantage in today's world (Stacey *et al.* 2000). This situation includes the emphasis on the period that Van-Eijnatten wrote alone in 2004 (van Eijnatten 2004), with other colleagues in 2002 and 2004 (Fitzgerald and van Eijnatten 2002; van Eijnatten and Putnik 2004). The authors mark a new century that begins with uncertainty, high mobility, speed, turbulence and vulnerabilities. Chaos will speak of itself as a new context for understanding this century. In other words, chaos will be the new guide and instructor of organizations in understanding the environment and organizational learning. However, for this reason, the meaning that the environment and the organization will attribute to chaos in order to learn itself appears as another important context.

LITERATURE VIEW

Contemporary management theories take into account the rapid changes in today's organizational environment and help to understand, interpret and explain the impact of changes on organizations (Porth and McCall 2001). In the literature, while many contemporary management theories such as resource-based theory, agency theory, institutional theory, contingency theory and systems theory are discussed in depth within the framework of the organization, it is seen that organizational ecology, chaos and theory are not examined in an integrated way. Organizational ecology and chaos theories are still difficult to understand and apply in contemporary organizations. In this study, it is aimed to make it easier to understand and apply these two theories in an integrated way by discussing them in depth and comparatively. When the studies conducted in recent years are examined, it is observed that there is an increase in research on chaos and organizational ecology theories in different application areas and different organizational forms. The studies conducted are listed below in chronological order.

Thietart and Forgues (1995) that deals with the theories of chaos and organization together, it is stated that the processes related to the management of organizations are actually included in the preferences and are embedded in the processes. The researchers, who went through 6 principles in the studies on the chaotic field, concluded that "similar actions should never lead to the same result during a single institutional lifetime or between two different organizations". Bayramoğlu (2016) emphasizes what needs to be done in order to gain a perspective and approach, based on the assumption that, despite the increasing number of studies on chaos, it is complex and does not have the desired competence in examining the relationship between chaos and organization theories. It is argued that this acquisition gains importance in ensuring success and that the chaos and complexity paradigm should be considered in this context. In another study dealing with chaos and organization theories, the topics of governance in projects, organizational design and governmentality were examined (Simard *et al.* 2018). In this research, a conceptual framework has been developed showing that governance, organizational design and managerialism are necessary for understanding projects. The paper offers a theoretical contribution to project studies by creating a bridge between process theory, the sensemaking perspective and the study of organizational project management.

Researchers have comparatively examined the theories of chaos, complexity and contingency in order for organizations to cope with the difficulties with the changes that have emerged with globalization and technological developments in the 21st century, the change in the nature of competition and the increase in unpredictable events. Looking at the concepts used for chaos; nonlinearity, feedback, bifurcation, odd attractors, fractals, self-organization for complexity theory; for the theory of non-linearity, dynamism, feedback, self-organization, emergence, and contingency; coherence, equifinality, effectiveness, and relevance were used. After all; inferences were put forward by comparing the working examples of the examined theories with their organizational applications (Lartey *et al.* 2020). Eight organizational theories related to supply chain management and their possible future research questions are identified and explained in the research (Prakash *et al.* 2020), which examines how humanitarian organizations should follow a path for their supply chain. Of these, the first four theories (i.e. resource-based theory, resource dependency theory, social exchange theory, and contingency theory) were initially applied in the humanitarian field, while the remaining theories (i.e., institutional theory, stakeholder theory, transactional cost theory, and information theory) have the potential to be applied in the future. In the context of creating and managing strategies for businesses, Arıcıoğlu *et al.* (2021) scanned the studies on chaos and selected the ones which are suitable for the purpose. They presented a short proposal title stating the importance of chaos for strategic management and how it guides managers. Using the propositions of chaos theory as an inclusive approach, Altinay and Arici (2021) evaluated the changing marketing channels in organizations providing accommodation service after the COVID-19 outbreak.

ORGANIZATIONAL ECOLOGY AND CHAOS ON LEARNING THE ENVIRONMENT DURING THE LIFE OF THE ORGANIZATION

Mankind acquired many things from nature in his relationship with the environment, but he uses it against nature. This exploitation isn't a new phenomenon (Adorno and Horkheimer 2010). On the other hand, learning to live with it by understanding the environment also has the same history as an awareness (Habermas and Kanat 1997).

Handling this relationship within the context of the organization does not depend on a very different perception and context. When associating Taylor's organization with the environment or explaining the existence of open system theory through the environment, the context in question is on this distinction: living together or using nature. However, the priority in both situations is learning the environment. For this reason, the definition and understanding of the environment are decisive. This is the subject that organizational theories also insist on.

One of the most interesting approaches on this subject stands out as Organizational Ecology and the other as Chaos Theory. The efforts for both of them to understand and define the environment actually bring with it the effort to define and understand the organization as well.

If the Organizational Ecology Theory is dealt with first, the two main issues that the theory seeks to answer are; the reasons for the existence of organizations and the different characteristics of organizations (Leblebici 2004). In ontological justification within these two issues; the understanding of order and universe explained with Newton's determinism leaves its place to regular chaos and differences are explained with fractal geometry (Poincaré and Maitland 2003; Chamberlain 1995; Moran 2018).

On the other hand, Organizational Ecology theory explains itself through three propositions by considering the relations between organization and environment (Baum 1999):

- Organizations are dynamic and new forms of organization emerge. However, these organizations live as much as the environment allows.
- Difficulties arise for organizations to respond to an uncertain and changing environment.
- There are differences and diversity in organizations in terms of their internal structures. On the other hand, it exists on three basic principles proposed for Chaos Theory.
- The reason for organizational mobility is complex movements related to human activities and human mobility in the environment.
- Organizations, as an open system, are naturally exposed to the effect of the environment and affected by these.
- The reactions of organizations affect their internal structures as much as they affect the environment.

Both theories advocate the importance of the environment and there is no one-way result in the interaction of the organization and environment.

On the other hand, Ecology Theory associates the survival of such species with evolution and states that diversification and reproduction occur during the evolutionary process (Leblebici 2004). Various opinions and thoughts have been put forward on the environment and environmental formation from past to present. The theories of Lamarck (1744-1829) and Darwin (1809-1882), which have an evolutionary perspective, form the basis of these. According to Lamarck, every being is formed according to the physical conditions in which it exists and it has to adapt to these physical conditions. Lamarck claims that living things create organs according to their needs, and that if they are not needed, these organs disappear by blunting over time. The transmission of these traits genetically to future individuals inherited has raised a number of unanswerable questions, and at this point, Darwin supported Lamarck's assumptions of genetical gravity and adaptation to the environment with a more scientific approach, with the findings of natural selection and survival. Darwin argues that living things can remain strong throughout their lives only by natural selection (Grandinetti 2018). He also argued that in order for living species to have a sustainable life, they must first show diversity and then adapt to the environment. The change that Darwin has mentioned at this point may be necessary according to the changing environmental conditions (Mayr 1972; Hancerlioglu 1995). As a matter of fact, ecology in a general expression states that organizations change in order to adapt to the changes in the environment and as a result of this change, there is a diversification in the organizations, as a result of this diversification, some organizations are chosen by the environment and are kept alive. It can be said that this point of view is the result of handling the life processes of organizations in a similar way to living things. Within this context, the theory focuses on the selection, survival, legitimacy and death of organizations. The theory focuses on organizational populations and communities rather than on an organization by making macro-scale explanations (**?**).

An important issue in theory is the process of change that causes diversification. Researchers have different views on the causes of change. In general terms, these are discussed under two headings as internal and external causes (Baum 1999). Political, legal, technical and institutional environment refers to external causes, while the interests of the organization, value judgments and degrees of dependency express internal causes. Another concept that draws attention to change is structural inertia, which refers to the unwilling stance and cumbersome structure of organizations against change. It is used to emphasize that organizations generally have a lower rate of change than the rate of change of the environment (Hannan and Freeman 1977). Hannan and Freeman advocate that the organization-environment relationship should be viewed from the perspective of environmental selection. Organizational ecology also pays attention to organizational features, but emphasizes the inherent organizational features that shape institutional environments and determine how specific organizations will respond to them. These include the cost of organizing, flexibility and stability or fragility (Abbott *et al.* 2016).

Another issue that has an important place in theory is organizational death and birth. Although there is no consensus on this issue, the entry of an organization into a new population is expressed as birth and exit from the population as death. Organizational deaths and births are important indicators in determining the characteristics (dynamics) of a population, that is, the organizational community formed by interacting organizations. Issues such as the total number of organizations in the population and the carrying capacity of the population, together with the death and birth rates, allow the determination of population dynamics (Baum and Oliver 1991). The basic view of Organizational Ecology theory is to understand the forces that shape organizational structures over the time span (Hannan and Freeman 1989).

Nevertheless, organizations, which are open systems, need to be able to respond quickly and rationally in this chaotic environment in order to survive the reactions from their environment. Otherwise, they will not be able to adapt to the changing conditions of the environment and will end their existence. Within this context, the environment that organizations are in is of great importance for organizations to survive this wind of change and ensure their sustainability. It is inevitable for organizations in terms of their sustainability to understand and correctly interpret ecology, which affects their activities and has an important effect on determining their lifespan. The key to survival for organizations, as in natural systems, is to develop rules that can keep an organization operating "on the brink of chaos" (Stacey *et al.* 2000).

The origin of modern chaos theory can be traced back to Hegel, Marx, and Engels, whose work focuses on historical evolution through dialectical processes between the opposing forces of stasis and change (Loye and Eisler 1987; Farazmand 2003). Henri Poincaré, who later noticed and became famous in the world, solved the problem of "three bodies", which was put forward on the stability of the solar system in 1889, causing the term "chaos" to be used for the first time in a technical sense. Poincaré laid the foundations of the chaos theory in New Science by proving that the solution of the solar system is sensitive to initial conditions and that the solar system can never be predicted whether it is stable or not because it is impossible to know the initial conditions of the universe (Gleick 1997). It was Lorenz who made Poincaré famous again. While forecasting the weather, as a result of his entry into the system by simplifying a number of sequences obtained

from previous research results, Lorenz realized that the results that appeared in the chart created a different table than the previous ones, while waiting to receive the same results. Lorenz's expectation is the way that a difference of one thousand unity (1/1000) created when entering sequences into the system will not affect the result. But this small change at the beginning affected the forecasts, and unlike the previous results, a bumpy, butterfly-like graph emerged (Gleick 2005). This revealed the "butterfly effect", which shows sensitivity to the initial state and forms the basis of Chaos Theory. Lorenz's results, by defining chaos as "a system with a uniform geometric structure that behaves randomly", emphasized that there is a "orderly disorder" in the system (Lorenz 1963). It is observed that small differences in variables can produce surprising results that cannot be predicted at the starting point. At this point Lorenz introduced two main features of the chaos theory. These; the principles of "Sensitive Dependence on Initial Conditions " and "Randomness" (Gleick 2005).

The general characteristic of chaos theory is that it is the "edge of chaos", which is defined as "the space in which the complex system spontaneously forms, adapts, and is alive", resulting from the fact that life stands between order and disorder (Heylighen 1999; Mitchell 1999).

Understanding and predicting practice and finding the exact practical equivalent of theories are some of the main goals of the theory. For this purpose, chaos theory has made an ontological differentiation in order to eliminate the deficiency in existing theories and evaluated the "disorder" situation from a different perspective (Aricioglu and Karabiyik 2019).

In this context, the following propositions summarize the chaos theory (Rockier 1991):

- Chaos theory helps to explain the nonlinear aspects of the universe.
- Combines the determinism of the Newtonian model with the randomness of quantum physics. It explains this partly through the concept of "strange attractors".
- Chaos theory shows that small changes in the beginning of a system can eventually lead to large differences.
- Understanding chaos leads us a perspective in which the universe is an open system.
- Human systems can be best explained by chaos theory. The nature of the human body and weather forecast are examples of this.
- It has a geometrically fractal structure (Fern).
- It has an original structure. No event repeats the same way (Snowflake).
- It can be stable (regular, cosmotic) within its own chaotic limits.
- It is not possible to be foreseen. Although it has a unique order, it also has an ambiguous side.

Chaos is not disorder; it represents the unpredictability of an evolutionary order system. Chaos Theory examines dynamical systems characterized by nonlinear, complex interactions and dynamic evolution over time (Levy 1994). It suggests that a small change in the initial condition of a nonlinear dynamic system can lead to unexpected results and makes it difficult to predict dynamical systems (Holmes 1995).

When the propositions of chaos are interpreted in the context of the organization-environment relationship; Small variables occurring in the system can bring unforeseen threats from the environment, which is an open system, and this can lead us to unexpected and effective results. This disorder has a unique and fragile structure and is not expected to be repeated. This whole range of uncertainty has an order in itself. In this context, being able to understand and respond to the organizational environment dominated by a regular disorder, to respond towards this and to develop sensors and to have a flexible structure are key to sustainability.

A PROPOSITION ABOUT THE FUTURE OF THE ENVIRONMENT

The report "Global Trends 2025", published by the US National Intelligence Council in 2008, predicts that in the future, chaos, violence and upheaval will dominate the world (Global Trends 2025: A Transformed World 2008). In today's world, where everything is so dependent and fragile, predictions have been realized, and the situation of uncertainty affects all stakeholders living on earth. There are a number of factors that trigger and accelerate disorder, uncertainty, chaos, and change. These factors are briefly described below.

Globalization: One of the most important phenomena of change is globalization, accompanied by regionalization (the European, American and Asian blocks) and fragmentation (the Soviet Union and Yugoslavia). What is meant by globalization is that most states in the world belong to a system with global interaction (Mannermaa 2009). Globalization is actually the result of a logical process. Human history shows that human systems tend to create new, technological, economic and socio-political levels of systems throughout the development process. Development from self-contained village communities to city-states, nation-states, regional systems is a natural process of systematic development. The characteristic of this development is that the birth of a new level of system means an increase in the complexity of the entire system. The removal of borders, the increase of mobility and the level of interaction have changed the existing world order and led to the birth of a chaotic environment. One of the most important features of the international system since the Cold War, globalization is not a process of chaotic ending that brought only chaos occurring around in the states, but completely covering and affecting the global environment have been turned into an event that is. There is a great similarity between the properties of the chaotic structure described in chaos theory and the properties of the concept of globalization.

Technological Developments and The Information Revolution: Information Technologies, one of the main elements of the globalization revolution, are the biggest element shaping the new global economy. The emergence of a single platform that brings together, connects individuals, organizations and objects, it has led to the change of many phenomena from the way individuals and organizations work to the way they work, logistics, production, communication, consumption, etc. In addition to the positive effects of this change, there are a number of negative effects. Removing borders, making access to information so easy, and thus the emergence of big data, in other words, overloading information, and therefore causing more confusion and chaos (Kotler and Caslione 2009).

Extreme Competition: The constant development and change of technological developments have made it difficult for organizations to have a sustainable competitive advantage and has led to the formation of a difficult competitive environment. In order to survive in markets where intense and fast competitive moves are made, current developments and competitors must be carefully followed and the counter move must be made in a timely and accurate manner. Globalization, attractive substitute goods, changing

consumer preferences and the emergence of new business models determine the pace of market disruptions in an intensely competitive environment. In order to resist competition in a chaotic environment, strategic foresight should be developed by organizational managers, importance should be given to the speed factor, and outsourcing and similar cooperation models should be implemented (Doherty and Delener 2001; D'aveni 2010).

Changing Balances in the World (The Rise of the Rest of the World): The phenomenon of power from an economic and political point of view is constantly changing from the past to the present. The role of countries in the global market may vary depending on this situation. A process is underway in which the United States and the European Union are increasingly losing their sovereign roles, money and power are transferred to nations rich in natural resources, to developing countries. The 2008 financial crisis, Brexit, the Covid-19 pandemic, etc. events reveal and accelerate the course of change.

Power is shifting for the third time in the history of the Modern world (Zakaria 2013). The agricultural and industrial revolution in the 15th century, the rise of the USA in the 19th century, and thirdly, the change and development of China and Asian countries today can be explained in this way. BRICS countries, the RCEP agreement (Regional Comprehensive Economic Partnership) and wealthy Middle Eastern countries show us the "rise of the rest of the world" as new rising powers in the perspective of chaos and turmoil (Time, 2020). In this context, today, when fragility and uncertainty are at the line stage, as a result of the power changes occurring between countries, an environment of chaos occurs throughout the global world. Organizations as well as countries should strategically evaluate the opportunities and threats that may arise.

CONCLUSION

"Turbulence" occurs anywhere or at any time when the number of triggers increases and reaches high levels, as can be seen in the process that started before the 2008 crisis and is still ongoing. Organizations that have an agile and flexible organizational structure, early warning systems and can remain vigilant will be able to notice the turmoil. Some turbulence can only be noticed when chaos manifests itself. When chaos is underestimated, it can be difficult to exploit strategies that will protect the organization from the weaknesses caused by chaos or allow it to seize the opportunities it creates (Kotler and Caslione 2009). For this reason, it is important that organizations are always on guard against a possible state of chaos that may occur at any time in terms of sustainability of the organization and minimizing the damage that may occur. The organizational environment should be well analyzed, the phenomenon of change and development should be understood by the entire organization and become part of the organizational culture.

Understanding the environment in this context, despite their different philosophical backgrounds, two similar theories, with their insistence on learning, their belief in sustainability and their increasing consistency, contribute to understanding the environment around the following differences:

In order for organizations to understand the environment, they need to understand chaos by prioritizing it, applying propositions carefully in context, and developing a number of strategies. Within the framework of the propositions of the theories, a number of strategies for organization sustainability are presented below, especially to learn to live in chaos:

Flexibility and agility: Physically, structures should be able to stretch when the ground swings. A similar situation applies to organizations competing in today's turbulent environment. Organizations that can predict market movements best, re-emerge from the worst system shocks and take advantage of the gaps left by those who cannot withstand the impact will win (Economist 2009). For most organizations, the path to organizational agility is through transformation, reducing inefficiency, and the ability to reorganize around core values. Basic processes need to be optimized. It is important for the organization to act in a flexible structure so that information system closed to outside/communication are maximized, the alignment of basic information sharing processes and become standardized. At this point, care should be taken not to disrupt communication and teamwork.

Development of an early warning system: It is known that the turbulence can come at any time, from anywhere, some can be detected in advance, and some cannot. The detected turbulence should be analysed by the organization, and then the opportunities and weaknesses that may arise should be identified. In this way, these deficiencies can be minimized or eliminated completely. If we liken the organization to a passenger plane preparing for flight, it can be used to direct pre-flight air traffic, weather, traffic, etc. we can say that the "tower" is the organization's early warning system, which allows the Prevention of disruptions caused by environmental factors. They can prevent disasters that may occur by developing an early warning system that acts as a tower in airports while performing their activities in organizations.

Another factor to consider in the early warning system is the external environment in which the organization operates. In some cases, organizations can ignore the external environment by focusing on internal factors. According to Gilad, this situation is called "mismatch in the sector" and occurs during periods when market realities exceed the strategy of the organization. In order to cope with this situation, organizations must identify, monitor risks and take the necessary measures by management (Gilad 2003).

Developing scenarios: The main element of a strategy in chaos management is the development of scenarios that the organization will likely encounter by bringing together the ideas of managers, experts and stakeholders at the head of all units of the organization's managers. Preparing different scenarios, including the worst, expected and best, is important in terms of first response to a possible threat from the environment and reducing damage. Developing scenarios can simultaneously benefit the organization. It allows you to manage, measure and classify uncertainty. It allows to reduce confusion and separate what is really unknown and really important. It creates a clear structure that will be used when working on options to overcome a number of possible outcomes, and avoids regrets (Hirt *et al.* 2020).

Chaos theory sets out various scenarios for understanding and predicting organizational behaviour and system evolution. Both computer simulations and experimental studies are needed to determine characteristics and strategic inferences in the organizational environment. Due to the sensitivity property of chaos systems, the selected variable must be measured precisely (Doherty and Delener 2001). In the research conducted, four different levels of uncertainty states are separated from each other. Level one has a foreseeable future and develops a single scenario. The second level develops a small number of scenarios and predicts the probability that each scenario will be implemented. The third level develops a number of scenarios due to the complexity of the underlying factors. It is impossible to make a prediction with certainty when there will be real ambiguity, and decisions are made at that moment by intuition. This can be considered Level Four. It

Table 1 Comparison of Organizational Ecology and Chaos Theories.

Elements	Organizational Ecology	Chaos
Background	Mutation that allowed Darwin and Lamarck to cling to the environment through	Anarchism or balance in disorder
Time/Period	Creating organizational characteristics of short-term processes over a wide period of time in the evolutionary process	An uncertain broad time or beyond future time
Motion/ Kinesis	Physical	Metaphysical
Making sense of the environment	Competitive understanding	Existence of requirement for entity
Universality of organization forms	Similarity or difference instead of universality	Fractal
Competitions	High competition	Balancing
Actors	Company / actor oriented	Governance approach
Sustainability	Competitive and adaptable	When life is learned with the environment

is impossible to establish a relationship because it constantly shifts the relationship between cause and effect. Atmosphere of chaos caused by the Covid-19 pandemic in global markets can qualify as a level 4.

Choice of scenario and strategy: In a world of extreme uncertainty, it will not be right in the long run to devise a strict, decisive plan. But making everything flexible in its entirety is also an expensive way, and may not achieve any of the organization's goals. Instead, a portfolio of strategic moves (scenarios) should be created that will collectively perform well in all possible scenarios, even if each scenario does not have a way out on its own.

After developing the most important scenarios, organization managers need to choose the most likely one from them. For each scenario, the optimal strategy must be found. Managers want to accept a strategy that coincides with a risk they are willing to take and as many opportunities as they want to evaluate. It is necessary to take into account the worst-case scenario and implement the strategy that will benefit the organization when the worst case occurs. This means minimizing maximum risk and is referred to in the literature as a mini-max strategy (Kotler and Caslione 2009). It is not possible to create a clear guide for scenario and strategy selection. Managers may want to take advantage of past experience, be timid/bold about taking risks, or argue that a scenario that mentions the existence of many opportunities may be the right choice. It is important to know that there are many unknowns, which scenario choice will be the right decision, as well as to be prepared for any turbulence and uncertainty that may occur.

Organizations should develop the capabilities, systems and processes to quickly identify and predict the upheavals that may arise in the environment in which they operate, identify their weaknesses, know and focus on their own values. It should be able to separate from the foggy and unpredictable environment created by the chaotic atmosphere with minimal damage and evaluate new opportunities that arise. In order to do this, they must constantly consider the environmental factor and take care of his relations with the environment. Considering that all uncertainties can come from the environment, the key to countering competition, reducing risk factors, following new developments in the market and ensuring the sustainability of the organization is to understand and analyze the environment in a good way. In order to predict any threat that may come from the environment, it is necessary to develop strategies and scenarios, evaluate opportunities, and teach managers and the organization to live with chaos as it does today. When these scenarios and strategies are understood by the entire organization, become part of everyday decision-making processes and are adopted in the organization as a culture, an organizational structure that chaos cannot shake arises. Organizations that have such an organizational structure will be able to live a sustainable life despite all the turmoil in today's world of chaos, where uncertainty increases every day and it becomes difficult to predict the future at any moment.

Conflicts of interest

The authors declare that there is no conflict of interest regarding the publication of this paper.

Availability of data and material

Not applicable.

LITERATURE CITED

Abbott, K. W., J. F. Green, and R. O. Keohane, 2016 Organizational ecology and institutional change in global governance. International Organization **70**: 247–277.

Adorno, T. W. and M. Horkheimer, 2010 Aydınlanmanın diyalektiği: felsefi fragmanlar. Kabalcı Yayınları, çev: Oğuz Özügül **1**.

Altinay, L. and H. E. Arici, 2021 Transformation of the hospitality services marketing structure: a chaos theory perspective. Journal of Services Marketing .

Arıcıoğlu, M. A., B. Erer, and N. Gülnar, 2021 A known innovation for strategy: A study on chaos. In *Financial Strategies in Competitive Markets*, pp. 179–191, Springer.

Aricioglu, M. A. and H. Ç. Karabiyik, 2019 Örgütlerin geleceğine bir önerme olarak kaos teorisi ve kaos olgusunu anlamak. Medeniyet ve Toplum Dergisi **3**: 145–156.

Baum, J. A., 1999 Organizational ecology. Studying organization: Theory and method pp. 71–108.

Baum, J. A. and C. Oliver, 1991 Institutional linkages and organizational mortality. Administrative science quarterly pp. 187–218.

Bayramoğlu, G., 2016 Karmaşiklik paradigmasi işiğinda örgüt teorilerinin yeniden değerlendirilmesi. Selçuk Üniversitesi Sosyal Bilimler Enstitüsü Dergisi pp. 49–63.

Chamberlain, L., 1995 Strange attractors in patterns of family interaction. .

D'aveni, R. A., 2010 *Hypercompetition*. Simon and Schuster.

Doherty, N. and N. Delener, 2001 Chaos theory: Marketing & management implications. Journal of Marketing Theory and Practice **9**: 66–75.

Economist, E., 2009 Organisational agility: How business can survive and thrive in turbulent times. The Economist pp. 1–27.

Farazmand, A., 2003 Chaos and transformation theories: A theoretical analysis with implications for organization theory and public management. Public Organization Review **3**: 339–372.

Fitzgerald, L. A. and F. M. van Eijnatten, 2002 Reflections: Chaos in organizational change. Journal of Organizational Change Management .

Gilad, B., 2003 *Early warning: Using competitive intelligence to anticipate market shifts, control risk, and create powerful strategies*. AMACOM Div American Mgmt Assn.

Gleick, J., 1997 Kaos: Yeni bir bilim teorisi, çev. Fikret Üçkan, TÜBİTAK, Ankara .

Gleick, J., 2005 Kaos: Yeni bir bilim teorisi, çev. Fikret Üçkan, TÜBİTAK, Ankara .

Grandinetti, R., 2018 Is organizational evolution darwinian and/or lamarckian? International Journal of Organizational Analysis .

Habermas, J. and C. A. Kanat, 1997 *Bilgi ve insansal ilgiler*. Küyerel Yayınları.

Hancerlioglu, O., 1995 Dört bin yıllık düşünce, sanat ve bilim tarihinin klasik yapıtları üzerine eleştirel inceleme. İstanbul: Remzi Kitabevi .

Hannan, M. T. and J. Freeman, 1977 The population ecology of organizations. American journal of sociology **82**: 929–964.

Hannan, M. T. and J. Freeman, 1989 *Organizational ecology*. Harvard university press.

Heylighen, F., 1999 The growth of structural and functional complexity during evolution. The evolution of complexity **8**: 17–44.

Hirt, M., S. Smit, C. Bradley, R. Uhlaner, M. Mysore, *et al.*, 2020 Getting ahead of the next stage of the coronavirus crisis. McKinsey & Company **4**.

Holmes, P., 1995 The essence of chaos (en lorenz). Siam Review **37**: 129–131.

Kotler, P. and J. A. Caslione, 2009 Kaos yönetimi: Çalkantılar çağında yönetim ve pazarlama (çev. kıvanç dündar). İstanbul: Optimist Yayınları pp. 12–58.

Lartey, F. M. *et al.*, 2020 Chaos, complexity, and contingency theories: a comparative analysis and application to the 21st century organization. Journal of Business Administration Research **9**: 44–51.

Leblebici, D. N., 2004 Örgüt-çevre ilişkisinde yeni perspektif arayişi: Dinamik örgütsel çevre ve örgütsel doku. Hacettepe Üniversitesi İktisadi ve İdari Bilimler Fakültesi Dergisi **22**: 285–307.

Levy, D., 1994 Chaos theory and strategy: Theory, application, and managerial implications. Strategic management journal **15**: 167–178.

Lorenz, E. N., 1963 Deterministic nonperiodic flow. Journal of atmospheric sciences **20**: 130–141.

Loye, D. and R. Eisler, 1987 Chaos and transformation: Implications of nonequilibrium theory for social science and society. Behavioral science **32**: 53–65.

Mannermaa, M., 2009 Globalization and information society—increasing complexity and potential chaos. Global Transformations and World Futures-II p. 88.

Mayr, E., 1972 Lamarck revisited. Journal of the History of Biology pp. 55–94.

Mitchell, W. M., 1999 Complexity. the emerging science at the edge of order and chaos, 1992.

Moran, G., 2018 *Chaos theory and psychoanalysis: The fluidic nature of the mind*. Routledge.

Poincaré, H. and F. Maitland, 2003 *Science and method*. Courier Corporation.

Porth, S. J. and J. McCall, 2001 Contemporary management theories and catholic social teaching. Review of Business **22**: 8–15.

Prakash, C., M. Besiou, P. Charan, and S. Gupta, 2020 Organization theory in humanitarian operations: a review and suggested research agenda. Journal of Humanitarian Logistics and Supply Chain Management .

Rockier, M. J., 1991 Thinking about chaos: Non-quantitative approaches to teacher education. Action in Teacher Education **12**: 56–62.

Simard, M., M. Aubry, and D. Laberge, 2018 The utopia of order versus chaos: A conceptual framework for governance, organizational design and governmentality in projects. International journal of project management **36**: 460–473.

Stacey, R. D., D. Griffin, and P. Shaw, 2000 *Complexity and management: Fad or radical challenge to systems thinking?*. Psychology Press.

Thietart, R.-A. and B. Forgues, 1995 Chaos theory and organization. Organization science **6**: 19–31.

van Eijnatten, F. M., 2004 Chaordic systems thinking: Some suggestions for a complexity framework to inform a learning organization. The Learning Organization .

van Eijnatten, F. M. and G. D. Putnik, 2004 Chaos, complexity, learning, and the learning organization: Towards a chaordic enterprise. The Learning Organization .

Zakaria, F., 2013 The rise of the rest. In *Debating a Post-American World*, pp. 42–51, Routledge.

How to cite this article: Arıcıoğlu, M. A. and Berk, O. N. A Comparative Proposal on Learning the Chaos to Understand the Environment. Chaos Theory and Applications, 4(1), 19-25, 2022.

CHAOS
Theory and Applications
in Applied Sciences and Engineering

e-ISSN: 2687-4539
RESEARCH ARTICLE
Vol.4 / No.1 / 2022 / pp.26-36
https://doi.org/10.51537/chaos.1022368

Nonchaotic Behavior and Transition to Chaos in Lorenz-like Systems Having Invariant Algebraic Surfaces

Marcelo Messias *,[1] **and Rafael Paulino Silva** *,[2]
*Departamento de Matemática e Computação, Faculdade de Ciências e Tecnologia, Universidade Estadual Paulista (UNESP), São Paulo, Brazil.

ABSTRACT The famous and well-studied Lorenz system is considered a paradigm for chaotic behavior in three-dimensional continuous differential systems. After the appearance of such a system in 1963, several Lorenz-like chaotic systems have been proposed and studied in the related literature, as Rössler system, Chen-Ueta system, Rabinovich system, Rikitake system, among others. However, these systems are parameter dependent and are chaotic only for suitable combinations of parameter values. This raises the question of when such systems are not chaotic, which can be seen as a dual problem regarding chaotic systems. In this paper, we give sufficient algebraic conditions for a generalized class of Lorenz-like systems to be nonchaotic. Using the general results obtained, we give some examples of nonchaotic behavior of some classical "chaotic" Lorenz-like systems, including the Lorenz system itself. The nonchaotic differential systems presented here have invariant algebraic surfaces, which contain the stable (or unstable) invariant manifolds of their equilibrium points. We show that, in some cases, the deformation of these invariant manifolds through the destruction of the invariant algebraic surfaces, by perturbing the parameter values, can reorganize the global structure of the phase space, leading to a transition from nonchaotic to chaotic behavior of such differential systems.

KEYWORDS
Chaotic and non-chaotic dynamics
Lorenz-like systems
Darboux theory of integrability
Invariant algebraic surface
Darboux invariant
Stable and unstable manifolds.

INTRODUCTION

Let $\mathbb{R}[x,y,z]$ be the ring of polynomial functions in the variables x,y,z, with coefficients in $\mathbb{R}$. Consider the system of first order ordinary differential equations (or differential system for short) defined in $\mathbb{R}^3$ given by

$$\dot{x} = P(x,y,z), \qquad \dot{y} = Q(x,y,z), \qquad \dot{z} = R(x,y,z), \quad (1)$$

where $P,Q,R \in \mathbb{R}[x,y,z]$ and the dot denotes derivative with respect to the independent variable t, usually called the time, mainly in physical systems. The degree of system (1) is defined as the maximum of the degrees of polynomials P,Q and R. When the maximum degree is two, system (1) is called *quadratic*.

Manuscript received: 11 November 2021,
Revised: 3 February 2022,
Accepted: 8 February 2022.

[1] marcelo.messias1@unesp.br (**Corresponding Author**)
[2] paulino.silva@unesp.br

Beyond its theoretical importance, system (1) appears frequently in mathematical modeling of several dynamical phenomena arising in different areas, like Physics, Engineering, Biology and Chemistry, among others, as shown in the references (Alligood *et al.* 1996; Argyris *et al.* 2015; Cencini *et al.* 2010; Guckenheimer and Holmes 2002; Ott 2002; Strogatz 2001; Wiggins 2003). In this way, the study of the behavior of solutions of system (1) in its phase space is important to understand the phenomena modeled by it. The possible behaviors include stable and unstable equilibrium points and periodic orbits, quasi-periodic orbits, and chaotic dynamics. In particular, the interest in studying systems like (1) with chaotic behavior increased a lot in the last decades, due to their appearance in the study of several phenomena. One of the first chaotic systems studied was the famous and well-known Lorenz system (Lorenz 1963), which was the precursor of several other differential systems presenting such a behavior, like Rössler system (Rössler 1976), Rabinovich system (Llibre *et al.* 2008), Chen-Ueta system (Chen and Ueta 1999), Rikitake system (Llibre and Messias 2009), among others. The chaotic dynamics of these polynomial differential systems is directly related to the degree and values

of coefficients (also called parameters) of the polynomials which determine them. In fact, although often called "chaotic systems" in the literature, the solutions of most of them present chaotic behavior only for certain combinations of their parameter values. For instance, it was shown by Edward Lorenz in 1963 that the solutions of system

$$\begin{aligned} \dot{x} &= s\,(y-x)\,, \\ \dot{y} &= rx - y - xz, \\ \dot{z} &= -bz + xy, \end{aligned} \tag{2}$$

which has degree two (so it is quadratic), presents chaotic behavior if $s = 10, b = \frac{8}{3}$ and $r = 28$ (Lorenz 1963). Later on, it was shown by several authors that Lorenz system (2) has chaotic behavior for many other combinations of parameter values (see for instance the nice book (Sparrow 1982) or the more recent review (Algaba *et al.* 2018) and references cited in them).

The Lorenz system (2) is a polynomial differential system with peculiar quadratic nonlinearities, which appear in the second and third equations and are given by the crossed product of variables (i.e. xz and xy). This motivated the definition of a more general class of quadratic differential systems called *Lorenz-like systems*, given by

$$\begin{aligned} \dot{x} &= a_1x + b_1y + c_1z + d_1yz, \\ \dot{y} &= a_2x + b_2y + c_2z + d_2xz, \\ \dot{z} &= a_3x + b_3y + c_3z + d_3xy, \end{aligned} \tag{3}$$

where $a_i,\ b_i,\ c_i,\ d_i \in \mathbb{R},\ i = 1,2,3$. This kind of system is often cited in the literature concerning chaotic systems, because several classical quadratic polynomial differential systems like Rössler, Rabinovich, Chen-Ueta, Rikitake, beyond the Lorenz system itself, can be obtained from system (3) by appropriate choice of the parameters $a_i,\ b_i,\ c_i,\ d_i$.

As the chaotic dynamics of several subclasses of system (3) were obtained in literature, a quite natural question arises in this context: can we determine conditions on the parameters of system (3) which can guarantee that it is *nonchaotic*? This is an important issue that can be seen as the dual problem of knowing when system (3) is chaotic. There are several papers dedicated to study the nonchaotic behavior of polynomial systems, especially the quadratic ones, see for instance the series of papers by Heidel and Zhang (Heidel and Zhang 1999, 2007; Zhang and Heidel 1997, 2012; Zhang *et al.* 2008), by Malasoma (Malasoma 2009, 2002) and Yang (Yang 2000, 2002; Yang and Chen 2002). The question about the nonchaotic behavior of differential systems is also related to the integrability theory (Dumortier *et al.* 2006; Llibre 2004; Llibre and Zhang 2012), because the phase space of integrable differential systems can be completely determined by their first integrals, hence they are not chaotic. Despite the existence of such studies, a general criterion for determining the nonchaotic behavior of polynomial differential systems defined in $\mathbb{R}^3$, or a general characterization of the ω-limit sets of their solutions, like the Poincaré-Bendixson theorem for planar differential systems (Dumortier *et al.* 2006), is far from being obtained, even in the quadratic case.

In (Messias and Silva 2018), by using some elements of Darboux Theory of Integrability, namely invariant algebraic surfaces and Darboux invariants, we stated and proved a sufficient algebraic criterion which guarantees the nonchaotic behavior of differential system (1), for P, Q, R polynomials of any degree. Using this criterion, we proved also in (Messias and Silva 2018) the nonchaotic behavior for a huge class of quadratic polynomial differential systems which have a symmetric Jacobian matrix, giving a partial answer for a conjecture proposed by Zeraoulia and Sprott, which states that "Three-dimensional quadratic continuous-time differential systems with a symmetric Jacobian matrix cannot be chaotic".

Later on, in (Messias and Silva 2020) we studied third order ordinary differential equations of the form

$$\dddot{x} = j\,(x, \dot{x}, \ddot{x})\,, \tag{4}$$

called *jerk equations*. When j is a polynomial, it can be called a polynomial jerk equation. From the physical point of view, the third derivative can be seen as the derivative of the acceleration of a particle with position x, velocity $\dot{x}$ and acceleration $\ddot{x}$, so this type of equations has great interest in applications. Using the algebraic criterion stated in (Messias and Silva 2018), we obtained general conditions on the polynomial j that guarantee the nonchaotic behavior of equation (4), which is equivalent to a subclass of system (1) by the natural change of coordinates $\dot{x} = y,\ \dot{y} = z,\ \dot{z} = j(x, y, z)$.

In the context above, in this paper our main goal is to determine sufficient conditions on the parameters which can guarantee the nonchaotic behavior of Lorenz-like system (3). The paper is organized as follows. In Section 2 we present some preliminary results from Darboux theory of integrability and use them to state a sufficient (but not necessary) algebraic criterion for the noncahotic behavior of system (1). Using this criterion, in Section 3 we state sufficient algebraic conditions for system (3) to be nonchaotic. In Section 4, we give some examples of classical systems derived from system (3) which we can guarantee that, for some combinations of parameter values, do not present chaotic behavior, as Lorenz system, Rabinovich system, Chen-Ueta system, and certain Lorenz-like systems with $D2$ symmetry (Anastassiou *et al.* 2002; Zhu C., Liu Y. and Guo Y. 2010). The nonchaotic differential systems presented here have invariant algebraic surfaces, which contain the stable or unstable invariant manifolds of their equilibrium points. In Section 5, we show that, in some cases, the deformation of these invariant manifolds through the destruction of the invariant algebraic surfaces, by perturbing the parameter values in system (3), can reorganize the global structure of the phase space, leading to a transition from nonchaotic to chaotic behavior of such differential systems. Finally, in Section 6 we present some concluding remarks and comments.

SOME PRELIMINARIES FROM DARBOUX THEORY OF INTEGRABILITY

Here, as in (Messias and Silva 2018), the existence of invariant algebraic surfaces and Darboux invariants are used to give a sufficient algebraic criterion which guarantees the nonchaotic behavior of three-dimensional polynomial differential systems (see Theorem 1 ahead). The definitions and results presented in this section also appear in (Messias and Silva 2018; Messias and Silva 2020) and in other classical texts about integrability theory (Dumortier *et al.* 2006; Llibre 2004; Llibre and Zhang 2012), but they are included here for the sake of completeness and to make the text easier to read.

The Darboux theory of integrability provides a link between the integrability of polynomial differential systems (or polynomial vector fields) and their invariant algebraic surfaces. A nice presentation of this theory for planar polynomial differential systems can be found in (Llibre 2004) and in Chapter 8 of (Dumortier *et al.* 2006). Here we are interested in quadratic polynomial differential systems defined in $\mathbb{R}^3$, hence we will present the results for system

(1) with degree two, which is naturally associated to the vector field

$$X(x,y,z) = P(x,y,z)\frac{\partial}{\partial x} + Q(x,y,z)\frac{\partial}{\partial y} + R(x,y,z)\frac{\partial}{\partial z}, \quad (5)$$

where P, Q and R are the polynomials in the right-hand side of system (1). In the next section we will apply the results in the study of the Lorenz-like system (3).

Definition 1 *Let U be an open subset of $\mathbb{R}^3$. If there exists a nonlocally constant differentiable function $H : U \to \mathbb{R}$, which is constant on all solution curves $(x(t), y(t), z(t))$ of system (1) (or of the vector field (5)) contained in U, then H is called a first integral of X in U. Clearly H is a first integral of system (1) if and only if $X(H) \equiv 0$ on U, i.e.*

$$X(H) = \frac{dH}{dt} = \frac{\partial H}{\partial x}P + \frac{\partial H}{\partial y}Q + \frac{\partial H}{\partial z}R = 0$$

on the orbits of X contained in U, where $H = H(x(t), y(t), z(t))$.

Definition 2 *An invariant of system (1) on an open subset $U \subset \mathbb{R}^3$ is a nonlocally constant differentiable function I in the variables x, y, z and t such that I is constant on all solution curves $(x(t), y(t), z(t))$ of system (1) contained in U, i.e.*

$$\frac{dI}{dt} = \frac{\partial I}{\partial x}P + \frac{\partial I}{\partial y}Q + \frac{\partial I}{\partial z}R + \frac{\partial I}{\partial t} = 0$$

on the orbits of X contained in U.

An invariant I can be seen as a first integral of system (1) which depends on the time t.

Definition 3 *Let $f \in \mathbb{K}[x,y,z]$ be a non-locally constant polynomial, where $\mathbb{K}$ is either $\mathbb{R}$ or $\mathbb{C}$. The surface $f(x,y,z) = 0$ is an invariant algebraic surface of system (1) if there exists a polynomial $K \in \mathbb{K}[x,y,z]$ such that*

$$X(f) = \frac{\partial f}{\partial x}P + \frac{\partial f}{\partial y}Q + \frac{\partial f}{\partial z}R = Kf.$$

The polynomial K is called the cofactor of the invariant algebraic surface $f = 0$.

Note that, as system (1) has degree 2, then the degree of the cofactor K is at most 1. Moreover, when $K = 0$, then f is a polynomial first integral of system (1).

Definition 4 *Let $g, h \in \mathbb{K}[x,y,z] \setminus \{0\}$ and assume that g and h are relatively prime polynomials in the ring $\mathbb{K}[x,y,z]$, or that $h = 1$, where $\mathbb{K}$ is either $\mathbb{R}$ or $\mathbb{C}$. Then the function $F = exp(g/h)$ is called an exponential factor of system (1) if for some polynomial $L \in \mathbb{K}[x,y,z]$ of degree at most $m-1$ we have that*

$$X(F) = \frac{\partial F}{\partial x}P + \frac{\partial F}{\partial y}Q + \frac{\partial F}{\partial z}R = LF.$$

We say that an invariant I of X is of *Darboux type* or a *Darboux invariant* if it can be written as

$$I(x,y,z,t) = {f_1}^{\lambda_1} \dots {f_p}^{\lambda_p} {F_1}^{\mu_1} \dots {F_q}^{\mu_q} e^{st}, \quad (6)$$

where $f_i = 0$ are invariant algebraic surfaces of X for $i = 1, \dots, p$; F_j are exponential factors of X for $j = 1, \dots, q$; $\lambda_i, \mu_j \in \mathbb{C}$ and $s \in \mathbb{R} \setminus \{0\}$.

The following result holds.

Proposition 1 *If $f(x,y,z) = 0$ is an invariant algebraic surface of system (1) with a constant cofactor $K = k \in \mathbb{R} \setminus \{0\}$, then $I = f(x,y,z)\, e^{-kt}$ is a Darboux invariant of this system.*

Proof. *Let $\phi(t) = (x(t), y(t), z(t))$ be a solution and $f = 0$ be an invariant algebraic surface of system (1) (or of the vector field (5)). Then we have*

$$\begin{aligned} \frac{d}{dt}I(\phi(t)) &= \frac{d}{dt}\left[f(\phi(t))\, e^{-kt}\right] = \\ &= \left[\tfrac{\partial f}{\partial x}P + \tfrac{\partial f}{\partial y}Q + \tfrac{\partial f}{\partial z}R\right] e^{-kt} - kf(\phi(t))e^{-kt} = \\ &= kf(\phi(t))e^{-kt} - kf(\phi(t))e^{-kt} = 0 \end{aligned}$$

While the knowledge of a first integral of system (1) in $\mathbb{R}^3$ allows to reduce its study in one dimension, the knowledge of a Darboux invariant provides information about the α and ω-limit sets of all orbits of system (1). Indeed, the following result, proved in (Llibre and Oliveira 2015) for planar polynomial differential systems, can be easily extended to polynomial differential systems defined in $\mathbb{R}^3$ and gives a relation between the existence of Darboux invariants and the α and ω–limit sets of the solutions of such systems.

Proposition 2 *Let $I(x,y,z,t) = f(x,y,z)e^{st}$ be a Darboux invariant of system (1). Let $p \in \mathbb{R}^3$ and $\varphi_p(t)$ be the solution of system (1) with maximal interval (α_p, ω_p) such that $\varphi_p(0) = p$. The following statements hold.*

(a) If $\omega_p = \infty$ then $\omega(p) \subset \overline{\{f(x,y,z) = 0\}} \cup \mathbb{S}^2$, where $\mathbb{S}^2$ is the boundary of the Poincaré ball (at infinity).

(b) If $\alpha_p = -\infty$ then $\alpha(p) \subset \overline{\{f(x,y,z) = 0\}} \cup \mathbb{S}^2$, where $\mathbb{S}^2$ is the boundary of the Poincaré ball (at infinity).

The definition of Poincaré ball is given, for instance, in (Llibre *et al.* 2008). Note that in Proposition 2 the function f is of the form $f = f_1^{\lambda_1} \dots f_p^{\lambda_p} F_1^{\mu_1} \dots F_q^{\mu_q}$, as in (6).

In (Messias and Silva 2018) we proved the following result.

Theorem 1 [Algebraic criterion for nonchaoticity] *Let X be the vector field (5), associated to differential system (1). If X has an invariant algebraic surface $f = 0$ with a constant cofactor $K = k \in \mathbb{R} \setminus \{0\}$, then the α and ω-limit sets of each orbit $\phi_p(t) = (x(t), y(t), z(t))$ with $\phi_p(0) = p \in \mathbb{R}^3$, are both contained in $\overline{\{f = 0\}} \cup \mathbb{S}^2$, where $\mathbb{S}^2$ represents the points at infinity of $\mathbb{R}^3$. In particular, X does not present chaotic behavior.*

The algebraic criterion stated in Theorem 1 gives a sufficient but not necessary condition for the nonchaotic behavior of the vector field (5). Indeed, there are several differential systems proved to be nonchaotic in the literature (Zhang and Heidel 1997, 2012; Zhang *et al.* 2008; Yang 2000, 2002; Yang and Chen 2002), which have no invariant algebraic surfaces. Furthermore, we observe that the hypothesis of a constant cofactor is essential in Theorem 1. Indeed, in (Jafari *et al.* 2016; Li *et al.* 2021) the authors gave examples of chaotic systems which have algebraic surfaces formed by equilibrium points (which are obviously invariant algebraic surfaces). However, we checked these cases and in all of them the cofactors of the invariant algebraic surfaces are not constant.

In the next section we will use Theorem 1 to obtain sufficient conditions for the nonchaotic behavior of Lorenz-like systems (3).

STATEMENT AND PROOF OF THE MAIN RESULTS: NON-CHAOTIC LORENZ-LIKE SYSTEMS

In the following result we give a huge class of Lorenz-like systems which do not present chaotic behavior.

Theorem 2 *Let $X = X(x,y,z)$ be the vector field associated to system (3). For the parameter values $a_1 = b_2 = \frac{1}{2}k, c_3 = k$, $d_3 \neq 0$ and the other parameters satisfying the system*

$$\begin{cases} (2a_2c_1 + kc_2)\, d_3 - 2a_3\,(a_2d_1 - b_1d_2) = 0, \\ (2b_1c_2 + kc_1) + 2b_3\,(a_2d_1 - b_1d_2) = 0, \end{cases} \tag{7}$$

the vector field $X = X(x,y,z)$ has the invariant algebraic surface

$$f(x,y,z) = -d_2x^2 - 2c_2x + d_1y^2 + 2c_1y - 2\frac{a_2d_1 - b_1d_2}{d_3}z \tag{8}$$

with cofactor $k \in \mathbb{R}$. Consequently, for these choice of parameters, system (3) does not present chaotic behavior.

Proof. *Consider the vector field $X = (P,Q,R)$ associated to system (3) with the choice of parameters given in Theorem 2. Then, the system reduces to*

$$\begin{aligned} \dot{x} &= P(x,y,z) = \frac{k}{2}x + b_1y + c_1z + d_1yz, \\ \dot{y} &= Q(x,y,z) = a_2x + \frac{k}{2}y + c_2z + d_2xz, \\ \dot{z} &= R(x,y,z) = a_3x + b_3y + kz + d_3xy, \end{aligned} \tag{9}$$

where the parameters $a_2, a_3, b_1, b_3, c_1, c_2, d_1, d_2$ satisfy system (7). In this way, the function (8) is a Darboux polynomial of system (9), with cofactor $k \in \mathbb{R}$. In fact, we have

$$\begin{aligned} &\langle \nabla f, X\rangle = \\ &\tfrac{\partial f}{\partial x}(x,y,z)P(x,y,z) + \tfrac{\partial f}{\partial y}(x,y,z)Q(x,y,z) + \tfrac{\partial f}{\partial z}(x,y,z)R(x,y,z) \\ &= -kd_2x^2 - kc_2x + 2c_1a_2x + kd_1y^2 + kc_1y - 2c_2b_1y - \\ &-2k\frac{(a_2d_1 - b_1d_2)}{d_3}z - 2a_3\frac{(a_2d_1 - b_1d_2)}{d_3}x - 2b_3\frac{(a_2d_1 - b_1d_2)}{d_3}y \\ &= k\left(-d_2x^2 - 2c_2x + d_1y^2 + 2c_1y - 2k\frac{(a_2d_1 - b_1d_2)}{d_3}z\right) \\ &+\frac{(2a_2c_1 + kc_2)\, d_3 - 2a_3\,(a_2d_1 - b_1d_2)}{d_3}x - \\ &-\frac{(2b_1c_2 + kc_1) + 2b_3\,(a_2d_1 - b_1d_2)}{d_3}y \\ &= kf(x,y,z). \end{aligned}$$

Hence, $f(x,y,z) = 0$ is an invariant algebraic surface of system (3), with cofactor $k \in \mathbb{R}$. Therefore, by Theorem 1 this system does not present chaotic behavior.

Remark Let $X = X(x,y,z)$ be the vector field associated to system (9) and $f(x,y,z) = 0$ the invariant algebraic surface given in Theorem 2. Then, we have that
a) $f(x,y,z)$ is a first integral of system (9) if, and only if, $k = 0$. In this case, the phase space is foliated by the invariant algebraic surfaces $f(x,y,z) = c$, $c \in \mathbb{R}$;
b) The vector field X is dissipative if, and only if, $k < 0$. If $k = 0$, then X is conservative.

Theorem 3 *Let $X = X(x,y,z)$ be the vector field associated to system (3) with the choice of parameters $a_1 = b_2 = c_3 = \frac{1}{2}k$, $b_1 = a_2\alpha$, and*

$$\begin{cases} c_1d_3 + a_3\,(d_2\alpha - d_1) = 0, \\ \alpha c_2d_3 - b_3\,(d_2\alpha - d_1) = 0, \end{cases} \tag{10}$$

where $\alpha, k \in \mathbb{R}$ and $\alpha d_3 \neq 0$. Then, system (3) presents the invariant algebraic surface

$$f(x,y,z) = -x^2 + \alpha y^2 - \frac{(d_2\alpha - d_1)}{d_3}z^2, \tag{11}$$

with cofactor $k \in \mathbb{R}$. Consequently, the system does not present chaotic behavior.

Proof. *Consider the vector field $X = (P,Q,R)$ associated to system (3) with the choice of parameters given in Theorem 3. Then, we have*

$$\begin{aligned} \dot{x} &= P(x,y,z) = \frac{k}{2}x + a_2\alpha y + c_1z + d_1yz, \\ \dot{y} &= Q(x,y,z) = a_2x + \frac{k}{2}y + c_2z + d_2xz, \\ \dot{z} &= R(x,y,z) = a_3x + b_3y + \frac{k}{2}z + d_3xy. \end{aligned} \tag{12}$$

In this way, the function (11) is a Darboux polynomial of system (12) with cofactor $k \in \mathbb{R}$. In fact, we have

$$\begin{aligned} &\langle \nabla f, X\rangle = \\ &= \tfrac{\partial f}{\partial x}(x,y,z)P(x,y,z) + \tfrac{\partial f}{\partial y}(x,y,z)Q(x,y,z) + \tfrac{\partial f}{\partial z}(x,y,z)R(x,y,z) = \\ &= -kx^2 + k\alpha y^2 - k\frac{(d_2\alpha - d_1)}{d_3}z^2 - 2c_1xz + 2\alpha c_2yz \\ &-2a_3\frac{(d_2\alpha - d_1)}{d_3}xz - 2b_3\frac{(d_2\alpha - d_1)}{d_3}yz \\ &= k\left(-x^2 + \alpha y^2 - \frac{(d_2\alpha - d_1)}{d_3}z^2\right) \\ &-2\frac{(c_1d_3 + a_3\,(d_2\alpha - d_1))}{d_3}xz + 2\frac{(\alpha c_2d_3 - b_3\,(d_2\alpha - d_1))}{d_3}yz \\ &= kf(x,y,z). \end{aligned}$$

Hence, $f(x,y,z) = 0$ is an invariant algebraic surface of system (3), with cofactor $k \in \mathbb{R}$. Therefore, by Theorem 1 this system does not present chaotic behavior.

It follows from the results above that system (3) has a plane as an invariant algebraic surface if and only if $d_1 = d_2 = d_3 = 0$, that is, only when it is linear. On the other hand, such system may have invariant algebraic surfaces with degrees $n \geq 3$, however we did not study these cases in this note, since the conditions on the coefficients are very huge and complicated, due to the great number of parameters.

EXAMPLES AND APPLICATIONS

We can relate the classes of nonchaotic systems obtained in Theorems 2 and 3 with some classical Lorenz-like systems which appear in the literature. Since some "chaotic" Lorenz-like systems are actually chaotic only for some parameter values, they can be nonchaotic for other choices of parameters. Some examples are presented below.

Lorenz system

The Lorenz systems (2) is maybe the most famous system which is known to be chaotic for certain parameter values (Algaba *et al.* 2018; Lorenz 1963; Sparrow 1982). Using Theorem 2 we can obtain some subclasses of Lorenz system which are not chaotic. We observe that a more general and detailed study of Lorenz system having invariant algebraic surfaces, including the dynamics at infinity via the Poincaré compactification, was made in (Llibre *et al.* 2010).

a) Consider in Theorem 2, the parameter values $a_3 = b_3 = c_1 = c_2 = d_1 = 0, b_1 = d_3 = 1, d_2 = -1, k = -2$ and $a_2 \in \mathbb{R}$, which corresponds to the Lorenz system (2) with parameters $s = 1, r = a_2$ and $b = 2$, that is

$$\begin{aligned} \dot{x} &= y - x, \\ \dot{y} &= a_2 x - y - xz, \\ \dot{z} &= -2z + xy, \end{aligned} \tag{13}$$

which has the parabolic cylinder $x^2 - 2z = 0$ as an invariant algebraic surface with cofactor $k = -2$, hence from Theorem 2, it is not chaotic.

b) Consider the choice of parameters in Theorem 3 as $a_3 = b_3 = c_1 = c_2 = d_1 = 0, d_2 = -1, d_3 = 1, \alpha = \frac{1}{a_2}, k = -2$, and $a_2 \neq 0$, which corresponds to the Lorenz system (2) with parameters $s = 1, r = a_2$ and $b = 1$. Then, we get the nonchaotic system

$$\begin{aligned} \dot{x} &= y - x, \\ \dot{y} &= a_2 x - y - xz, \\ \dot{z} &= -z + xy, \end{aligned} \tag{14}$$

which has the cone $-x^2 + \frac{1}{a_2}\left(y^2 + z^2\right) = 0$ as an invariant algebraic surface with cofactor $k = -2$.

The phase portraits of systems (13) and (14) on the respective invariant algebraic surfaces are shown in Figures 1 and 2.

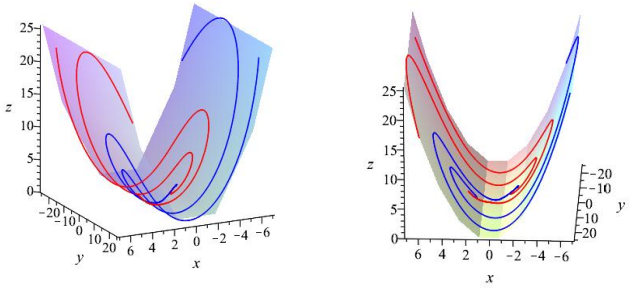

Figure 1 Phase portrait of system (13) with $a_2 = 3$.

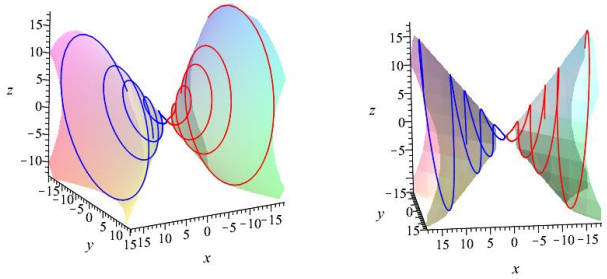

Figure 2 Phase portrait of system (14) with $a_2 = 1$.

Rabinovich system

The Rabinovich system (Llibre *et al.* 2008) is an example of Lorenz-like system. It is given by

$$\begin{aligned} \dot{x} &= hy - v_1 x + yz, \\ \dot{y} &= hx - v_2 y - xz, \\ \dot{z} &= -v_3 z + xy, \end{aligned} \tag{15}$$

with $h, v_1, v_2, v_3 \in \mathbb{R}$. It is known that system (15) presents chaotic behavior for the parameter values $v_1 = 4, v_2 = v_3 = 1$ and $h = 6,75$ (Llibre *et al.* 2008). Using Theorem 2, we can obtain the following cases in which the Rabinovich system has an invariant algebraic surface with constant cofactor, thus the system does not present chaotic behavior in theses cases.

a) Following Theorem 3 and considering the parameters $a_3 = b_3 = c_1 = c_2 = 0, d_1 = d_3 = 1, d_2 = -1, b_1 = a_2$, and $k = -2v$ in system (15), we obtain $v_1 = v_2 = v, v_3 = 2v$ with $v \in \mathbb{R}$ and $h = a_2$, which lead to the following system

$$\begin{aligned} \dot{x} &= hy - vx + yz, \\ \dot{y} &= hx - vy - xz, \\ \dot{z} &= -2vz + xy, \end{aligned} \tag{16}$$

which has the invariant algebraic surface $x^2 + y^2 - 4hz = 0$ with constant cofactor $-2v \in \mathbb{R}$. From Theorem 3 follows that system (16) is not chaotic.

b) Following Theorem 3 and considering the parameters $a_3 = b_3 = c_1 = c_2 = 0, d_1 = d_3 = 1, d_2 = -1, \alpha = 1$ and $k = -2v$ with $v \in \mathbb{R}$ in system (15), we obtain $v_1 = v_2 = v_3 = v, h = a_2$ and the system

$$\begin{aligned} \dot{x} &= hy - vx + yz, \\ \dot{y} &= hx - vy - xz, \\ \dot{z} &= -vz + xy, \end{aligned} \tag{17}$$

which has the invariant algebraic surface $-x^2 + y^2 + 2z^2 = 0$, with constant cofactor $-2v \in \mathbb{R}$, therefore it is not chaotic.

The phase portraits of systems (16) and (17) on the invariant algebraic surfaces described above are shown in Figures 3 (a) and (b), respectively.

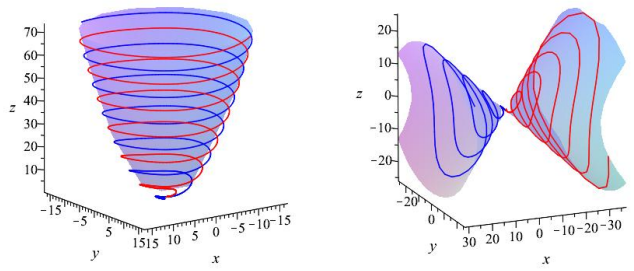

(a) $h = v = 1$ (b) $h = v = 1$

Figure 3 (a) Phase portrait of system (16); (b) Phase portrait of system (17). In both cases, $v = h = 1$.

Chen-Ueta system

As a subclass of the Lorenz-like system (3) there is the known Chen-Ueta system, given by (Chen and Ueta 1999)

$$\begin{aligned} \dot{x} &= a\,(y - x)\,, \\ \dot{y} &= (c - a)\,x + cy - xz, \\ \dot{z} &= -bz + xy, \end{aligned} \tag{18}$$

where $a, b, c \in \mathbb{R}$. System (18) has chaotic behavior for the parameter values $a = 35, b = 3$ and $c = 28$, as shown in (Chen and Ueta 1999). The global dynamical behavior of system (18) having invariant algebraic surfaces, including the behavior at infinity using Poincaré compactification, was done in (Llibre *et al.* 2012). Using Theorem 2, we can give some examples of Chen-Ueta system without chaotic behavior.

Considering Theorem 2 and taking the parameters $a_3 = b_3 = c_1 = c_2 = d_1 = 0, a_2 = k, b_1 = -\frac{1}{2}k, d_2 = -1, d_3 = 1, c_2 = 0, k = 2r$ with $r \in \mathbb{R}$ in system (18) we obtain $a = -r, c = r, b = -2r$ and the nonchaotic system

$$\begin{aligned} \dot{x} &= -r\,(y - x)\,, \\ \dot{y} &= 2rx + ry + xz, \\ \dot{z} &= 2rz - xy, \end{aligned} \tag{19}$$

which has $x^2 - 2rz = 0$ as invariant algebraic surface, with constant cofactor $k = 2r$. The phase portrait of system (19) on this surface is given in Figure 4.

Lorenz-like system with $D2$ Symmetry

In (Anastassiou *et al.* 2002), the authors studied the following differential system, derived from Lorenz-like system (3):

$$\begin{aligned} \dot{x} &= a_1 x + d_1 yz, \\ \dot{y} &= b_2 y + d_2 xz, \\ \dot{z} &= c_3 z + d_3 xy, \end{aligned} \tag{20}$$

where $a_1, b_2, c_3, d_1, d_2, d_3 \in \mathbb{R}$. System (20) has several types of symmetry, as pointed out in (Anastassiou *et al.* 2002), and has

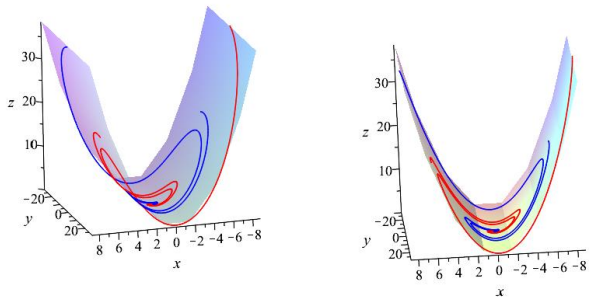

Figure 4 Phase portrait of Chen system (19) with $r = 1$.

chaotic behavior for some choices of parameter values a_1 and b_2. They also showed that the function $V(x, y, z) = x^2 + y^2 + 2z^2$ is a Lyapunov function for system (20) if $a_1, b_2 > 0$ and $c_3 = d_1 = d_2 = 1, d_3 = \pm 1$.

Considering in Theorem 3 the parameter values $a_2 = a_3 = b_3 = c_1 = c_2 = 0$ and taking $a_1 = b_2 = c_3 = k/2$ we obtain the following subclass of system (20)

$$\begin{aligned} \dot{x} &= \frac{k}{2}x + d_1 yz, \\ \dot{y} &= \frac{k}{2}y + d_2 xz, \\ \dot{z} &= \frac{k}{2}z + d_3 xy. \end{aligned} \tag{21}$$

From Theorem 3, it follows that system (20) has no chaotic dynamics in this case, for any parameters $d_1, d_2, d_3 \in \mathbb{R}$, with $d_3 \neq 0$, since it has the invariant algebraic surface

$$f(x, y, z) = -x^2 + \alpha y^2 - \frac{(d_2\alpha - d_1)}{d_3}z^2 = 0, \tag{22}$$

with constant cofactor $k \in \mathbb{R}$, for any $\alpha \in \mathbb{R}$.

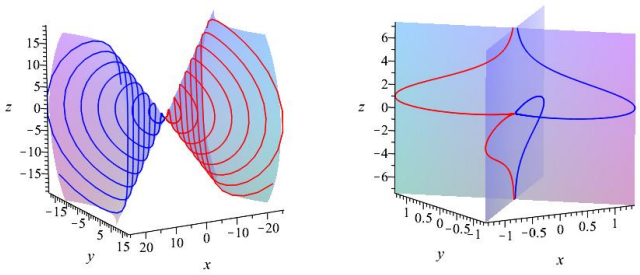

(a) $\alpha = 2$ (b) $\alpha = 1$

Figure 5 Phase portrait of $D2$ system in the case of system (21) for the parameters $k = 2, d_1 = d_2 = 1, d_3 = -1$, and: (a) $\alpha = 2$; (b) $\alpha = 1$.

From these calculations, we can see that for the choice of parameters $c_1 = d_1 = d_2 = 1, d_3 = -1$, system (20) has a cone and two planes intersecting at the z-axis as invariant algebraic surfaces. In fact, taking $\alpha = 1$, we obtain from equation (22) that $-x^2 + y^2 = 0$ is an invariant algebraic surface with cofactor k. Furthermore, for $\alpha = 2$ we obtain $-x^2 + 2y^2 + z^2 = 0$, which implies that system (20) has an invariant cone (see Figure 5 (a)), and for $\alpha = 1$ this system has two invariant planes, see Figure 5 (b)). These results complement the ones obtained in (Anastassiou *et al.* 2002).

Zhu-Liu-Guo symmetric Lorenz-like system

In (Zhu C., Liu Y. and Guo Y. 2010), the authors studied the Lorenz-like system given by

$$\begin{aligned} \dot{x} &= -x - \beta_1 y + yz, \\ \dot{y} &= \beta_2 y - xz, \\ \dot{z} &= -\beta_3 z + xy, \end{aligned} \tag{23}$$

where $\beta_1, \beta_2, \beta_3 \in \mathbb{R}$. This system has the symmetry $(x, y, z) \mapsto (-x, -y, z)$ and present chaotic behavior for certain parameter values, as shown in (Zhu C., Liu Y. and Guo Y. 2010). Considering Theorem 2, and choosing $a_2 = a_3 = b_3 = c_1 = c_2 = 0, d_1 = d_3 = 1, d_2 = -1$, with $b_1 \neq 0$ and $k = -2$, we obtain $\beta_1 = -b_1, \beta_2 = -1, \beta_3 = 2$ and the subclass of system (23) given by

$$\begin{aligned} \dot{x} &= -x - b_1 y + yz, \\ \dot{y} &= -y - xz, \\ \dot{z} &= -2z + xy, \end{aligned} \tag{24}$$

which has the invariant algebraic surface $x^2 + y^2 + 2b_1 z = 0$, with cofactor $k = -2$. It follows from Theorem 1 that system (24) do not present chaotic behavior, see their phase portrait on the respective invariant algebraic surface in Figure 6.

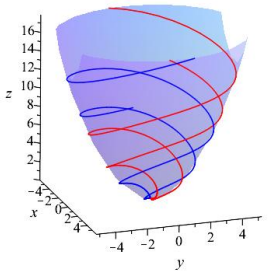

Figure 6 Phase portrait of Zhu system (24), with $b_1 = -1$.

TRANSITION FROM NONCHAOTIC TO CHAOTIC BEHAVIOR IN LORENZ-LIKE SYSTEMS

In this section we will study the transition from nonchaotic to chaotic behavior in some Lorenz-like systems. The nonchaotic differential systems presented in the previous sections have invariant algebraic surfaces with constant cofactor, hence their equilibrium points are contained in the invariant algebraic surfaces, which therefore contain the stable (or unstable) manifolds of these equilibria. We will see that a small perturbation in the parameters of a nonchaotic system can destroy the invariant algebraic surface and, consequently, deform the invariant manifolds and reorganize the global structure of the phase space, leading to the creation of chaotic behavior in these systems. In order to show this transition from nonchaotic to chaotic behavior, via perturbation, we will analyze the Rabinovich system (15). As already mentioned, this system presents chaotic behavior for the parameter values $v_1 = 4, v_2 = v_3 = 1$ and $h = 6.75$, having in this case the chaotic attractor shown in Figure 7.

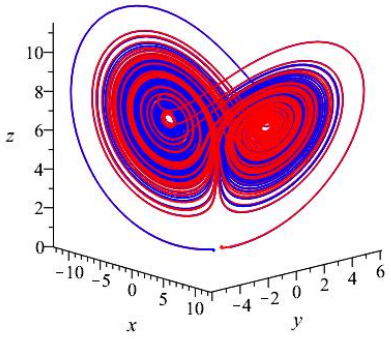

Figure 7 Chaotic attractor of Rabinovich system (15) with parameter values $h = 6.75, v_1 = 4, v_2 = v_3 = 1$.

Considering now system (15) in the conditions of Theorem 3, taking the parameter values $h = a_2, v_1 = v_2 = v_3 = v$, we obtain system (17), which presents the cone $-x^2 + y^2 + 2z^2 = 0$ as an invariant algebraic surface with cofactor $k = -2v \in \mathbb{R}$, hence it has no chaotic behavior (see Figure 3 (b)). In order to destroy the invariant algebraic surface in such a way that system (17) can generate chaotic behavior, we will use the following variation of this system

$$\begin{aligned} \dot{x} &= hy - v_1 x + yz, \\ \dot{y} &= hx - vy - xz, \\ \dot{z} &= -vz + xy, \end{aligned} \tag{25}$$

where $v_2 = v_3 = v$ are fixed and equal to 1 and $h = 6.75$. Then, we will vary v_1 in order to deform the invariant cone and produce chaotic behavior. Varying v_1 in the interval $[1, 3.8]$, we obtained the solutions of system (25) with initial conditions $(\pm 0.6, \pm 0.6, 0)$, shown in Figures 8 to 12. In these figures, we can see the deformation of the invariant cone and the transition of solutions ranging from nonchaotic to chaotic behavior.

We observe that, when the parameter $v_1 = 1$, system (25) presents a cone as an invariant algebraic surface and three singular points belonging to the invariant cone: a saddle at the origin and two stable foci. Hence, the stable manifolds of the foci are contained in the invariant cone. When v_1 is different from 1, the structure given by the invariant cone and the singular points is deformed and the system has no longer invariant algebraic surfaces, so the invariant manifolds are deformed. As v_1 moves away from $v_1 = 1$, the behavior of solutions become more and more complex and, for $v_1 = 3.8$ the chaotic attractor is created, as shown in Figure 12.

We can conclude that the formation of chaotic dynamics was due to the deformation of the invariant manifolds of the equilibrium points, which were initially (for $v_1 = 1$) contained on the invariant cone, with the destruction of this cone (for $v_1 \neq 1$).

The same type of analysis can be done for the Rabinovich chaotic system presented in (Llibre *et al.* 2008). In such work, the authors have shown that system (15) presents a four-wings chaotic attractor for the parameter values given by $h = 0.04$, $v_1 = -1.5$, $v_2 = -0.3$ and $v_3 = -1.67$, as shown in see Figure 13. Let us see that this chaotic attractor can be obtained by the deformation of an invariant algebraic surface through the variation of the parameter values.

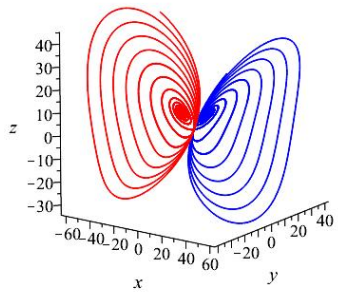

Figure 8 Two solutions of Rabinovich system (25) with parameter values $h = 6.75, v = v_1 = 1$ and initial conditions $(\pm 0.6, \pm 0.6, 0)$.

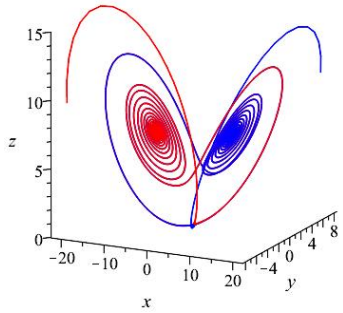

Figure 9 Two solutions of Rabinovich system (25) with parameter values $h = 6.75, v = 1, v_1 = 1.5$ and initial conditions $(\pm 0.6, \pm 0.6, 0)$.

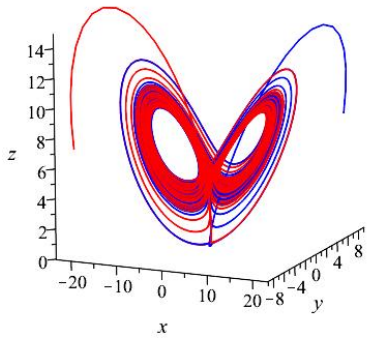

Figure 10 Two solutions of Rabinovich system (25) with parameter values $h = 6.75, v = 1, v_1 = 2$ and initial conditions $(\pm 0.6, \pm 0.6, 0)$.

Consider the Rabinovich system (15) with $h = 0.0$, $v_1 = v_3$ and $v_2 \in \mathbb{R}$. In this case, system (15) is in the hypothesis of Theorem 3, having the invariant algebraic surface $-x^2 + z^2 = 0$, given by two intersecting invariant planes, with constant cofactor $-2v_1$, hence it does not present chaotic behavior. In order to study the deformation of the invariant planes of system (15), we will vary the parameter h in the interval $[0, 0.0201]$ and consider also $v_1 \neq v_3$.

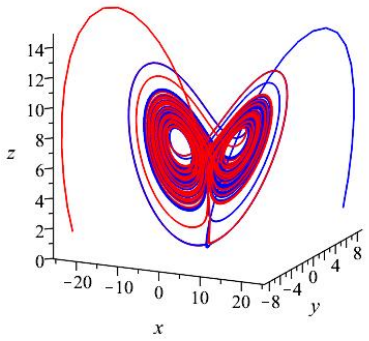

Figure 11 Two solutions of Rabinovich system (25) with parameter values $h = 6.75, v = 1, v_1 = 3$ and initial conditions $(\pm 0.6, \pm 0.6, 0)$.

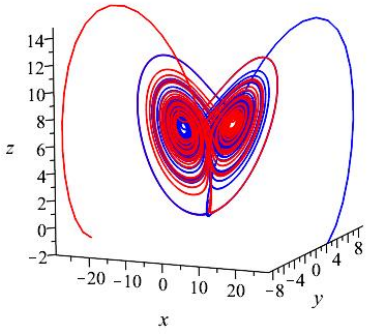

Figure 12 Two solutions of Rabinovich system (25) with parameter values $h = 6.75, v = 1, v_1 = 3.8$ and initial conditions $(\pm 0.6, \pm 0.6, 0)$.

As the invariant algebraic planes $-x^2 + z^2 = 0$ does not depend on the variable y, we can modify the second equation of the system without changing the invariant algebraic surface, hence based on our knowledge on the existence of the four-wings attractor shown in Figure 13, we will take the parameter values $v_1 = v_3 = -1.5$ and $v_2 = 0.3$. In this case, system (15) has five singular points belonging to the invariant algebraic surface $-x^2 + z^2 = 0$: four unstable foci and one saddle at the origin (see Figure 14). Hence, the global two-dimensional unstable manifolds of the unstable foci are contained in the invariant planes $-x^2 + z^2 = 0$ and the global one-dimensional unstable manifold of the saddle at the origin is given exactly by the intersection of these planes.

Keeping $h = 0.0$, taking the parameter $v_1 = -1.5$ and changing slightly the parameter v_3 to $v_3 = -1.6$, we can see that system (15) has no longer the two invariant planes, but it is not yet chaotic, see Figure 15. The same occurs for $v_3 = -1.67$, as shown in Figure 16. In Figures 15 and 16, we have taken the initial conditions $(0.6, 1.5, 0.6)$, $(-0.6, 1.5, -0.6)$, $(-0.6, -1.5, 0.6)$ and $(0.6, -1.5, -0.6)$.

In order to deform the two invariant planes with the structure contained on them (five singular points), to generate the chaotic behavior, we will now vary the parameter h. Taking $h \in [0, 0.01]$ we obtain solutions topologically equivalent to

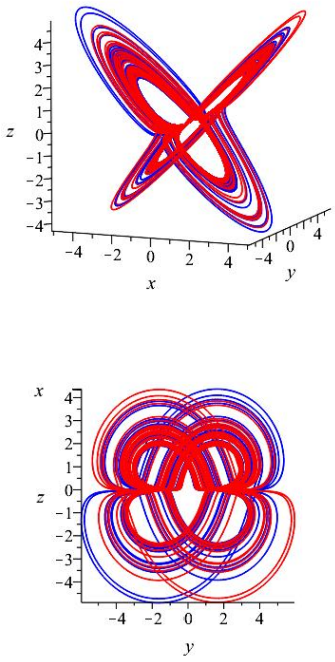

Figure 13 Four-wings chaotic attractor of Rabinovich system with parameters $h = 0.04, v_1 = -1.5, v_2 = 0.3, v_3 = -1.67$, and its projection on the yz-plane. Initial conditions: $(\pm 0.6, \pm 1.5, \pm 0.6)$. Time integration: $t \in [800, 1100]$.

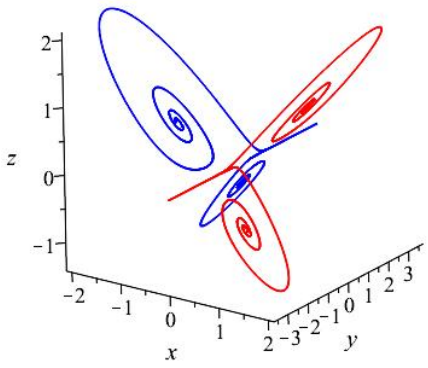

Figure 14 Phase portrait of the system (15) with parameters $h = 0.0$, $v_1 = v_3 = -1.5$, and $v_2 = 0.3$. The system has two invariant planes and five equilibrium points: a saddle at the origin and four unstable foci. Initial conditions $(0.6, 1.5, 0.6)$, $(-0.6, 1.5, -0.6)$, $(-0.6, -1.5, 0.6)$ and $(0.6, -1.5, -0.6)$.

the ones shown in Figure 17, where we have taken the same initial conditions $(0.6, 1.5, 0.6)$, $(-0.6, 1.5, -0.6)$, $(-0.6, -1.5, 0.6)$ and $(0.6, -1.5, -0.6)$ and the time of integration $t \in [300, 350]$ in order to exclude the transient part of the solutions and to obtain only the representation of the $\omega-$limit set.

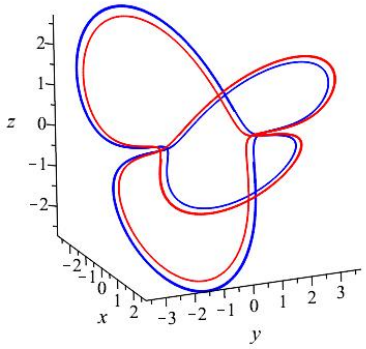

Figure 15 Phase portrait of system (15) with parameters $h = 0.0$, $v_1 = -1.5$, $v_3 = -1.6$, $v_2 = 0.3$ The system has no longer the invariant planes, but there is no chaotic behavior yet. Time integration: $t \in [120, 150]$.

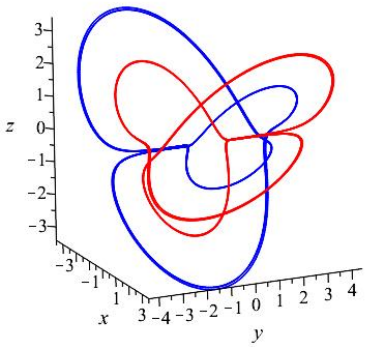

Figure 16 Phase portrait of system (15) with parameters $h = 0.0$, $v_1 = -1.5$, $v_3 = -1.67$, $v_2 = 0.3$ Time integration: $t \in [120, 150]$.

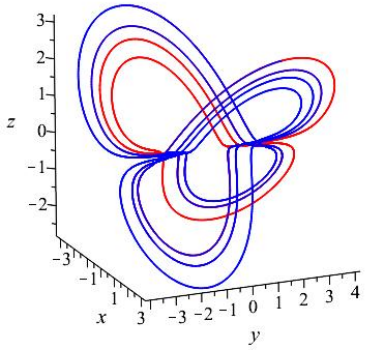

Figure 17 Phase portrait of system (15) with parameters $h = 0.01$, $v_1 = -1.5$, $v_3 = -1.67$, $v_2 = 0.3$ Time integration: $t \in [300, 350]$.

Taking $h = 0.015$ and the same initial conditions, we observe that the solutions become more complex, as shown in Figure 18.

Now taking $h \in [0, 0.02]$ and the same initial conditions, we

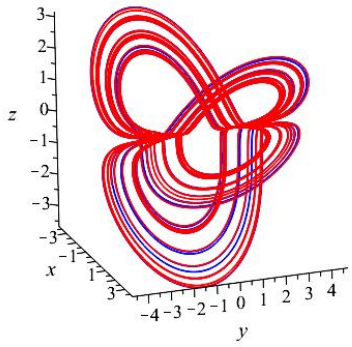

Figure 18 Phase portrait of system (15) with parameters $h = 0.015$, $v_1 = -1.5$, $v_3 = -1.67$, $v_2 = 0.3$ Time integration: $t \in [600, 800]$.

finally obtain a four-wings chaotic attractor, shown in Figure 19, which is similar to the attractor of Figure 13.

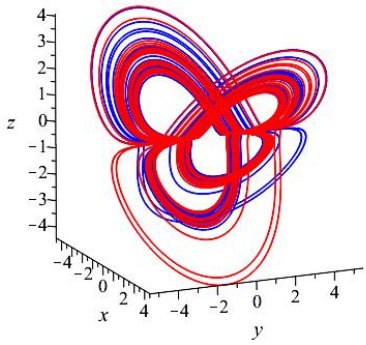

Figure 19 Phase portrait of system (15) with $h = 0.02$, $v_1 = -1.5$, $v_3 = -1.67$, $v_2 = 0.3$ Observe the existence of a four-wings chaotic attractor. Time integration: $t \in [800, 1000]$.

We can see from Figures 14 to 19 that the deformation of the invariant manifolds of the equilibrium points of system (15), which are contained on the invariant planes for $h = 0.0$ and $v_1 = v_3$, through the variation of the parameter values, lead to the transition from nonchaotic to chaotic behavior of this system.

CONCLUSIONS

In this paper we gave sufficient algebraic conditions for some classes of the generalized Lorenz-like system (3) to be nonchaotic. More precisely, these systems have no chaotic behavior when they have an invariant algebraic surface with constant cofactor, as stated in Theorem 1. We also have shown that, in some cases, the deformation of the invariant manifolds of equilibrium points, contained on the invariant surfaces of nonchaotic Lorenz-like systems, by perturbing their parameter values, can deform and reorganize the global phase space structure, leading to the chaotic behavior of these systems. The results presented here are quite general and can be used to study other Lorenz-like systems than the examples presented here.

We believe that the results presented here are somehow related to the works (Osinga and Krauskopf 2002, 2004) on the determination of global one or two-dimensional stable and unstable manifolds of critical elements (mainly singular points and periodic orbits) of chaotic differential systems (as the Lorenz system), in order to describe how these manifolds organize the global phase space of such systems. In these studies, a better understanding of the global behavior of chaotic dynamics were obtained. Analogously, in this paper we could see that the invariant algebraic surfaces of nonchaotic Lorenz-like systems contain the stable (or unstable) manifolds of critical elements because, as the cofactor of these surfaces are constant, all the equilibrium points of the nonchaotic systems are contained on them. Also, the deformation of these invariant algebraic surfaces may lead do the creation of chaotic dynamics, as shown for instance in the Rabinovich system. We think that this ideas may be further developed, aiming to obtain a better understanding of the organization of phase space for nonchaotic and chaotic differential systems by the stable and unstable manifolds of their equilibrium points.

We can conclude saying that, in order to have a better understanding of the complex dynamical behavior of continuous three-dimensional differential systems, it is important to study also the nonchaotic differential systems, beyond the chaotic ones.

Acknowledgements

The first author was supported by State of São Paulo Foundation (FAPESP) grant number 2019/10269-3 and by CNPq/Brazil grant number 311355/2018-8. The second author was supported by CAPES/Brazil through a PhD fellowship.

Conflicts of Interest

The authors declare that there is no conflict of interest regarding the publication of this paper.

Availability of data and material

Not applicable.

LITERATURE CITED

Algaba, A., Dominguez-Moreno, M. C., Merino, M. and Rodríguez-Luis, A. J., 2018 A Review on Some Bifurcations in the Lorenz System. Nonlinear Systems, **1**:3–36.

Alligood, K. T., Sauer, T. and Yorke, J., 1996 Chaos: An Introduction to Dynamical Systems. Springer-Verlag, New York.

Anastassiou, S., Pnevmatikos, S. and Bountis T, 2002 Quadratic Vector Fields Equivariant Under the D_2 Symmetry Group. Internat. J. Bifur. Chaos Appl. Sci. Engrg. **23**, 1350017.

Argyris, J., Faust, G., Haase, M. and Friedrich, R., 2015 An Exploration of Dynamical Systems and Chaos. Springer-Verlag, Berlin.

Cencini, M., Cecconi, F. and Vulpiani, A., 2010 Chaos: From Simple Models to Complex Systems. World Scientific, Singapore.

Chen, G. and Ueta, T., 1999 Yet another chaotic attractor. Internat. J. Bifur. Chaos Appl. Sci. Engrg. **9**:1465–1466.

Dumortier, F., Llibre, J. and Artés, J.C., 2006 Qualitative Theory of Planar Differential Systems. Springer-Verlag, New York.

Guckenheimer, J. and Holmes, P. [2002] "Nonlinear Oscillations, Dynamical Systems and Bifurcations of Vector Fields", (Appl. Math. Sci. 42, Springer-Verlag, New York).

Heidel, J. and Zhang, F., 1999 Nonchaotic behavior in three-dimensional quadratic systems II. The conservative case. Nonlinearity **12**:617–633.

Heidel, J. and Zhang, F., 2007 Nonchaotic and chaotic behaviour in three-dimensional quadratic systems: Five–one conservative cases. Internat. J. Bifur. Chaos Appl. Sci. Engrg. **17**:2049–2072.

Jafari, S., Sprott, J. C., Pham, V-T, Volos, C., and Li, C., 2016 Simple chaotic 3D flows with surfaces of equilibria. Nonlinear Dynamics **86**:1349–1358.

Li, C., Peng, Y., Tao, Z., Sprott, J. C. and Jafari, S., 2021 Coexisting Infinite Equilibria and Chaos. Internat. J. Bifur. Chaos Appl. Sci. Engrg. **31**(5), 2130014, 17p.

Llibre, J., 2004 Integrability of polynomial differential systems. Handbook of differential equations, Elsevier/North-Holland, Amsterdam.

Llibre, J. and Messias, M., 2009 Global dynamics of the Rikitake system. Phys D: Nonlinear Phenomena **238**:241–252.

Llibre, J., Messias, M. and da Silva, P.R., 2008 On the global dynamics of the Rabinovich system. J. Phys. A: Math. Theor. **41**, 275210, 21p.

Llibre, J., Messias, M. and da Silva, P.R., 2010 Global dynamics of the Lorenz system with invariant algebraic surfaces. Internat. J. Bifur. Chaos Appl. Sci. Engrg. **20**:3137–3155.

Llibre, J., Messias, M. and da Silva, P.R., 2012 Global dynamics in the Poincaré ball of the Chen system having invariant algebraic surfaces. Internat. J. Bifur. Chaos Appl. Sci. Engrg. **22**, 1250154, 17p.

Llibre, J. and Oliveira, R. D. S., 2015 Quadratic systems with invariant straight lines with total multiplicity two having Darboux invariants. Comm. in Contemporary Math. **17**, 1450018.

Llibre, J. and Zhang, X., 2012 On the Darboux integrability of the polynomial differential systems. Qualit. Th. Dyn. Sys. **11**:129–144.

Lorenz, E.N., 1963 Deterministic nonperiodic flow. J. Atmos. Sci. **20**:130–141.

Malasoma, J. -M., 2002 A new class of minimal chaotic flows equation for continuous chaos. Phys. Lett. A. **305**:52–58.

Malasoma, J. -M., 2009 Non-chaotic behavior for a class of quadratic jerk equations. Chaos, Solitons Fractals **39**:533–539.

Messias, M. and Silva, R. P., 2018 Nonchaotic Behavior in Quadratic Three-Dimensional Differential Systems wiht a Symmetric Jacobian Matrix. Internat. J. Bifur. Chaos Appl. Sci. Engrg. **28**, 1830006.

Messias, M. and Silva, R. P., 2020 Determination of nonchaotic behavior for some classes of polynomial jerk equations. Internat. J. Bifur. Chaos Appl. Sci. Engrg. **30**, 2050117, 12p.

Osinga, H. M. and Krauskopf, B., 2002 Visualizing the structure of chaos in the Lorenz system. Computers and Graphics **26**(5):815–823.

Osinga, H. M. and Krauskopf, B., 2004 The Lorenz manifold as a collection of geodesic level sets. Nonlinearity **17** C1.

Ott, E., 2002 Chaos in Dynamical Systems. Cambridge University Press, London.

Rössler, O. E., 1976 An equation for continuous chaos. Phys. Lett. A **57**:397–398.

Sparrow, C., 1982 The Lorenz Equations. Bifurcations, Chaos, and Strange Attractors. Springer-Verlag, New York.

Strogatz, S.H., 2001 Nonlinear Dynamics and Chaos: with applications to physics, biology, chemistry and engineering. Westview Press, New York.

Zhang, F. and Heidel, J., 1997 Nonchaotic behaviour in three-dimensional quadratic systems. Nonlinearity **10**:1289–1303.

Zhang, F. and Heidel, J., 2012 Chaotic and nonchaotic behaviour in three-dimensional quadratic systems: 5-1 dissipative cases. Internat. J. Bifur. Chaos Appl. Sci. Engrg. **22**, 1250010.

Zhang, F., Heidel, J. and Le Borne, R., 2008 Determining nonchaotic parameter regions in some simple chaotic jerk functions. Chaos, Solitons and Fractals **11**:1413–1418.

Zhu C., Liu Y. and Guo Y., 2010 Theoretic and Numerical Study of a New Chaotic System. Intelligent Information Management **2**:104-109.

Yang, X. S., 2000 Nonchaotic behavior in nondissipative quadratic systems. Chaos, Solitons and Fractals **11**:1799–1802.

Yang, X. S., 2002 On non-chaotic behavior of a class of jerk systems. Far East J. Dyn. Syst. **4**:27–38.

Yang, X. S. and Chen, G., 2002 Non-chaotic behavior in a class of continuous dynamical systems. Far East J. Dyn. Syst. **4**:87–95.

Wiggins, S., 2003 Introduction to Applied Nonlinear Dynamical Systems and Chaos. Texts in Appl. Math. 2, Springer-Verlag, New York.

How to cite this article: Messias, M. and Silva, R. P. Nonchaotic Behavior and Transition to Chaos in Lorenz-like Systems Having Invariant Algebraic Surfaces. Chaos Theory and Applications, 4(1), 26-36, 2022.

CHAOS
Theory and Applications
in Applied Sciences and Engineering

e-ISSN: 2687-4539
RESEARCH ARTICLE
Vol.4 / No.1 / 2022 / pp.37-44
https://doi.org/10.51537/chaos.1000608

Determination of Romantic Relationship Categories and Investigation of Their Dynamical Properties

Kadir Can Erbaş *,[1]
*Department of Biomedical Engineering, Faculty of Engineering, Başkent University, Ankara, Turkey.

ABSTRACT In studies on dynamical modeling of romantic relationships, it is seen that individuals are divided into four different romantic styles. Most of these studies focused on the mathematical analysis of the dynamic expression of individuals' attitudes or tried to determine what kind of relationship evolution randomly assigned romantic style parameters will create. The categorization of relationship types and finding the general characteristics of the relationships in each category by identifying all combinations of four different romantic styles, to our knowledge, have not been attempted before. To fill this gap in the literature, this study divided individuals into four different romantic styles and identified ten different types of relationships formed by the combination of these four styles. The evolution of the love/hate situation of individuals in each type of relationship was modeled with a linear differential equation system and the short-term development of the relationship to evolve from an initial state was determined. According to the results, it was observed that in some types of relationships, couples achieved harmony in the love/hate mood over time, while in some types of relationships, a couple was reluctant. It has even been determined that the willingness in the relationship enters a periodic cycle. With the findings obtained, it can be determined what kind of relationship the couples are in, guidance can be provided and feedback correction can be provided to their attitudes in the relationship. Overall, this study aimed to be a starting point for the applicability of dynamic modeling with psychometric research.

KEYWORDS
Linear systems
Mathematical sociology
Human behaviour
Dynamics of love
Fixed points

INTRODUCTION

The expression of romantic relationships using a time-dependent system of differential equations has been studied by different researchers since Rapoport (Rapoport and Anatol 1960). Differential modeling studies on love dynamics have increased, especially after Strogatz's short paper, which made the topic popular in the literature. The most general form of the method discussed in the literature may be expressed as

$$\frac{dx}{dt} = f(x,y,t) \ , \frac{dy}{dt} = g(x,y,t) \tag{1}$$

Here x is the love/hate of individual 1 against individual 2 and y is the love/hate of individual 2 against individual 1 as functions of time. Functions f and g give an expression for the time derivatives (speeds of the feelings) in terms of instantaneous love quantities (x and y) and time (t) explicitly. Different researchers have used different forms of functions f and g including linear, nonlinear, homogeneous, and non-homogeneous.

In 1988, Strogatz published a one-page paper that describes the evolution of the romantic relationship between Romeo and Juliet by systems of coupled ordinary differential equations (Strogatz 1988). His study is based on a simple linear model and it may be the simplest attempt to model love affairs. It is mathematically stated as

$$\frac{dR}{dt} = -aJ \ , \frac{dJ}{dt} = bR \tag{2}$$

R and J represent the feelings of Romeo and Juliet, respectively. The coefficient 'a' describes the extent to which Romeo is encouraged by Juliet's feelings, while 'b' is the extent to which Juliet is encouraged by Romeo's feelings (Wauer *et al.* 2007).

Manuscript received: 25 September 2021,
Revised: 26 December 2021,
Accepted: 18 January 2022.

[1] kcerbas@gmail.com (**Corresponding Author**)

After Strogatz, many papers have been published to describe romantic relations in terms of systems of differential equations including linear, nonlinear, and non-homogeneous models. Among the linear studies, Rinaldi expressed the evolution of love with linear minimal models. Rinaldi proposed an improved linear model that is more realistic than that described by Strogatz although it is still a minimal model. The aspects of love dynamics, namely forgetting process (oblivion), the pleasure of being loved (return), and reaction to the partner appeal (instinct), are expressed by Eqs.3, 4 (Rinaldi 1998). He proposed the equation system below:

$$\dot{x}_1 = -\alpha_1 x_1 + \beta_1 x_2 + \gamma_1 A_2 \tag{3}$$

$$\dot{x}_2 = -\alpha_2 x_2 + \beta_2 x_1 + \gamma_2 A_1 \tag{4}$$

Variables x_1 and x_2 are measures of the love of individuals for their respective partners. Positive values of x represent positive feelings, ranging from friendship to passion, while negative values are associated with antagonism and disdain. Complete indifference is identified by $x = 0$. Another linear study was conducted by Patro with determined and dependent indeterminacy models. Patro modeled romantic relationships by applying neutrosophic logic to the dynamics of love. He used a linear model and stated that an indeterminacy must be calculated in love dynamics (Patro 2016).

Bae modeled other factors such as the opinions of friends, parents, or other family members by adding a time-dependent external force term to the equation (Bae 2015). Chaotic phenomena appeared in the study with some choice of external forces. Barley and Cherif studied stochastic and deterministic models with nonlinear return functions. Their results showed that deterministic models tend to approach locally stable emotional behavior, but these complex and exotic patterns of emotional behaviors were observed in the presence of stochasticity in the models (Barley and Cherif 2011).

Satsangi and Sinha suggested that the effect of learning and adaptation and synergism after living together should be considered. This suggests that the emotional interaction of two individuals must be considered in the modeling process. By considering that the emotion of an individual with respect to another cannot increase infinitely, they assumed that it is proportional to $x_1.x_2$. Therefore, the term $x_1.x_2$ was added to the linear differential system of equations (Satsangi and Sinha 2012).

In studies of some researchers, hopf bifurcations were detected by nonlinear models with time delays (Deng *et al.* 2017; Liao and Ran 2007; Gragnani *et al.* 1996). Deng et al. have reported that Hopf bifurcation occurs when time delay passes through the critical value among three individuals, which is called a love triangle model (Deng *et al.* 2017). Liao and Ran investigated a love dynamical model with nonlinear couples and two delays and found that Hopf bifurcation occurs when the sum of the two delays varies and passes a sequence of critical values (Liao and Ran 2007). Rinaldi has detected three types of bifurcation curves, namely, supercritical Hopf, fold, and homoclinic, around a Bogdanov–Takens codimension-2 bifurcation point (Gragnani *et al.* 1996).

Other studies on the effects of time delays were conducted by different researchers. Bielczyk et al. showed that an unstable system without time delay can become stable when a certain range of time delay is included in a linear or nonlinear system (Bielczyk *et al.* 2013). It is possible for linear systems with only delays for different choices of the terms. In a different study, it was proved that changes in the stability of the stationary points occur for various intervals of the parameters that determine the intensity of interactions (Bielczyk *et al.* 2013). Son and Park investigated the effect of time delay on a dynamic model of love and found that time delay on the return function can cause a Hopf bifurcation and cyclic love dynamics (Son and Park 2011).

Ozalp and Koca have described and analyzed a fractional order nonlinear dynamic model of interpersonal relationships and obtained a stability condition for equilibrium points with a numerical example (Ozalp and Koca 2012). Owolabi has developed the Adams–Bashforth method to approximate the Caputo, Caputo–Fabrizio, and Atangana–Baleanu fractional derivatives. In his work, simulations of fractional-order have shown that interpersonal and romantic love affairs between two individuals can exhibit some chaotic scenarios (Owolabi 2019). Ahmad and Khazali proposed a fractional-order model of love to describe the dynamics of a love triangle under different structures and demonstrated that such a system can produce chaos in the presence of nonlinearity (Ahmad and El-Khazali 2007). Goyal et al. have tried different fraction values to compare the results of a fractional variational iteration method (FVIM) and fractional homotopy perturbation transform method (FHPTM). They have shown that the FVIM is successfully applied to obtain a rapidly convergent approximate numerical solution of a coupled nonlinear dynamical fractional model of romantic and interpersonal relationships for marriages (Goyal *et al.* 2019).

There are several attempts to use interesting approaches to a love model. Jafari et al. used complex numbers to represent the feelings of partners. They assumed that the feelings could be a combination of love and hate, so could be modeled by a complex variable that has a magnitude and a phase between 0° and 180° (Jafari *et al.* 2016). Bagarello et al. studied love dynamics from quantum mechanical and operator points of view (Bagarello and Oliveri 2010; Bagarello 2011).

It is seen that the studies in the literature summarized above try to determine the differential equation of relationships (Eq.1) and examine the related equation from the perspective of bifurcation, chaos and stability. Therefore, the subjects such as the equations that can be used in modeling romantic relationships, the situations in which these equations will create chaos, their stability will change, or bifurcation diagrams have been studied extensively. However, no research has categorized romantic relationships, how many types of relationships can be between individuals and to determine the general characteristics of these relationship types. Such a classification study is necessary to make dynamic modeling more applicable in relationships and to predict the course of romantic relationships between two individuals. In this way, individuals' romantic styles can be determined by questionnaires or observations, and feedback can be provided on how the romantic futures of various styles will work.

MATERIALS AND METHODS

Construction of the Mathematical Model

As Rinaldi highlights, measuring the parameters that explain romantic styles in a typical differential equation is hard (Rinaldi *et al.* 2015). Especially in nonlinear models, it is difficult to propose an equation and to predict the parameters from the characteristics of the individual. For this reason, it is a major problem that theoretical studies do not have an area of use and cannot be presented for the benefit of humanity.

The primary aim of this study was to make dynamic modeling of romantic relationships applicable and measurable. Therefore, it was made the analysis as qualitative as possible and the following assumptions were made.

- As a function of time, instead of the love/hate state of the

individual, the affection/indifference in a relationship that has begun or rapprochement/distancing has been chosen.
- In all relationships, it has been accepted that the interest of individuals toward each other can be linearized around the equilibrium point in a narrow time interval. Thus, homogeneous models linearized around the equilibrium point are adopted and the results are generalized to predict the relationship evolution in the short term.
- Determining the romantic style for each individual is reduced to determining the two parameters (ai and bi) in the linear model. According to the signs of these parameters, romantic styles were considered in four categories (eager beaver, cautious lover, narcissistic nerd, and hermit).

In summary, each individual was reduced to one of four specified romantic styles, and ten types of relationship formed by the combination of all different styles were named. It was assumed that all couples will fit into one of the ten types of relationship identified here. In this way,

- Counseling can be offered to couples.
- Algorithms can be developed to find the ideal match.
- Couples can be guided in their relationships.
- Couples and individuals can self-criticize and correct their romantic styles.

Our model is based on a system of linear differential equations describing the evolution of love into a romantic relationship between couples. There are two individuals whose emotions are represented by the functions $x_1(t)$ and $x_2(t)$ depending on time. The time derivatives x_1 and x_2, denoted by $\dot{x}_1$ and $\dot{x}_2$, represent the rate at which emotions change over time. If the derivative is positive, the interest/love will tend to increase; if it is negative, it will tend to decrease. Therefore, the rate of change in emotions may depend on both functions of emotions of the individuals. Mathematically, a linear relationship can be suggested with Eqs.5-8.

$$\dot{x}_1(t) = a_1 x_1(t) + b_1 x_2(t) \tag{5}$$

$$\dot{x}_2(t) = b_2 x_1(t) + a_2 x_2(t) \tag{6}$$

$$\frac{d}{dt}\begin{pmatrix} x \\ y \end{pmatrix} = \begin{pmatrix} a_1 & b_1 \\ b_2 & a_2 \end{pmatrix}\begin{pmatrix} x \\ y \end{pmatrix} \tag{7}$$

$$\dot{\vec{x}} = \hat{R}\vec{x} \tag{8}$$

The coefficients a_1, b_1, a_2 and b_2 are related to the romantic styles of individuals. The main point is the determination of the parameters. It is difficult to measure them accurately but one can categorize individuals with respect to the value of the romantic style parameters. For a partner, the parameters *'a'* and *'b'* can be both positive and negative, so the combinations of signs can determine the style of the individual (Barley and Cherif 2011).

Different researchers used these parameters with different names. Gottman et al. (2002) use the term *'behavioral inertia'* for the parameter *'a'* and *'influence function'* for *'b'* (Gottman *et al.* 2002). Rinaldi named *'a'* and *'b'* forgetting coefficient and reactiveness, respectively (Rinaldi 1998). Wauer states that coefficient *'a'* describe the extent to which person 1 is encouraged by his/her own feelings and *'b'* are the extent to which he/she is encouraged by the feelings of person 2 (Wauer *et al.* 2007). How to measure these parameters and the questionnaires to be prepared for this purpose are so complicated that they are a separate study, so the measurement of the parameters is not mentioned here (Bagarello and Oliveri 2010; Bagarello 2011).

Two parameters define an individual's romantic styles: behavioral inertia *'a'* and reactivity *'b'*. According to the signs of the parameters, four different styles can be defined (Table 1). There is no need to consider that the parameters are zero, as a zero value in styles can be treated as a sub-case.

Ten combinations are obtained by coupling different romantic styles (Table 2). In Table 2, different relationships are named R_{ij}, which means that the relationship is between style i and j in Table 1. The relation matrices in Eq.7 are also given in Table 1. Analyzing the matrices according to Eq.8 will give the possible results of the processes improving in the relation.

Analysis of the Relationships

Generally, a relation matrix has the form

$$R = \begin{pmatrix} a_1 & b_1 \\ b_2 & a_2 \end{pmatrix} \tag{9}$$

For a 2×2 matrix, the types of phase portraits with respect to the parameters of the matrix are shown in Fig.1. The relation matrix has four real numbers. The determinant of R is $\Delta = a_1 a_2 - b_1 b_2$ and its sign indicates whether the fixed point is a saddle or not. If $\Delta<0$, the origin is a saddle node. If $\Delta>0$, the origin is a node or spiral. If the trace of the matrix $\tau = a_1 + a_2$ is positive, nodes, lines, or spirals are always unstable. The sign of the discriminant $D = \tau^2 - 4\Delta = (a_1 - a_2)^2 + 4b_1 b_2$ determines whether the fixed point is a focus or node (see Fig.1). Five types of fixed point can be assigned to analyze the relation matrix: saddle point, stable node, unstable node, stable spiral, and unstable spiral.

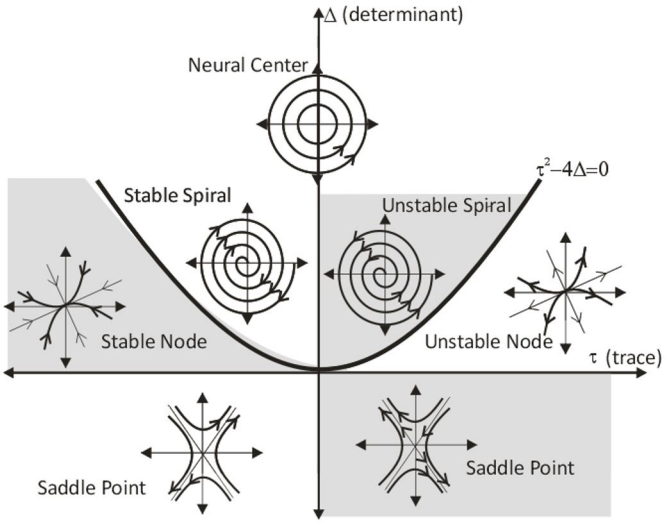

Figure 1 Phase portraits for a system of linear first-order differential equations.

On a phase portrait showing the relationship process (e.g., Fig.2), the first quadrant means that both individuals agree with the relationship or love. Similarly, the third quadrant means that the pairs agree with separation or apathy. However, the second and fourth quadrants point to a disagreement or inconsistency between the pairs. One individual is unwilling while the other desires him/her. According to Fig.1 and the explanation in Table 2, types of possible phase portraits are examined in Table 3.

Table 1 Romantic styles with their parameters

Style	a	b	Name	Description of a	Description of b
S_1	(+)	(+)	Eager beaver	Unstable in his own feeling	Positive reaction to the interest
S_2	(+)	(-)	Narcissistic nerd	Unstable in his own feeling	Negative reaction to the interest
S_3	(-)	(+)	Secure or cautious lover	Stable in his own feeling	Positive reaction to the interest
S_4	(-)	(-)	Hermit	Stable in his own feeling	Negative reaction to the interest

Table 2 Matrices of the types of relationship

.	S_1 = [+ +]	S_2 = [+ -]	S_3 = [- +]	S_4 = [- -]
S_1 = [+ +]	$R_{11} = \begin{bmatrix} + & + \\ + & + \end{bmatrix}$	$R_{12} = \begin{bmatrix} + & + \\ - & + \end{bmatrix}$	$R_{13} = \begin{bmatrix} + & + \\ + & - \end{bmatrix}$	$R_{14} = \begin{bmatrix} + & + \\ - & - \end{bmatrix}$
S_2 = [+ -]		$R_{22} = \begin{bmatrix} + & - \\ - & + \end{bmatrix}$	$R_{23} = \begin{bmatrix} + & - \\ + & - \end{bmatrix}$	$R_{24} = \begin{bmatrix} + & - \\ - & - \end{bmatrix}$
S_3 = [- +]			$R_{33} = \begin{bmatrix} - & + \\ + & - \end{bmatrix}$	$R_{34} = \begin{bmatrix} - & + \\ - & - \end{bmatrix}$
S_4 = [- -]				$R_{14} = \begin{bmatrix} - & - \\ - & - \end{bmatrix}$

Table 3 Examination of matrices according to their traces (τ), determinants (Δ), and discriminant (D) via Fig.1 and Fig.2.

	τ	Δ	D	Fixed points (0,0)	Fig.2
R_{11}	+	±	+	Saddle I or unstable node	a, e
R_{12}	+	+	±	Unstable node or spiral	e, h
R_{13}	±	-	+	Saddle I	a
R_{14}	±	±	±	All possibilities (saddle IV)	a, e-i
R_{22}	+	±	+	Saddle II or unstable node	b, e
R_{23}	±	±	±	All possibilities (saddle III)	c, e-i
R_{24}	±	-	+	Saddle II	b
R_{33}	-	±	+	Saddle I or unstable node	a, f
R_{34}	-	+	±	Stable node or spiral	f, g
R_{44}	-	±	+	Stable node or saddle II	b, f

RESULTS AND DISCUSSION

The following criteria should be considered when interpreting the results.

- Because the model is linear, it should be viewed as a first-order approximation of a much more complex equation. The time interval should be kept short for the linearization to converge realistically. Therefore, predicting short-term movements after a certain traumatic onset give more realistic results.
- The x and y parameters in the equations were taken as care/indifference instead of the love/hate determined by Strogatz. Unlike other studies, it refers to the state of interest/indifference of individuals who are in a relationship with each other, rather than the process of initiating a relationship. These parameters (x and y) have an interval scale. Therefore, a value of zero is a shift toward homogenizing the system of equations rather than expressing a lack of emotion. For example, if $x = 2$ units and $y = -1$ unit of interest are the equilibrium point for the relationship, the $(x, y) = (2, -1)$ point is taken as the origin.
- Any extraordinary event during the relationship creates a new starting point. For example, in a fight that may arise from a jealousy crisis, the woman may fall into a situation where her interest has decreased (cooled down) and the man has increased it (trying to forgive). That is, they may have started the routine of daily life when their emotional state was at the point (female, male) = $(x, y) = (-1.5, 2.3)$. After this point, how the relationship will evolve can be predicted by following the arrows in the phase diagram. After such a starting point, as the R_{11} relationship moves toward reconciliation with time, R_{12} can also enter a periodic cycle. In fact, the woman may get much colder in R_{14}, or both individuals may become colder toward each other over time in R_{23}.
- Quadrant 1 in the phase portrait is an ideal region where couples reciprocate their interests together. The third quadrant is the region where both partners cool off toward each other. The second and fourth quadrants can be interpreted as the region where one person in the couple escapes and the other chases after them. In short, quadrants 1 and 3 represent parallel and 2 and 4 represent opposite emotions. While interpreting the phase portrait, it is more appropriate to understand the relationship by determining in which regions to spend more time or target.

The analysis of relationships according to the above criteria is given in Fig.2 which is prepared by (Hollis 2010) and Table 4. For detailed analysis, the phase portraits in Fig.2 can be examined. The general characteristics of romantic relationship types are summarized in Table 4.

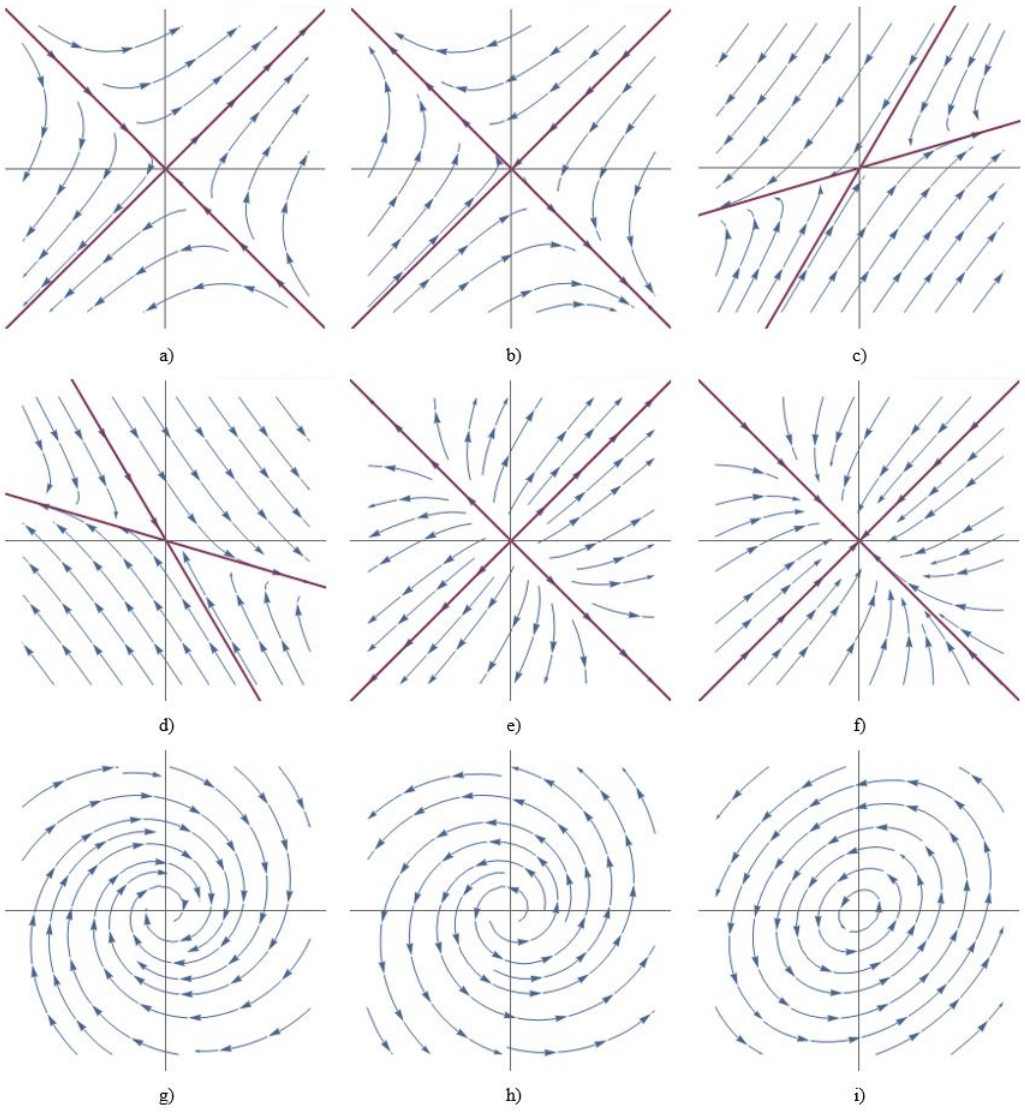

Figure 2 a) Saddle I: R=[1 2 ; 2 1]. Unstable in incompatible regions (2nd and 4th quadrants). According to the quantity of parameters and emotions, it evolves into the positive or negative compatible regions (1st and 3rd quadrants). **b)** Saddle II: R=[-1 -2 ; -2 -1]. Unstable in compatible regions (1st and 3rd quadrants). According to the quantity of parameters and emotions, it evolves into the positive or negative incompatible regions (2nd and 4th quadrants). **c)** Saddle III: R=[1 -2 ; 1 -3]. In this type of situation, x is luckier than y because when x has positive emotions, both partners go into positive compatible territory. The same is true when x is negative. But still compatible regions are targeted. **d)** Saddle IV: R=[1 2; -1 -3]. In this type of situation, incompatible regions are targeted. In the positive compatible region, y moves away from his/her partner over time, while in the negative fit region he/she gets closer. **e)** Unstable node: R=[2 1; 1 2]. Whatever the initial condition, the type of emotion grows over time without much change. **f)** Stable Node: R=[-2 -1; -1 -2]. Whatever the initial condition, the type of emotion decay over time without much change. **g)** Stable spiral: R=[-0.5 2; -2 -0.5]. As they make periodic transitions to different emotional states, their emotions decay over time with each periodic repetition. **h)** Unstable spiral: R=[0.5 -2; 2 0.5]. As they make periodic transitions to different emotional states, their emotions growth over time with each periodic repetition. **i)** Center: R=[0.5 -2; 2 -0.5]. As they make periodic transitions to different emotional states, their emotions remain the same with each periodic repetition.

Table 4 Summary of the properties of relationships

Type	Explanation
R_{11}	It is a compatible type of relationship. The attitudes of individuals toward each other turn into mutual love or mutual indifference.
R_{12}	It cannot be said that there is a stable relationship. Sometimes periodically, sometimes regularly, they move away from their initial equilibrium point. They cannot aim for a stable level of love.
R_{13}	It is rare for one to chase after the other. They quickly move into a state of harmonious interest.
R_{14}	It is rare for them to have harmonious feelings and they cannot stay in this state for long. They quickly move toward an opposite emotional state.
R_{22}	It is a negative type of relationship. They easily go into an opposite mood.
R_{23}	They usually target the positive territory, even if they are likely to go through a cyclical process.
R_{24}	It is perhaps the most negative type of relationship. They tend to gravitate toward an area where one is interested and the other less.
R_{33}	It is generally a balanced relationship. It does not take long for individuals to tend to oppose each other.
R_{34}	It is generally a balanced relationship. Sometimes they come to equilibrium by making loops.
R_{44}	They cannot stay in the compatible area for long. They either go into balance or into negative territory.

CONCLUSION

In this study, possible phase portraits obtained by coupling individuals with different romantic styles were examined and it was deduced how the relationship would evolve. When these portraits were examined, the state of emotions was observed in the regions where the love/interest status of individuals was similar (1^{st} and 3^{rd} quadrants) and in the regions where they were opposite (2^{nd} and 4^{th} quadrants), and accordingly the compatibility or incompatibility of the relationship was determined.

It can be seen from the analysis that R_{13} and R_{33} are the most compatible and R_{22} and R_{24} are the most incompatible among the types of relationship. The most ambiguous and most sensitive to romantic parameters were determined as R_{14} and R_{23}. If the above results are analyzed, it is seen that the most fortunate or successful romantic styles in relationships are S_1 (eager beaver) and S_3 (cautious lover), while the most unlucky or unsuccessful ones are S_2 (narcissistic nerd) and S_4 (hermit). From the common features of these styles, it is seen that the most important romantic feature is to show a positive attitude toward attention/love. It can be concluded that the types who run away when they see interest/love or chase when they do not see it create a problematic relationship in every relationship combination. The second important romantic style characteristic is attachment to one's own feelings. It can be surmised that those who are stable (a<0) are slightly more fortunate than those who are not (a>0).

Conflicts of Interest

The author declares that there is no conflict of interest regarding the publication of this paper.

Availability of data and material

Not applicable.

LITERATURE CITED

Ahmad, W. M. and R. El-Khazali, 2007 Fractional-order dynamical models of love. Chaos, Solitons & Fractals **33**: 1367–1375.

Bae, Y., 2015 Chaotic behavior in a dynamic love model with different external forces. International Journal of Fuzzy Logic and Intelligent Systems **15**: 283–288.

Bagarello, F., 2011 Damping in quantum love affairs. Physica A: Statistical Mechanics and its Applications **390**: 2803–2811.

Bagarello, F. and F. Oliveri, 2010 An operator-like description of love affairs. SIAM Journal on Applied Mathematics **70**: 3235–3251.

Barley, K. and A. Cherif, 2011 Stochastic nonlinear dynamics of interpersonal and romantic relationships. Applied Mathematics and Computation **217**: 6273–6281.

Bielczyk, N., U. Foryś, and T. Płatkowski, 2013 Dynamical models of dyadic interactions with delay. The Journal of mathematical sociology **37**: 223–249.

Deng, W., X. Liao, T. Dong, and B. Zhou, 2017 Hopf bifurcation in a love-triangle model with time delays. Neurocomputing **260**: 13–24.

Gottman, J., J. Murray, C. Swanson, R. Tyson, and K. Swanson, 2002 The mathematics of marriage: Dynamic nonlinear approach.

Goyal, M., A. Prakash, and S. Gupta, 2019 Numerical simulation for time-fractional nonlinear coupled dynamical model of romantic and interpersonal relationships. Pramana **92**: 1–12.

Gragnani, A., S. Rinaldi, and G. Feichtinger, 1996 Complex dynamics in romantic relationships .

Hollis, S., 2010 Eigenvalues and linear phase portraits.

Jafari, S., J. C. Sprott, and S. Golpayegani, 2016 Layla and majnun: a complex love story. Nonlinear Dynamics **83**: 615–622.

Liao, X. and J. Ran, 2007 Hopf bifurcation in love dynamical models with nonlinear couples and time delays. Chaos, Solitons & Fractals **31**: 853–865.

Owolabi, K. M., 2019 Mathematical modelling and analysis of love dynamics: A fractional approach. Physica A: Statistical Mechanics and its Applications **525**: 849–865.

Ozalp, N. and I. Koca, 2012 A fractional order nonlinear dynamical model of interpersonal relationships. Advances in Difference Equations **2012**: 1–7.

Patro, S. K., 2016 On a model of love dynamics: A neutrosophic analysis. Florentin Smarandache, Surapati Pramanik p. 279.

Rapoport, A. and R. Anatol, 1960 *Fights, games, and debates*. University of Michigan Press.

Rinaldi, S., 1998 Love dynamics: The case of linear couples. Applied Mathematics and Computation **95**: 181–192.

Rinaldi, S., F. Della Rossa, F. Dercole, A. Gragnani, and P. Landi, 2015 *Modeling love dynamics*, volume 89. World Scientific.

Satsangi, D. and A. K. Sinha, 2012 Dynamics of love and happiness: a mathematical analysis. International Journal of Modern Education and Computer Science **4**: 31.

Son, W.-S. and Y.-J. Park, 2011 Time delay effect on the love dynamical model. arXiv preprint arXiv:1108.5786 .

Strogatz, S. H., 1988 Love affairs and differential equations. Mathematics Magazine **61**: 35–35.

Wauer, J., D. Schwarzer, G. Cai, and Y. Lin, 2007 Dynamical models of love with time-varying fluctuations. Applied Mathematics and Computation **188**: 1535–1548.

How to cite this article: Erbaş, K.C. Determination of Romantic Relationship Categories and Investigation of Their Dynamical Properties. Chaos Theory and Applications, 4(1), 37-44, 2022.

CHAOS
Theory and Applications
in Applied Sciences and Engineering

e-ISSN: 2687-4539
RESEARCH ARTICLE
Vol.4 / No.1 / 2022 / pp.45-58
https://doi.org/10.51537/chaos.1069002

Lyapunov Exponent Enhancement in Chaotic Maps with Uniform Distribution Modulo One Transformation

Günyaz Ablay *,[1]
*Department of Electrical-Electronics Engineering, Abdullah Gül University, Kayseri, Turkey.

ABSTRACT Most of the chaotic maps are not suitable for chaos-based cryptosystems due to their narrow chaotic parameter range and lacking of strong unpredictability. This work presents a nonlinear transformation approach for Lyapunov exponent enhancement and robust chaotification in discrete-time chaotic systems for generating highly independent and uniformly distributed random chaotic sequences. The outcome of the new chaotic systems can directly be used in random number and random bit generators without any post-processing algorithms for various information technology applications. The proposed Lyapunov exponent enhancement based chaotic maps are analyzed with Lyapunov exponents, bifurcation diagrams, entropy, correlation and some other statistical tests. The results show that excellent random features can be accomplished even with one-dimensional chaotic maps with the proposed approach.

KEYWORDS
Chaos
Lyapunov exponent
Random numbers
Cryptography
Image encryption

INTRODUCTION

Chaotic maps have a wide-range application areas in many disciplines including engineering, cryptography, statistics, physics, biology, art and philosophy (El-Hameed *et al.* (2021); Benamara *et al.* (2016); Strogatz (2015); Ruelle (1997); Banerjee *et al.* (2012)). Specifically, the need for highly secure cryptosystems is always increasing because the information technologies are continuously developing and reaching more and more people everyday in various platforms (e.g., e-banking, IoT, e-purchasing, etc.). The chaos-based cryptography is a great tool to produce secure and independent random number sequences for information security. On the other hand, only few number of chaotic maps are inherently suited for data encryption since the majority of chaotic systems are not satisfying the statistically independendent and unbiased uniform distribution which are the main properties of random key generators. Many chaotic maps have a limited key space due to their narrow chaotic ranges, which causes security issues against intruders (Luo *et al.* (2020)). In addition, the chaotic random number generators must be sufficiently fast, and there should not be any collapsing effect in long turn run.

To deal with the aforementioned issues, there is a great interest in developing novel chaotic maps with highly mixing feature by making various modifications on the available chaotic maps. The researchers have constructed some general frameworks to get new chaotic maps with increased complexity and improved performances in some applications, including mixing two 1D maps (Garasym *et al.* (2016)), weakly or cross-coupling of 1D chaotic maps (Ablay (2016)), parameter switching based combination of multiple chaotic maps (Wang and Liu (2021)), mixing linear-nonlinear coupled map lattices (Zhou *et al.* (2014)), sine transform of chaotic maps (Hua *et al.* (2019a)), polynomial combination of chaotic maps (Asgari-Chenaghlu *et al.* (2019)), beta-function-based chaotification (Zahmoul *et al.* (2017)), modulo transform based chaotification (Hu and Li (2021); Hua *et al.* (2020); Murillo-Escobar *et al.* (2017); Zhou *et al.* (2014)), modulo operator based generalized Newton complex map (Jafari Barani *et al.* (2020)), cosine transform based chaotic maps (Hua *et al.* (2019b); Liu *et al.* (2016); Talhaoui *et al.* (2021)), composition of chaotic maps with many parameters (Parvaz and Zarebnia (2018)), multi-delayed Chebyshev map (Liu *et al.* (2016)), improvement in chaotic maps with a perturbed parameter (Xiang and Liu (2020)), combination of chaotic maps with floor operator (Pak and Huang (2017)), and mixing three maps with composition, addition and modulo operators (Lan *et al.* (2018)). Most of these approaches cannot fit the uniform distribution which is the central feature of the random numbers. However, the modulo operator based approaches are capable of producing outputs in the uniform distribution range. In (Zhou *et al.* (2014)), a 1D chaotic system is proposed by summing two 1D chaotic maps followed by a modulo operator. In (Murillo-Escobar *et al.* (2017)), the modulo operator is applied to logistic map and an enhanced

Manuscript received: 6 February 2022,
Revised: 25 February 2022,
Accepted: 26 February 2022.

[1] gunyaz.ablay@agu.edu.tr (**Corresponding Author**)

pseudo-random number generator algorithm is obtained. In (Hua *et al.* (2020)), the modulo N operator is applied to the 2D chaotic maps for getting a bounded transformation and improvement in chaos complexity. In (Jafari Barani *et al.* (2020)), the modulo operator and complex folding functions are utilized to get a generalized Newton complex map. In (Hu and Li (2021)), two 1D chaotic maps are coupled by their control parameters for mixing the chaotic behaviors of the seed maps, and then the modulo operator is applied to get an outcome in the range of standard uniform distribution. In general, these chaotic frameworks as random number sources have varying features affecting the throughput efficiency and complexity of the post-processing steps. Most of these chaotic frameworks use several parameters or functions that are not easy to adjust. Some of these chaotic frameworks are completely dependent on the seed chaotic map, and may not produce high quality outputs for other maps.

In this work, a chaotic framework based on a nonlinear transformation via a gain plus modulo-1 operator is proposed to obtain highly complex chaotic behaviors with Lyapunov exponent enhancements and to satisfy the standard uniform distribution $U(0,1)$. The Lyapunov exponent of the chaotic maps and complexity of modulo operator based methods are significantly improved with a gain parameter in this work. The proposed method uses one- or higher-dimensional chaotic maps as seeds and produces completely new chaotic sequences. The method eliminates the time-consuming post-processing steps in chaos-based random number generators. The produced novel chaotic systems significantly broaden the chaotic range of the seed discrete chaotic systems. In addition, the approach removes the periodic windows of existing chaotic systems, and produces robust chaos for practical applications. The uniformity and independence of the chaotic sequences are assured with statistical analyses. The efficiency and feasibility of the proposed approach are illustrated with the random bit generations and image encryption applications.

A GAIN PLUS UNIFORM DISTRIBUTION MODULO ONE TRANSFORMATION IN CHAOTIC MAPS

There is a sea of chaotic maps available for statistical studies, modeling, simulations, cryptography and some other technological applications. These chaotic maps or in general discrete-time chaotic systems can be utilized to generate shaped chaotic algorithms with nonlinear transformations for direct usage in applications including information technologies. Therefore, two main goals of this work are Lyapunov exponent enhancement and achievement of standard uniform distribution in chaotic maps. Consider a discrete-time chaotic map described by

$$x_{k+1} = f(\sigma, x_k) \tag{1}$$

where $f(\cdot)$ represents a real function, $f : R \to R$, and σ is a real-valued parameter. The existence of chaos in any system is usually shown with positive Lyapunov exponent (LE) calculations (Vallejo and Sanjuán (2019)). LEs are computed to characterize the rate of separation of infinitesimally close trajectories, and a positive LE is a requirement for existence of chaos. The positive LE calculation methods start with exponential divergence of nearby trajectories when the trajectory is on the attractor (Awrejcewicz *et al.* (2018)). An exponential separation of nearby phase-space trajectories is given by

$$d_k \approx d_0 e^{\lambda_s k} \tag{2}$$

where λ_s is the LE, d_k is the trajectory separation after k iterates, and d_0 is the initial trajectory separation. By taking the logarithm of both sides and using the property $d_k = f^k(x_0 + d_0) - f^k(x_0)$ for an initial condition x_0, the LE for chaotic map (1) can be given by

$$\lambda_s = \lim_{N\to\infty} \frac{1}{N} \sum_{k=0}^{N-1} \log |f'(x_k)| \tag{3}$$

where $f' = df/dx$ and it defines the variational (linearized) map as

$$u_{k+1} = f'(x_k) u_k \tag{4}$$

where $u_0 \neq 0$. A positive λ_s indicates the presence of chaos in general. The positive LE is also used to measure unpredictability of the chaotic dynamics in Kolmogorov-Sinai entropy (KSE) calculations.

Definition 1 (Pesin's theorem) (Dorfman (1999)): For an ergodic map, the KSE is equal to the sum of the positive LEs and given by

$$h_{KSE} = \sum_n \lambda_s^+ \tag{5}$$

Similarly, the Ruelle's inequality (Ruelle (1997)) states that the KSE is always less than or equal to the sum of the positive LEs, that is $h_{KSE} \leq \sum_n \lambda_s^+$. This definition indicates that for chaotic maps, the greater LE means the greater KSE and the higher randomness. This gives an idea that if we can increase the values of positive LEs, then more complex chaotic information can be obtained. It is possible to enhance the value of positive LE by nonlinear transformation of the chaotic map (1).

An LE-enhanced uniform distribution modulo one transformation of (1) with a gain α and $\mod 1$ operator is proposed as

$$x_{k+1} = \alpha f(\sigma, x_k) \mod 1 \tag{6}$$

where α is a real-valued gain defined as $\alpha > 1$, $\mod 1$ denotes keeping of the fractional part, $f(\cdot)$ represents the seed chaotic map (1), and the new LE-enhanced chaotic map holds $[0,1] \to [0,1]$. The first goal is the LE enhancement, which can be shown with LE calculations.

Theorem 1: Let the LEs of seed map (1) and transformed map (6) be λ_s and λ, respectively. Then, these LEs are related with $\lambda > \lambda_s$ for $\alpha > 1$.

Proof: For the proposed chaotic map (6), since the linearization slope is $\alpha f'(x_k)$, the LE is given by

$$\lambda = \lim_{N\to\infty} \frac{1}{N} \sum_{k=0}^{N-1} \log |\alpha f'(x_k)| \tag{7}$$

The equation (7) can be expanded as

$$\begin{aligned} \lambda &= \lim_{N\to\infty} \frac{1}{N} \sum_{k=0}^{N-1} \log |f'(x_k)| + \frac{1}{N} \sum_{k=0}^{N-1} \log \alpha \\ &= \lim_{N\to\infty} \frac{1}{N} \log |u_N| + \frac{1}{N} \log \alpha^N \\ &= \lambda_s + \log \alpha \end{aligned} \tag{8}$$

where u_N is computed from the variational map (4) and we have $\lambda > \lambda_s$ since $\alpha > 1$.

This means that the Lyapunov exponent of (6) takes higher values than the seed chaotic map (1) so that a more complex chaotic behavior can be obtained. High-dimensional maps can be obtained by weakly-coupling or cross-coupling of the one-dimensional (1D) chaotic maps (Ablay (2016)). For example, the same or different 1D chaotic maps can be used to create the weakly-coupled (WC) maps as given below

$$\begin{aligned} x_{k+1} &= f_1(\sigma, x_k) + p y_k \\ y_{k+1} &= f_2(\sigma, y_k) - p x_k \end{aligned} \tag{9}$$

where $f_1(\cdot)$ and $f_2(\cdot)$ represent 1D chaotic maps, and p is a small coupling coefficient. The maximal one-dimensional LE of this map is given by (Pikovsky and Politi (2016))

$$\lambda_c = \lim_{N\to\infty} \frac{1}{N} \sum_{k=0}^{N-1} \log \|F'(x_k, y_k)\| \tag{10}$$

and F' denotes the Jacobian matrix and it defines the variational (linearized) map as

$$\begin{bmatrix} u_{k+1} \\ v_{k+1} \end{bmatrix} = F'(x_k, y_k) \begin{bmatrix} u_k \\ v_k \end{bmatrix} \tag{11}$$

where $u_0, v_0 \neq 0$. An LE-enhanced uniform distribution modulo one transformation of coupled-chaotic map (9) is proposed as

$$\begin{aligned} x_{k+1} &= \alpha(f_1(\sigma, x_k) + p y_k) \mod 1 \\ y_{k+1} &= \alpha(f_2(\sigma, y_k) - p x_k) \mod 1 \end{aligned} \tag{12}$$

where $\alpha > 1$ is a real-valued gain, mod1 denotes keeping of the fractional part, and the new chaotic map holds $[0,1] \to [0,1]$. It can be shown with LE calculations that the maximum LE of (12) is larger than the seed map (9).

Theorem 2: Let the maximum LEs of seed map (9) and transformed map (12) be λ_c and λ, respectively. Then, these maximum LEs are related with $\lambda > \lambda_c$ for $\alpha > 1$.

Proof: For the proposed chaotic map (12), since the Jacobian matrix of the map is $\alpha F'(x_k, y_k)$, the maximum LE is given by

$$\lambda = \lim_{N\to\infty} \frac{1}{N} \sum_{k=0}^{N-1} \log \|\alpha F'(x_k, y_k)\| \tag{13}$$

By using the entry-wise matrix norm, the maximal one-dimensional LE can be written as

$$\begin{aligned} \lambda &= \lim_{N\to\infty} \frac{1}{N} \sum_{k=0}^{N-1} \log \|F'(x_k, y_k)\| + \frac{1}{N} \sum_{k=0}^{N-1} \log \alpha \\ &= \lim_{N\to\infty} \frac{1}{N} \log\left(|u_N| + |v_N|\right) + \frac{1}{N} \log \alpha^N \\ &= \lambda_c + \log \alpha \end{aligned} \tag{14}$$

where u_N and v_N are computed from the variational map (11) and it is obvious that $\lambda > \lambda_c$ since $\alpha > 1$.

Theorem 2 can be applied to any high-dimensional chaotic maps in order to increase the complexity of chaotic systems.

The second main goal is to ensure that the probability density function of the generated random numbers fits the standard uniform distribution $U(0,1)$, because the $U(0,1)$ is at the center of random variable generation. The applications of this distribution include hypothesis testing, random sampling, finance, etc. However, it is important to note that in any application, there is the unchanging assumption that the probability of falling in an interval of fixed length is constant (Dekking *et al.* (2005)). The proposed LE-enhanced chaotic maps have the features of standard uniform distribution, and this will be demonstrated with histograms, statistical property calculations, entropy and correlation evaluations.

Seed chaotic map examples

Practically all chaotic maps can be considered as a seed map. Three different chaotic maps, cubic, signum and sinh maps (Ablay (2016)), are considered in this work. The cubic map is given by

$$x_{k+1} = \sigma x_k - x_k^3 \tag{15}$$

There are three fixed points, $x_e = (0, \pm\sqrt{\sigma - 1})$ for $\sigma > 1$, and the origin is unstable. A chaotic behavior exists for $2.25 < \sigma < 3$ as seen in Fig. 1a. The signum map is defined by

$$x_{k+1} = -\sigma x_k + sign(x_k) \tag{16}$$

where the $sign(\cdot)$ is defined as $sign(x) = x/|x|$ if $x \neq 0$ and $sign(x) = 0$ if $x = 0$. There are three fixed points with unstable origin, $x_e = (0, \pm 1/(\sigma + 1))$ for $\sigma > 0$. The map is chaotic for $1 < \sigma < 2$ as seen in Fig. 2a. The hyperbolic-sine (sinh) map is defined by

$$x_{k+1} = \sigma x_k - \sinh(x_k) \tag{17}$$

The map has three fixed points at $x_e = (0, \pm\gamma)$ for $\sigma > 1$, where $(\sigma - 1)\gamma - \sinh\gamma = 0$. Again the origin is unstable and a symmetric chaotic behavior is available for $3.1 < \sigma < 3.5$ as illustrated in Fig. 4a. In the following sections, the given 1D chaotic maps (15), (16) and (17) will serve as seed maps for developing LE-enhanced chaotic maps.

Performance analysis of LE-enhanced chaotic maps

Many 1D and coupled chaotic maps are able to produce complex chaotic outputs, but not able to generate uniformly distributed random numbers. The LE-enhanced chaotic maps (6) can solve this problem by increasing the complexity and by producing uniformly distributed numbers. In this section, the performances of the LE-enhanced chaotic maps will be analyzed in terms of the Lyapunov exponents, bifurcation diagrams, histograms, entropies and correlation coefficients.

Lyapunov exponents: LEs of the seed and LE-enhanced chaotic maps are shown in Fig. 1. The seed chaotic maps consist of 1D seed maps (1), i.e., cubic map (15), signum map (16), sinh map (17), and weakly coupled (WC) maps (9). LE-cubic, LE-signum and LE-sinh denote the LE-enhanced maps (6); LEWC-cubic, LEWC-signum and LEWC-sinh maps denote LE-enhanced weakly coupled (LEWC) maps (12). The numerical results are obtained for initial values $x_0 = 0.1234$, $y_0 = 0.1234$ and $p = 0.01$ for the 1D and WC chaotic maps. The gain parameter is taken as $\alpha = 1 \times 10^5$ for LE-cubic and LEWC-cubic maps and $\alpha = 1 \times 10^2$ for LE-signum, LE-sinh, LEWC-signum and LEWC-sinh maps. The LEs of enhanced chaotic maps (blue), compared with the LEs of seed chaotic maps (red), have a broad range of positive LE values. As explained and proved above, the LE enhanced chaotic maps have larger positive LE values than the seed maps, and thus they can exhibit much more complex chaotic behavior. The LE spectrum results given in Fig. 1 are compatible with the bifurcation diagrams (see Fig. 4).

For comparison purposes, the LEs of various models are provided in Fig. 2. The proposed LE-enhanced approach is compared with the unit transform based models given in Refs. (Hu and Li (2021); Zhou *et al.* (2014)), the sine transform based model given in Ref. (Hua *et al.* (2019a)) and the cosine transform based model given in Ref. (Hua *et al.* (2019b)). In the LE computations, summation of two different seed chaotic map functions, $f_1(\sigma_1, x_k) + f_2(\sigma_2, x_k)$ (i.e., cubic + signum, cubic + sinh, and signum + sinh map functions), are utilized to obtain seed chaotic maps, because the given reference studies use this form. Namely,

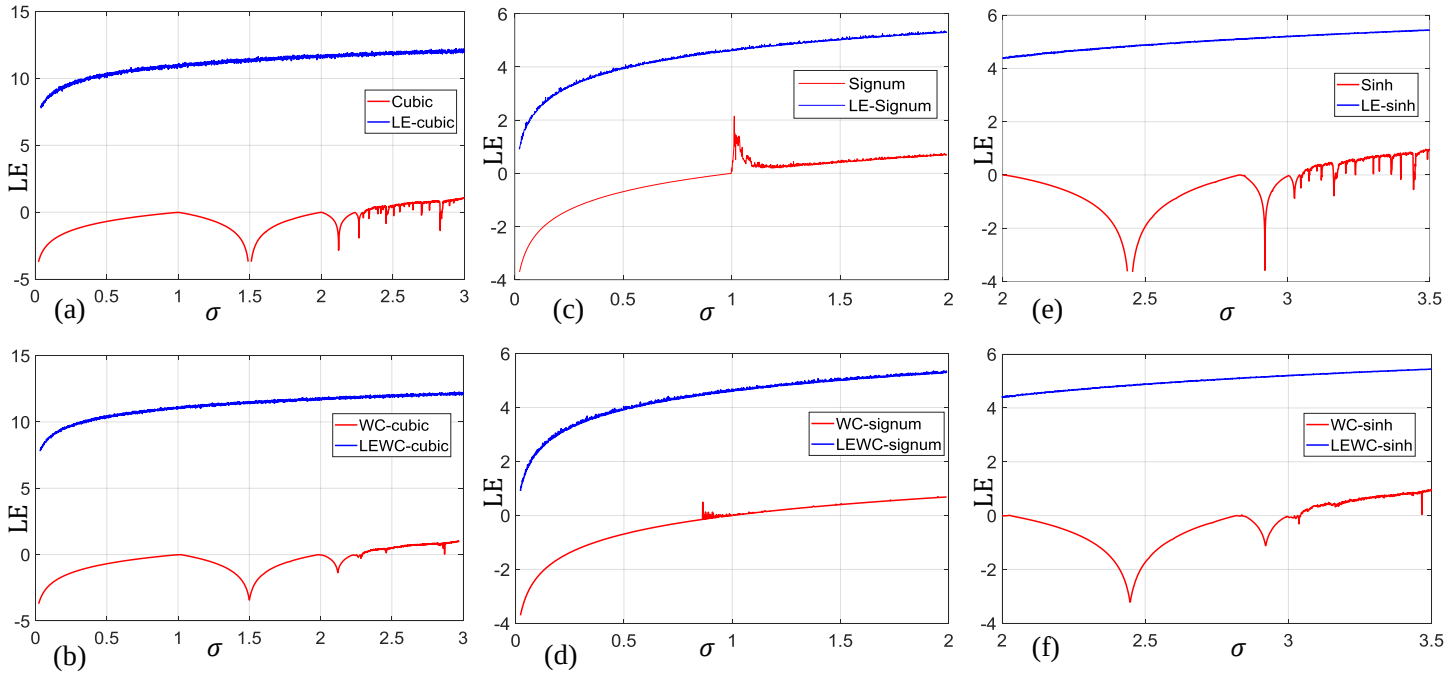

Figure 1 Lyapunov exponents (λ vs σ); (a) cubic maps, (b) weakly-coupled cubic maps; (c) signum maps, (d) weakly-coupled signum maps; (e) sinh maps, (f) weakly-coupled sinh maps.

by considering the LE-enhanced map (6) two different map functions are integrated with the addition operator as

$$x_{k+1} = \alpha(f_1(\sigma_1, x_k) + f_2(\sigma_2, x_k)) \mod 1 \tag{18}$$

where the functions f_1 and f_2 represent different seed chaotic map functions defined in right hand-sides of (15), (16) and (17). It is seen from Fig. 2 that the proposed LE-enhanced chaotification approach provides positive LE values in all parameter ranges of the seed maps. On the other hand, the models provided in Refs. (Hu and Li (2021); Hua *et al.* (2019b,a); Zhou *et al.* (2014)) have seed map dependent efficiency such that Fig. 2c shows that these methods are not valid when the signum + sinh map is the seed map. The efficiency of unit transform (modulo operator) based method is significantly improved with a gain operator in this work, and it is obvious that the proposed method has the best performance among the given methods.

The effect of gain operator α can be illustrated on the cubic map. Figure 3 shows the LEs and bifurcation diagrams of the cubic map (15), LE-enhanced cubic map (6) for $\alpha = 1$ and LE-enhanced cubic map (6) for $\alpha = 1 \times 10^5$. When the gain is $\alpha = 1$, then only mod 1 operator is implemented, and compared with Fig. 3a, it is clear from Fig. 3b that the modulo operator transforms the data to $x \in [0, 1]$, but slightly improves the chaotic features or randomness of data. On the other hand, when the gain is $\alpha = 1 \times 10^5$, then the gain plus mod 1 operator is implemented, and the chaotic and randomness features of the map are significantly improved because LE is always positive and there are no periodic windows in the bifurcation diagram as seen in Fig. 3c.

Bifurcation diagrams: Bifurcation diagrams of the seed maps (1) and (9) and LE-enhanced chaotic maps (6) and (12) are illustrated in Fig. 4. For $\sigma \in [1.5, 3]$, the cubic (15) and WC-cubic (12) maps exhibit a period-doubling route to chaos (Figs. 4a and 4c), but the LE-cubic (6) and LEWC-cubic (12) maps exhibit chaotic behavior within the whole parameter ranges (Figs. 4b and 4d). Besides, the outputs of LE-enhanced chaotic maps fit the range of standard uniform distribution (i.e., $x_k \in [0, 1]$). The signum map for $\sigma \in [0.5, 2]$ and hyperbolic-sine map for $\sigma \in [2.5, 3.5]$ also exhibit similar behaviors as seen in Figs. 4e-4l. It is seen that the WC-chaotic maps increase complexity of the maps, but still we can observe non-uniform distributions and periodic windows. However, the LE-enhanced chaotic maps (6) and (12) provide excellent chaotic features compared with the seed chaotic maps (1) and (9). Note that, the LEWC-chaotic maps (12) provide more complex chaos compared with the 1D LE-chaotic maps (6). For example, the LE-signum map (Fig. 4f) encounters collapse (trajectory approaches to fixed point in long-term run) at $\sigma = 1$, but the LEWC-signum map (Fig. 4h) has no collapse.

Phase diagrams: Phase diagrams of the seed and LE enhanced chaotic maps are illustrated in Fig. 5. The 1D chaotic maps have the data points that are spread evenly across the symmetric lines. The weakly-coupled (WC) chaotic maps increase complexity (randomness) of the chaotic data, but have non-uniform distributions (Figs. 5b,f,j). On the other hand, the phase diagrams of LE-enhanced chaotic maps have completely random data distribution and have quite complex and uniformly distributed chaotic properties.

Entropy and correlation coefficients: The splitting of the outcome space converts the chaotic map into an ergodic information source. Therefore, it is quite convenient to utilize the information theory for analyzing this source. The average level of randomness in the outcome of a variable is determined by the entropy in information theory.

Definition 2 (Shannon entropy) (Karmeshu and Pal (2003)): Entropy H_m of the ensemble $(X_1, p_1), \ldots, (X_m, p_m)$ is given by the expression

$$H_m(p) = -\sum_{i=1}^{m} p_i \log(p_i) \tag{19}$$

where p_i denotes the probability mass associated with the variable

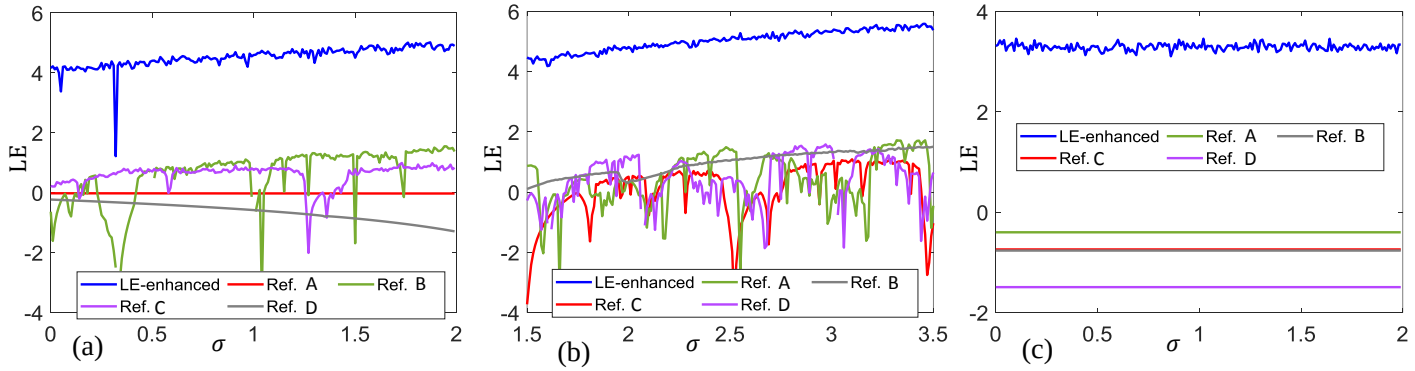

Figure 2 Comparison of Lyapunov exponents (λ vs σ) of different models; (a) cubic+signum, (b) cubic+sinh, and (c) signum+sinh map functions. (Ref.A: Hua *et al.* (2019b), Ref.B: Hu and Li (2021), Ref.C: Zhou *et al.* (2014), Ref.D: Hua *et al.* (2019a))

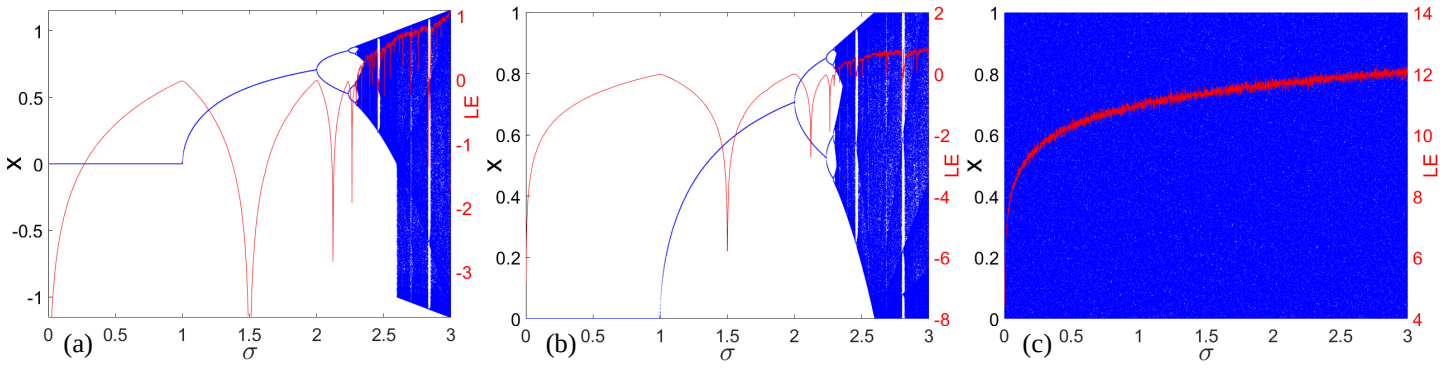

Figure 3 Lyapunov exponents (red) and bifurcation diagrams (blue); (a) cubic seed map, (b) LE-enhanced cubic map with $\alpha = 1$ and (c) LE-enhanced cubic map with $\alpha = 1 \times 10^5$.

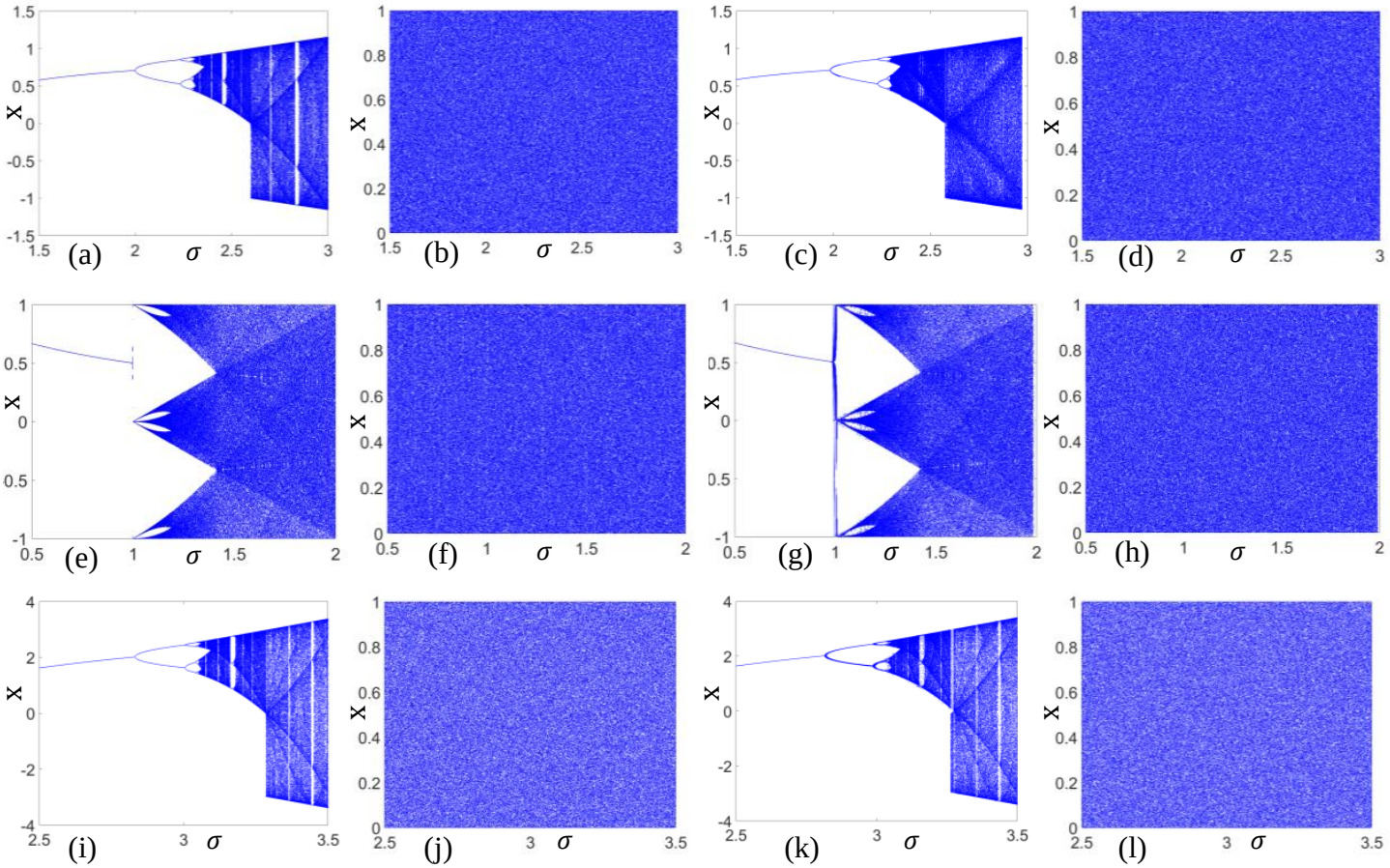

Figure 4 Bifurcation diagrams (x_k vs σ); (a) cubic seed map, (b) LE enhanced cubic map, (c) weakly-coupled cubic map, (d) LE enhanced weakly-coupled cubic map; (e) signum seed map, (f) LE enhanced signum map, (g) weakly-coupled signum map, (h) LE enhanced weakly-coupled signum map; (i) sinh seed map, (j) LE enhanced sinh map, (k) weakly-coupled sinh map, and (l) LE enhanced weakly-coupled sinh map.

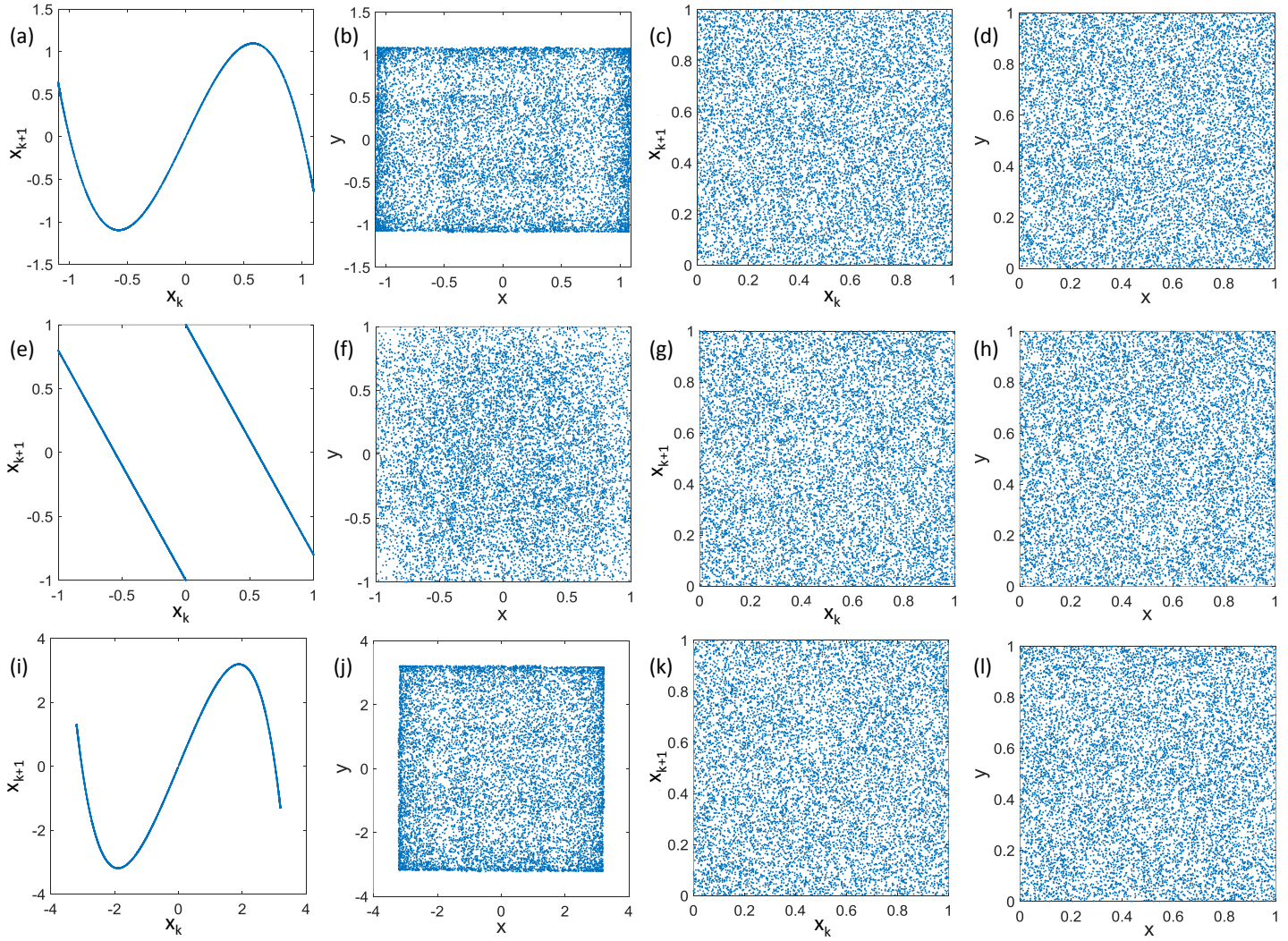

Figure 5 Phase diagrams; (a) cubic map, (b) weakly-coupled cubic map; (c) LE enhanced cubic map, (d) LE enhanced weakly-coupled cubic map, (e) signum map, (f) weakly-coupled sign map; (g) LE enhanced signum map, (h) LE enhanced weakly-coupled signum map, (i) sinh map, (j) weakly-coupled sinh map; (k) LE enhanced sinh map, (l) LE enhanced weakly-coupled sinh map.

X_i such that $\sum p_i = 1$, and the maximum entropy value is given by $H_{max} = \log_2 m$. This definition of the Shannon entropy has a relation with KSE in terms of its supremum as (Falniowski (2014))

$$h_{KSE} = \sup_X \lim_{m\to\infty} \frac{1}{m} H_m(p) \tag{20}$$

The KSE can be interpreted as a generalization of Shannon entropy. Both entropies measure the unpredictability of a deterministic system, and the higher the entropy means the higher the unpredictability. Deciding if generated chaotic sequences are statistically independent can be tested with many statistical test methods. The correlation coefficient is one of these methods that must be satisfied by the chaotic random number generators.

Definition 3 (Correlation coefficient) (James (2006)): For two random variables (x, y) with n observations, the correlation coefficient is defined as

$$R(x,y) = \frac{1}{n-1} \sum_{i=1}^{n} \left(\frac{x_i - \mu_x}{\sigma_x}\right)\left(\frac{y_i - \mu_y}{\sigma_y}\right) \tag{21}$$

where μ_x and μ_y are the means, and σ_x and σ_y are the standard deviations of x and y. The correlation coefficient of two random variables is a measure of their linear independence, and it can be positive, negative or zero. The maximum value of correlation coefficient is $|R| = 1$. Hence, the absolute value of correlation coefficient should be around zero for high random outcomes.

Table 1 shows the calculated entropy and correlation coefficient values. In the probability mass calculations, 1000 subintervals are taken into account, and thus the maximum entropy value is $H_{max} = 9.9658$. As seen in Table 1, the entropies of all chaotic maps are very high, but the LE-enhanced chaotic maps provide almost the maximimum entropy value. The correlation coefficient is calculated for very small initial value differences. The initial conditions are taken as $x_0 = 0.123400$ and $y_0 = 0.123401$ for all chaotic maps. It is seen from Table 1 that all the chaotic maps have almost no correlation since the correlation coefficient is $|R| \approx 0$ for the selected parameter values.

Histograms: The histogram allows measuring the initial condition insensitivity which is related to the splitting of the output space into a number of subintervals, and analyzing the evolution in these regions. Consider a set of equally distributed m subintervals such that

$$X = X_1, \ldots, X_m,\ X_i \cap X_j = \varnothing,\ \text{for } i \neq j \tag{22}$$

Then the randomness in deterministic chaos can be specified through the probabilities. Histogram describes the distribution of the numerical data in each subinterval. The height of each histogram subinterval (or bin) represents the average frequency density for the interval. If the total number of observations are n, the number of subintervals can be calculated from the square-root choice as $m = \sqrt{n}$. The histograms of the chaotic maps are shown in Fig. 6. The total number of observations for each chaotic map are taken as $n = 1 \times 10^6$, so the number of bins can be calculated from the square-root choice as $m = 1000$. Figure 6 displays the histograms of seed cubic, WC cubic, LE-enhanced cubic and LE-enhanced WC cubic maps. The cubic and WC cubic maps have completely non-uniform distributions (Figs. 6a and 6c), while the WC cubic map has a better distribution than the 1D cubic map. On the other hand, the histograms of LE enhanced 1D and WC cubic maps (Figs. 6b and 6d) have a random pattern without any periodic, upward or downward trends. Existence of some significant outliers is an indication of problems in the random number generators. It is clear that there are no obvious outliers in the histograms of LE-enhanced chaotic maps, i.e., data points are spreaded evenly which is a good indication of uniformity. The histograms verify that the data follows the features of standard uniform distribution such that there is almost the same number of observations in each subinterval. Similarly, the histograms of signum, WC signum, sinh and WC sinh maps have non-uniform distributions (Figs. 6e,g,i,k), but their LE-enhanced counterparts have uniformly distributed histograms (Figs. 6f,h,j,l).

Throughout this paper, the system parameters are chosen as follows: $x_0 = 0.1234$ and $y_0 = 0.1234$ for all maps, $\sigma = 2.82$ for cubic maps, $\sigma = 1.8$ for signum maps, $\sigma = 3.4$ for sinh maps, $\alpha = 1 \times 10^5$ for LE-enhanced cubic maps, $\alpha = 1 \times 10^2$ for LE-enhanced signum and sinh maps, $p = 0.01$ for all weakly-coupled (WC) maps.

In practice, the probability density function (pdf) estimations and histograms are closely related. The distribution of the numerical data in each subinterval of the histogram can directly be used to obtain pdf with normalization. Hence, the histograms provide a visual assessment on the pdf estimations. Besides, the statistical properties of the chaotic maps must match the properties of the related distributions. Since the physical origin based random numbers (e.g., radioactive particle emissions) follow the uniform distribution, the LE-enhanced chaotic map should also follow this distribution. The statistical properties of the standard uniform distribution $U(0,1)$ are given by $mean = 0.5$, $median = 0.5$, $variance = 0.0833$, $skewness = 0$, $kurtosis = 1.8$, $pdf = 1$ and $cdf = x$ for $x \in [0,1]$. The probability of falling in the interval of fixed length $[0,1]$ is constant in the uniform distribution. Table 1 shows the statistical properties of chaotic maps for total number of observations $n = 1 \times 10^6$. It is seen that the LE-enhanced chaotic maps successfully follow the statistical properties of standard uniform distribution $U(0,1)$. Note that the parameters α and σ of LE-enhanced chaotic maps ((6) and (12)) have significant effects on the randomness features of chaotic sequences, so they should be selected suitably in practical applications.

APPLICATIONS

LE-enhanced chaotic maps as random bit generators

Random bit generators are significant for many applications in statistical physics, stochastic modeling, numerical simulations, and cryptography. A random bit generator must provide statistically independent and unbiased bits (namely, fully unpredictable bits). The ranges of sequences produced from most of the chaotic systems do not match the random bit generator requirements, so many authors have proposed chaotic map specific post-processing algorithms (Pulido-Luna *et al.* (2021); Jafari Barani *et al.* (2020); Hamza (2017)). On the other hand, since the proposed LE-enhanced chaotic maps produce uniformly distributed random numbers, a binary converter algorithm can directly be used to generate random bits, such as a comparator is defined by

$$b_k = \begin{cases} 1 & \text{if } x_k \geq 0.5 \\ 0 & \text{otherwise} \end{cases} \tag{23}$$

where b_k represents random bits, $b_k \in \{0,1\}$, and the threshold is selected as the mean value of the LE-enhanced chaotic maps (6). If a chaotic system is not providing uncorrelated and unbiased bits, the de-skewing techniques (Stallings (2006)) (e.g., Von Neumann technique) can be used to remove possible correlations and biases in the binary sequences. However, the proposed LE-enhanced chaotic maps (6) are able to produce high quality random numbers

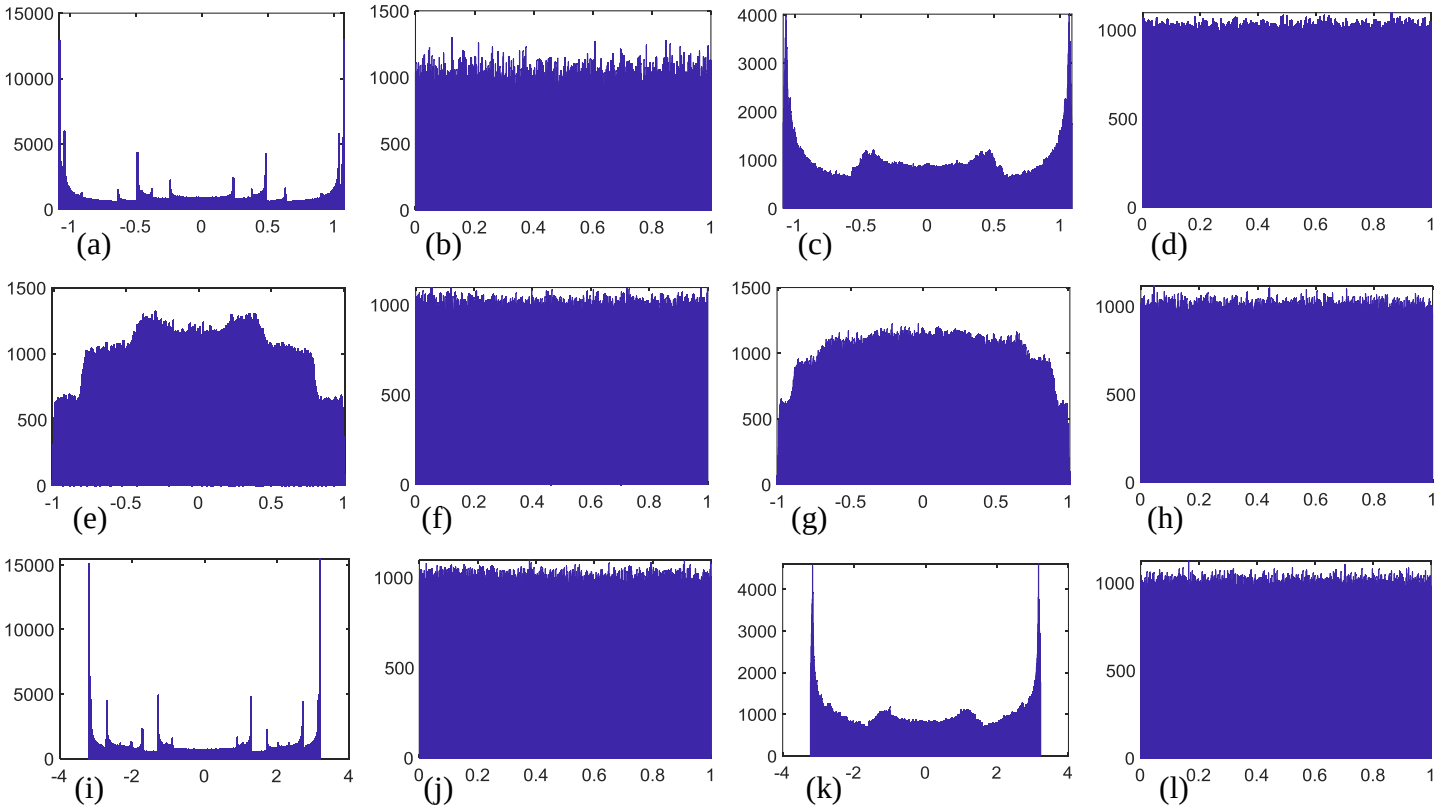

Figure 6 Histograms (counts vs x_k): (a) cubic seed map, (b) LE-enhanced cubic map, (c) weakly-coupled cubic map, (d) LE-enhanced weakly-coupled cubic map; (e) signum seed map, (f) LE-enhanced signum map, (g) weakly-coupled signum map, (h) LE-enhanced weakly-coupled signum map; (i) sinh seed map, (j) LE-enhanced sinh map, (k) weakly-coupled sinh map, and (l) LE-enhanced weakly-coupled sinh map.

Table 1 Randomness test results for the LE-enhanced chaotic maps.

Property	Cubic Map	Sign Map	Sinh Map	WC Cubic Map	WC Sign Map	WC Sinh Map	LE Cubic Map	LE Sign Map	LE Sinh Map	LEWC Cubic Map	LEWC Sign Map	LEWC Sinh Map
Mean	0	0	0.002	0	0	0	0.5	0.5	0.5	0.5	0.5	0.5
Median	0	0	0.005	0	0	0	0.5	0.5	0.5	0.5	0.5	0.5
Variance	0.4784	0.278	4.500	0.4844	0.2771	4.345	0.0837	0.0834	0.0834	0.0834	0.0833	0.0833
Skewness	0.001	0.001	0.002	0.001	0.002	0.001	0.003	0.001	0.003	0.000	0.000	0.001
Kurtosis	1.751	1.947	1.609	1.718	1.948	1.664	1.796	1.799	1.798	1.799	1.799	1.799
Range	(-2,2)	[-1,1]	(-4,3)	(-2,2)	[-1,1]	(-4,4)	[0,1]	[0,1]	[0,1]	[0,1]	[0,1]	[0,1]
Correlation	0.0018	0.0009	0.0013	0.0013	0.0012	0.0003	0.0008	0.0011	0.0008	0.0015	0.0011	0.0005
Entropy	9.7400	9.9334	9.7000	9.8540	9.9363	9.8645	9.9604	9.9650	9.9651	9.9651	9.9651	9.9650

as proved in the previous section, which can eliminate the use of a de-skewing algorithm. This is an important advantage because the post-processing steps are eliminated. This is an advantage in terms of less time consuming and short algorithm developments, for instance, the random bit generation can easily be implemented with in-line codes rather than function calls. More importantly, the usage of a de-skewing technique provides less than 25% efficiency with respect to the random bit throughput, but the proposed LE-enhanced approach has 100% efficiency.

The commonly used statistical testing methods for randomness analysis of binary values are provided in NIST SP 800-22 test suite (Bassham *et al.* (2010)). The output file containing 5120000 random bits are generated to be tested with the NIST statistical test suite. The test results are given in Table 2. The LE-enhanced chaotic maps successfully pass the statistical tests, implying that these maps can be used in cryptosystems. Clearly, the statistical tests may not determine the quality of the produced random bits alone, but some conclusions can be drawn about it. In practice, the quality of applications must be checked with application specific randomness analysis tests. In addition, since chaotic systems have high sensitivity to initial conditions, for the unpredictability of chaotic random bit generators an efficient approach can be connecting the initial condition of chaotic maps with an input device of the application environment, e.g., thermal noise, port value and mouse movement.

LE-enhanced chaotic maps based Image encryption

The proposed chaotic random bit generators are applied to an image encryption scheme in this section. Today, almost all image encryption schemes use different chaotic systems with many different sophisticated encryption algorithms (Khan and Kayhan (2021); Wang and Liu (2021); Talhaoui *et al.* (2021)). Here, for image encryption and decryption, the key bits are generated from the LE-enhanced sinh map, and the symmetric-key encryption method is implemented. The grayscale image of size KL pixels is converted into one-dimensional array of pixels M_i, $i = 1, 2, .., KL$, and then each M_i pixel is represented with 8-bit blocks (i.e., 256 shades per pixel). Hence, the bit length of binary sequence for the given figure is equal to $K \times L \times 8$ bits. The same number of random bits are generated from the LE-enhanced sinh map and represented with 8-bit blocks for using in the pixel-by-pixel encryption scheme. The XORing operator is implemented between the key and image bit sequences for encryption. For decryption of the image, the XORing operator is implemented between the key and decrypted image bit sequences.

Histogram analysis: Histogram of a digital image displays the distribution of grayscale values of all the pixels. For an 8-bit grayscale image there are $2^8 = 256$ different possible intensities, which are visualized by the histograms. Four grayscale images, their encrypted images and corresponding histograms are illustrated in Fig. 7. The histograms of plain-text images are one of the most common cryptosystem attacks (Farajallah *et al.* (2016)), because they exhibit the characteristic properties of the images as seen in Figs. 7b,f,j,n. On the other hand, all the plain-text images become indistinguishable noise-like ciphers after encryption as seen in Figs. 7c,g,k,o. The histograms of four cipher-text images just show indistinguishable and identical properties (see Figs. 7d,h,l,p). All 256 gray levels appear with almost the same probability in encrypted images, and the histograms are not leaking any significant information to the statistical attacks.

The chi-square goodness-of-fit test can be used to determine whether the histogram data sample fits the uniform probability distribution (James (2006)). By taking into account the histogram data, the chi-square test statistic can be calculated as

$$\chi^2 = \sum_{i=1}^{256} (O_i - E_e)^2 / E_e \tag{24}$$

where O_i is the observed counts of gray level i in an image, and $E_e = KL/256$ represents the expected counts for grayscale image of size KL pixels. The test statistic has an approximate chi-square distribution of 256 degrees of freedom, and the hypothesis at the 5% significance level can be accepted if $\chi^2 < \chi^2_{0.05}(256) = 320$, otherwise it can be rejected. The χ^2-test statistics of images shown in Fig. 7 (both plain-text and cipher-text images) are listed in Table 3. It is seen from Table 3 that the statistics of the cipher-text images are small and satisfy the hypothesis, while the plaintext images have much larger values and are not satisfying the hypothesis. This means that the histograms of cipher-text images are approximately uniformly distributed.

Correlation analysis: The correlation between adjacent pixels of an image data is high due to natural image properties. Hence, an image encryption algorithm must eliminate this high correlation and provide an adequate resistance against statistical attacks. To test correlation dimensions of images, 30000 pairs of adjacent pixels from vertical and horizontal directions in plain-text images and cipher-text images are randomly selected, and the corresponding correlation coefficients are calculated using (21) and listed in Table 3. It is seen that the plain-text images have high correlation (around 1) in vertical and horizontal directions. On the other hand, the correlation coefficients of the cipher-text images are approximately zero, indicating that there are almost no correlations between adjacent pixels. That is, the proposed LE-enhanced chaotic maps produce highly random bits.

Mean square error analysis: The difference between original and encrypted image pixels (each pixel has 256 shades of gray) is measured with the mean square error (MSE). The MSE can be defined as

$$MSE = \frac{1}{KL} \sum_{i=1}^{K} \sum_{j=1}^{L} (O_{ij} - E_{ij})^2 \tag{25}$$

where O_{ij} is the original image pixel, E_{ij} is the encrypted image pixel, and K and L represent the pixel size of the original or encrypted image. The MSE result is equal to zero if the images are the same, but it should be as high as possible if the compared images are different. A higher MSE value means the cipher-text image is more immune to attacks. The calculated MSE values for different cipher-text images are tabulated in Table 3. The MSE values are much higher than zero ($MSE \gg 0$), and thus the LE-enhanced chaotic map based encryption provides highly satisfactory results.

Entropy analysis: In the probability mass calculations, 256 subintervals are taken into account, and thus the maximum entropy value is $H_{max} = \log_2 256 = 8$. The formula (19) is used to calculate entropy of cipher-text images. Table 3 shows that the entropy values of the cipher-text images are practically equal to the maximum entropy value (around 8), indicating that the unpredictability level of the cipher-text images is maximum.

Table 2 Randomness (NIST) test results for the LE-enhanced chaotic maps.

Test Name	LE Cubic Map	LE Sign Map	LE Sinh Map	LEWC Cubic Map	LEWC Sign Map	LEWC Sinh Map
Frequency	10/10	10/10	10/10	10/10	10/10	10/10
Block frequency	10/10	10/10	10/10	9/10	10/10	10/10
Cumulative sums Forward	10/10	10/10	8/10	10/10	10/10	9/10
Cumulative sums Reverse	10/10	10/10	9/10	10/10	10/10	10/10
Runs	10/10	9/10	10/10	10/10	10/10	10/10
Longest run	10/10	9/10	10/10	10/10	10/10	10/10
Rank	10/10	10/10	10/10	10/10	9/10	10/10
FFT	10/10	10/10	10/10	10/10	10/10	10/10
Non-overlapping template	10/10	10/10	10/10	10/10	10/10	10/10
Overlapping template	10/10	10/10	10/10	10/10	10/10	10/10
Universal	9/10	9/10	10/10	9/10	10/10	10/10
Approximate entropy	10/10	10/10	9/10	10/10	9/10	10/10
Random excursions	4/4	4/4	2/2	4/4	3/3	5/5
Random excursions variant	4/4	4/4	2/2	4/4	3/3	5/5
Serial	9/10	10/10	10/10	10/10	10/10	10/10
Linear complexity	10/10	10/10	10/10	10/10	10/10	10/10

Table 3 Statistical analysis results of the encrypted images.

Images	Correlation plain-image (vertical)	Correlation cipher-image (vertical)	Correlation plain-image (horizontal)	Correlation cipher-image (horizontal)	χ^2 plain-image	χ^2 cipher-image	MSE	Entropy
coins.png	0.9726	0.0047	0.9676	0.0066	3×10^5	306	21519	7.9969
peppers.png	0.9917	0.0051	0.9860	0.0021	4×10^5	267	21674	7.9990
corn.tif	0.9662	0.0071	0.0514	0.0067	4×10^4	251	21627	7.9986
moon.tif	0.9949	0.0011	0.0282	0.0005	3×10^6	312	21577	7.9988
football.jpg	0.9437	0.0018	0.9347	0.0022	2×10^5	237	21474	7.9979

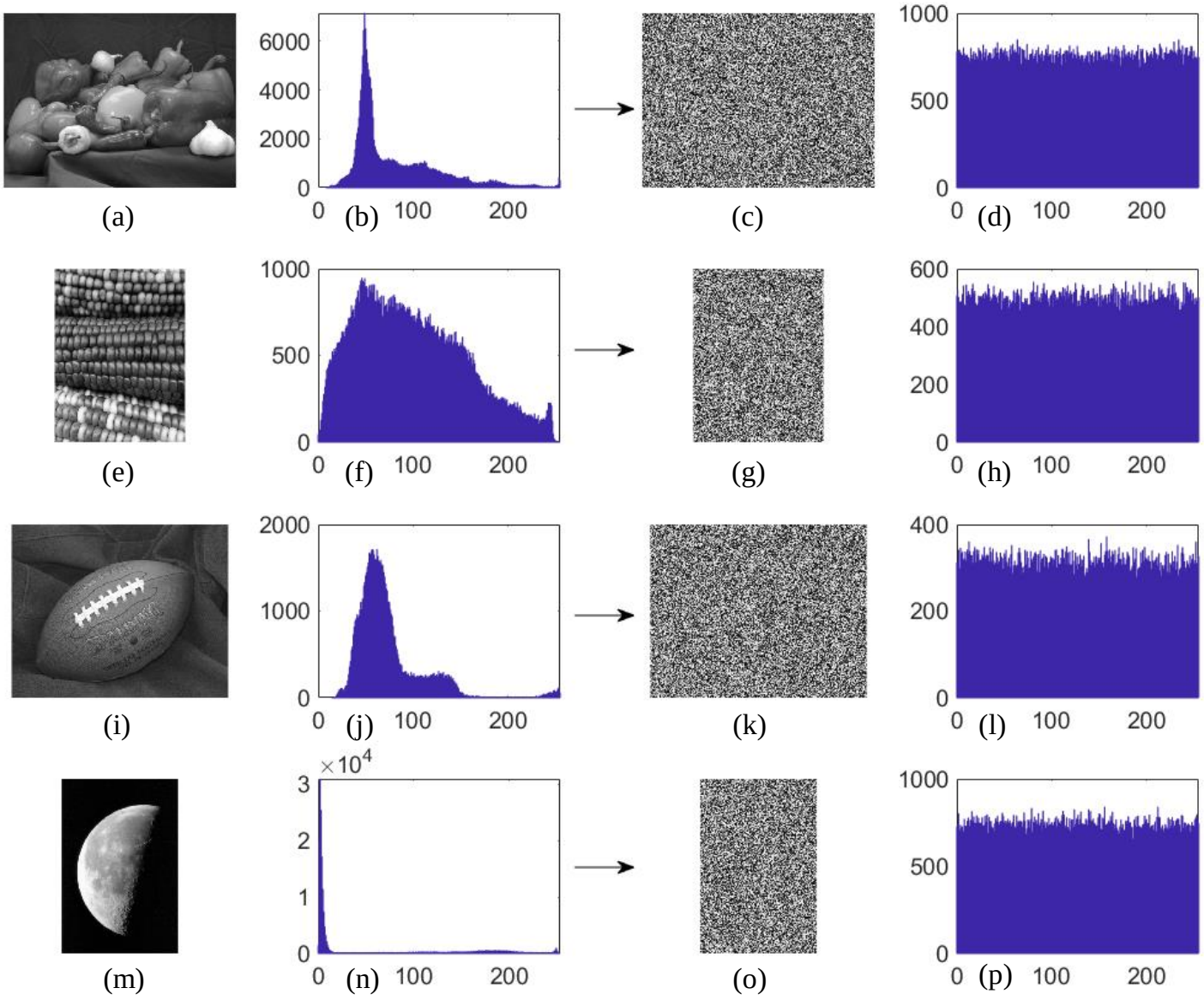

Figure 7 Histogram analysis: (a) peppers; (b) histogram of (a); (c) encrypted peppers; (d) histogram of (c); (e) corn; (f) histogram of (e); (g) encrypted corn (c); (h) histogram of (g); (i) football; (j) histogram of (i); (k) encrypted football; (l) Histogram of (k); (m) moon; (n) histogram of (m); (o) encrypted moon; (p) histogram of (o).

CONCLUSION

The uniformity and statistically independence are two key features that a chaotic random number generator must satisfy for cryptographic and scientific applications. A gain plus modulo-1 operator based chaotic framework is proposed in this work to enhance the Lyapunov exponent of the seed chaotic maps and to assure that the chaotic outcomes follow the standard uniform distribution $U(0,1)$ with highly random chaotic sequences. It is shown that the gain plus modulo-1 operator based approach greatly broadens the chaotic range of seed chaotic maps and generates robust chaos. The proposed approach produces chaotic sequences that are replicable, fast, portable and closely approximate the ideal statistical properties of uniformity and independence. The proposed chaotic framework successfully passes the fundamental statistical and visual tests. The approach can eliminate the use of post-processing approaches (e.g., de-skewing) and provide 100% efficiency with respect to the random bit throughput. The efficiency and feasibility of the approach are verified with an image encryption application. The proposed method has a high potential in science, technology and cryptography applications.

Conflicts of Interest

The author declares that there is no conflict of interest regarding the publication of this paper.

Availability of data and material

Not applicable.

LITERATURE CITED

Ablay, G., 2016 Chaotic map construction from common nonlinearities and microcontroller implementations. International Journal of Bifurcation and Chaos **26**: 1650121.

Asgari-Chenaghlu, M., M.-A. Balafar, and M.-R. Feizi-Derakhshi, 2019 A novel image encryption algorithm based on polynomial combination of chaotic maps and dynamic function generation. Signal Processing **157**: 1–13.

Awrejcewicz, J., A. V. Krysko, N. P. Erofeev, V. Dobriyan, M. A. Barulina, *et al.*, 2018 Quantifying Chaos by Various Computational Methods. Part 1: Simple Systems. Entropy **20**: 175.

Banerjee, S., L. Rondoni, and M. Mitra, editors, 2012 *Applications of Chaos and Nonlinear Dynamics in Science and Engineering - Vol. 2*. Springer-Verlag, Berlin Heidelberg.

Bassham, L. E., A. L. Rukhin, J. Soto, J. R. Nechvatal, M. E. Smid, *et al.*, 2010 A Statistical Test Suite for Random and Pseudorandom Number Generators for Cryptographic Applications. Technical report, National Institute of Standards & Technology, Gaithersburg, MD, United States.

Benamara, O., F. Merazka, and K. Betina, 2016 An improvement of a cryptanalysis algorithm. Information Processing Letters **116**: 192–196.

Dekking, F. M., C. Kraaikamp, H. P. Lopuhaä, and L. E. Meester, 2005 *A Modern Introduction to Probability and Statistics: Understanding Why and How*. Springer-Verlag, London.

Dorfman, J. R., 1999 *An Introduction to Chaos in Nonequilibrium Statistical Mechanics*. Cambridge Lecture Notes in Physics, Cambridge University Press, Cambridge.

El-Hameed, H. A. A., N. Ramadan, W. El-Shafai, A. A. M. Khalaf, H. E. H. Ahmed, *et al.*, 2021 Cancelable biometric security system based on advanced chaotic maps. The Visual Computer .

Falniowski, F., 2014 On the Connections of Generalized Entropies With Shannon and Kolmogorov–Sinai Entropies. Entropy **16**.

Farajallah, M., S. El Assad, and O. Deforges, 2016 Fast and secure chaos-based cryptosystem for images. International Journal of Bifurcation and Chaos **26**: 1650021(1–21).

Garasym, O., I. Taralova, and R. Lozi, 2016 New Nonlinear CPRNG Based on Tent and Logistic Maps. In *Complex Systems and Networks: Dynamics, Controls and Applications*, edited by J. Lü, X. Yu, G. Chen, and W. Yu, Understanding Complex Systems, pp. 131–161, Springer, Berlin, Heidelberg.

Hamza, R., 2017 A novel pseudo random sequence generator for image-cryptographic applications. Journal of Information Security and Applications **35**: 119–127.

Hu, G. and B. Li, 2021 Coupling chaotic system based on unit transform and its applications in image encryption. Signal Processing **178**: 107790.

Hua, Z., Y. Zhang, and Y. Zhou, 2020 Two-Dimensional Modular Chaotification System for Improving Chaos Complexity. IEEE Transactions on Signal Processing **68**: 1937–1949.

Hua, Z., B. Zhou, and Y. Zhou, 2019a Sine Chaotification Model for Enhancing Chaos and Its Hardware Implementation. IEEE Transactions on Industrial Electronics **66**: 1273–1284.

Hua, Z., Y. Zhou, and H. Huang, 2019b Cosine-transform-based chaotic system for image encryption. Information Sciences **480**: 403–419.

Jafari Barani, M., P. Ayubi, M. Yousefi Valandar, and B. Y. Irani, 2020 A new Pseudo random number generator based on generalized Newton complex map with dynamic key. Journal of Information Security and Applications **53**: 102509.

James, F., 2006 *Statistical Methods In Experimental Physics*. World Scientific, Hackensack, NJ, second edition.

Karmeshu and N. R. Pal, 2003 Uncertainty, Entropy and Maximum Entropy Principle — An Overview. In *Entropy Measures, Maximum Entropy Principle and Emerging Applications*, edited by Karmeshu, Studies in Fuzziness and Soft Computing, pp. 1–53, Springer, Berlin, Heidelberg.

Khan, J. S. and S. K. Kayhan, 2021 Chaos and compressive sensing based novel image encryption scheme. Journal of Information Security and Applications **58**: 102711.

Lan, R., J. He, S. Wang, T. Gu, and X. Luo, 2018 Integrated chaotic systems for image encryption. Signal Processing **147**: 133–145.

Liu, L., S. Miao, M. Cheng, and X. Gao, 2016 A pseudorandom bit generator based on new multi-delayed Chebyshev map. Information Processing Letters **116**: 674–681.

Luo, Y., S. Zhang, J. Liu, and L. Cao, 2020 Cryptanalysis of a Chaotic Block Cryptographic System Against Template Attacks. International Journal of Bifurcation and Chaos **30**: 2050223.

Murillo-Escobar, M. A., C. Cruz-Hernández, L. Cardoza-Avendaño, and R. Méndez-Ramírez, 2017 A novel pseudorandom number generator based on pseudorandomly enhanced logistic map. Nonlinear Dynamics **87**: 407–425.

Pak, C. and L. Huang, 2017 A new color image encryption using combination of the 1D chaotic map. Signal Processing **138**: 129–137.

Parvaz, R. and M. Zarebnia, 2018 A combination chaotic system and application in color image encryption. Optics & Laser Technology **101**: 30–41.

Pikovsky, A. and A. Politi, 2016 *Lyapunov Exponents: A Tool to Explore Complex Dynamics*. Cambridge University Press, Cambridge.

Pulido-Luna, J. R., J. A. López-Rentería, N. R. Cazarez-Castro, and E. Campos, 2021 A two-directional grid multiscroll hidden attractor based on piecewise linear system and its application in pseudo-random bit generator. Integration **81**: 34–42.

Ruelle, D., 1997 Chaos, predictability, and idealization in physics. Complexity **3**: 26–28.

Stallings, W., 2006 *Cryptography and Network Security: Principles and Practice*. Prentice Hall.

Strogatz, S. H., 2015 *Nonlinear Dynamics and Chaos: With Applications to Physics, Biology, Chemistry, and Engineering*. CRC Press, Boulder, CO, second edition.

Talhaoui, M. Z., X. Wang, and M. A. Midoun, 2021 A new one-dimensional cosine polynomial chaotic map and its use in image encryption. The Visual Computer **37**: 541–551.

Vallejo, J. C. and M. A. F. Sanjuán, 2019 *Predictability of Chaotic Dynamics : A Finite-time Lyapunov Exponents Approach*. Springer Series in Synergetics, Springer International Publishing, Switzerland, second edition.

Wang, X. and P. Liu, 2021 Image encryption based on roulette cascaded chaotic system and alienated image library. The Visual Computer .

Xiang, H. and L. Liu, 2020 An improved digital logistic map and its application in image encryption. Multimedia Tools and Applications **79**: 30329–30355.

Zahmoul, R., R. Ejbali, and M. Zaied, 2017 Image encryption based on new Beta chaotic maps. Optics and Lasers in Engineering **96**: 39–49.

Zhou, Y., L. Bao, and C. L. P. Chen, 2014 A new 1D chaotic system for image encryption. Signal Processing **97**: 172–182.

How to cite this article: Ablay, G. Lyapunov Exponent Enhancement in Chaotic Maps with Uniform Distribution Modulo One Transformation. Chaos Theory and Applications, 4(1), 45-58, 2022.